Some Aspects of Dimensional Deconstruction

Koichiro Kobayashi

Supervisor: Prof. Kiyoshi Shiraishi

Doctoral thesis submitted to Yamaguchi University

Yamaguchi University
Graduate school of Science and Engineering

March, 2011

Abstract

We introduce two novel models ("Democratic Three Site Higgsless Model" and "Vortices and Superfields on a Graph") that are based on the technique of Dimensional Deconstruction.

Background

Nowadays, in the (elementary) particle physics, the Glashow-Weinberg-Salam (GWS) Model [1] is well known theory as the Electroweak (Unified) Theory. In this model, the symmetry of the gauge field $SU(2)_L \otimes U(1)_Y$ is spontaneously broken to the electromagnetic symmetry $U(1)_{em}$. In the process of symmetry breaking, some gauge fields become massive and the Higgs particle (a massive scalar particle) is produced. This mechanism is called the Higgs mechanism [2]. The GWS Model symmetry group $SU(2)_L \otimes U(1)_Y$ forms the electroweak gauge sector of the Standard Model (SM) of particle physics. The SM is the very successful theory, as decades of experiments have confirmed it predictions to a high level accuracy. Nevertheless there are some questions that have not been answered. We introduce two of them.

One is the missing Higgs particle problem. This is the problem that the existence of the Higgs particle has never observed. Therefore the Higgs particle is the missing piece of the GWS Model.

The other is the gauge hierarchy problem. As the further unification, there is the Grand Unified Theory (GUT). GUT (for example $SU(5)$ GUT) unifies both Electroweak Theory and Quantum Chromodynamics (the fundamental theory of the strong interactions). The unification energy scale of the GUT is about 10^{14} GeV. On the other hand, the unification energy scale of the Electroweak Theory is about 100 GeV. The gap of the order between these two unification energy scale is about 12. This large gap of the energy scale is enormous hierarchy. The gauge hierarchy problem is that what the origin of this hierarchy is. This problem leads to why there are no physical objects between these unification scale.

To solve these two problems, we introduce the extra-dimensional gauge theory of the Electroweak Theory. In this thesis, we have an interest in the five-dimensional gauge theory. The fifth-component of the gauge field plays the role of the Higgs particle and the Kaluza-Klein (KK) mode of the four-dimensional gauge fields explains the gauge hierarchy problem. The Electroweak Theory which do not need the Higgs mechanism, is called Higgsless Theory.

We are interested in the low energy scale physics, near the electroweak unified energy scale. We focus on the Higgsless Theory of the deconstructed extra-dimensional gauge theory. The technique of discretizing the dimension is called "Dimensional Deconstruction" (DD), in this thesis, we use this technique in fifth-dimension. DD was introduced by Harvard group [3] and Fermi lab group [4] independently. In the (dimensionally) deconstructed theory, we use the moose diagram which denotes the theory framework. For the example of the Higgsless Theory, we show the deconstructed five-dimensional $SU(2)$ gauge theory. This theory is four-dimensional [effective] $SU(2) \otimes [SU(2)]^N \otimes U(1)$ gauge theory, where N represents the degree of the discretization. Since we are interested in the low-energy scale physics, we search the highly deconstructed theory of the Three Site Higgsless Model ($SU(2) \otimes [SU(2)] \otimes U(1)$, $N = 1$).

We call the theory based on [15] "the Original Three Site Higgsless Model", $SU(2)_L \otimes SU(2)_V \otimes U(1)_Y$. This is the highly deconstructed model of the five-dimensional $SU(2)_L \otimes SU(2)_R \otimes U(1)_{B-L}$ gauge theory. This model investigates fermions such as leptons and quarks. The property of $SU(2)_L$ and $U(1)_Y$ gauge fields are similar to the GWS Model. There are four SM-like gauge bosons and three heavier gauge bosons, and a set of SM-like fermions and heavy copies of those fermions.

We are also interested in (topological) solitons, such as monopole and vortex. Soliton means a solitary particle. Solitons are the particular classical solutions of the non-linear field equations. We think that topological configurations are a key ingredient in recent studies in theoretical physics.

We have an interest in the application of the moose diagram. We try to generalize DD with the help of Graph Theory.

The moose diagram is a figure which consists of sites and links. In the Higgsless Theory (of the deconstructed extra-dimensional gauge theory), gauge fields live in each site and scalar field live in each link. A connection between sites and links shows the interactions between fields. Therefore the shape of the moose diagram represents the theory space (theory framework).

We generalize the relation between gauge fields and scalar fields in the context of Graph Theory. In the language of the Graph Theory, site corresponds to vertex and link corresponds to edge. Introducing the orientated edge, we have some variations of the connections between vertices. We can express the relation between gauge fields and scalar fields in a graph, which is just a complex moose. We wish to call this theory based on a graph as "Graph Dimensional Deconstruction" (GDD).

Democratic Three Site Higgsless Model

We attempt another approach for the Three Site Higgsless Model. We extend the Three Site Higgsless Model by using the Democratic Condition. We call the model of this approach "Democratic Three Site Higgsless Model". In this model, "Democratic" means that each $SU(2)$ gauge field has equivalent property. We consider $[SU(2)]^2 \otimes U(1)$ gauge it is taken from $[SU(2)]^3$ broken by [effective] adjoint scalar. When $SU(2)$ is broken to $U(1)$ by the Higgs mechanism, the theory has monopole configuration. As the result of searching, we find that it is difficult to represent the real electroweak phenomenology in the Democratic Condition. We need to improve the Democratic Three Site Model.

Vortices and Superfields on a Graph

We extend the DD by utilizing the knowledge of Graph Theory. In the DD, one uses the moose diagram to exhibit the structure of the "theory space". We generalize the moose diagram to a general graph with oriented edges. We consider only the $U(1)$ gauge symmetry.

We also introduce supersymmetry (SUSY) into our model by use of superfields. We suppose that vector superfields reside at the vertices and chiral superfields at the edges of a given graph. Then we can consider multi-vector, multi-Higgs models. In our model, $[U(1)]^p$ (where p is the number of vertices) is broken to a single $U(1)$. Therefore for specific graphs, we get vortex-like classical solutions in our model. We show some examples of the graphs admitting the vortex solutions of simple structure as the Bogomolnyi solution.

概要

本論文では次元脱構築の方法を基礎にした２つの新たなモデル (「デモクラティックスリーサイトモデル」、「グラフ上でのボーテックスと超場」) を提案した。

背景

素粒子物理では、電磁気力と弱い力を統一的に記述する理論 (電弱統一理論) としてグラショウ-ワインバーグ-サラム (GWS) モデル [1] が知られている。このモデルでは、理論の持つゲージ対称性が $SU(2)_L \otimes U(1)_Y$(電弱対称性) から $U(1)_{em}$(電磁気対称性) に自発的に破れる (壊れる)。この対称性の破れの過程において、幾つかのゲージ場 (W、Z ボソン) は質量を獲得する。また、質量をもつヒッグス粒子がみいだされる。この対称性の破れの過程はヒッグスメカニズム [2] と呼ばれている。GWS モデルと強い力を記述する理論 (量子色力学) は２つを合わせて素粒子のスタンダードモデル (SM) と呼ばれている。SM は大成功を収めている理論で、これまでのところ実験事実をよく説明している。しかしながら、幾つかの問題点や疑問点も含んでいる。ここでは、それらのうちの２つに注目した。

１つは、ヒッグス粒子が未発見の問題である。もう１つは、ゲージ階層性問題と呼ばれるものである。SM を越えるさらなる統一理論として、大統一理論 (GUT) が存在する。GUT では、SM に含まれるゲージ理論が、統一的に一つのゲージ対称性のもとで記述される。GWS モデルでは統一のエネルギースケールが 100GeV なのに対し、GUT では 10^{14}GeV と、12 桁もの違いがある。この大きな違いの起源は何なのかという問題が、ゲージ階層性問題とよばれるものである。この問題は、このように大きなエネルギースケールの間に何らかの物理があるのではないかという疑問にもつながる。

これらの問題を解く鍵として、電弱統一理論としての余剰次元ゲージ理論を紹介した。余剰次元を持つ理論を考えることにより、粒子の質量の起源が説明される。余剰次元ゲージ理論において、ゲージ場の余剰次元成分がヒッグス場の役目を果たすことで、ゲージ場の質量に説明がつく。またゲージ場の質量スペクトルの存在により、ゲージ階層性の疑問点が説明される。このヒッグス粒子が現れない電弱統一理論はヒッグスレス理論と呼ばれている。

電弱統一のエネルギースケールにより近いという意味での低エネルギー物理に興味をもっている。次元脱構築 (DD) の方法を用いた余剰次元ゲージ理論が考えられている。この方法は、ハーバードグループ [3] とフェルミラボグループ [4] でそれぞれ独立に導入された。余剰次元を離散化し、離散化具合をムースダイアグラム (MD) と呼ばれる図形に対応させて理論的枠組みを

記述する。低エネルギー物理に興味があるので、離散化度合いの高いスリーサイトモデル ($SU(2) \otimes [SU(2)] \otimes U(1)$) に注目した。

エネルギーの塊であるソリトン (モノポール、ボーテックスなど) にも興味を持っている。

DD で用いられる MD の応用にも興味を持っている。DD を用いたヒッグスレス理論おいては、MD によってゲージ場同士の相互作用の形が決まる。つまりは、MD により理論の枠組みを制限することができる。MD はサイトとリンクからなる図形である。グラフの言葉で言い替えれば、サイトは頂点、リンクは辺となる。辺に向き付けを加えたものを (有向) グラフと言い、向きを持たせることで理論をさらに制限することができる。このように、MD を一般のグラフに拡張することで、DD の応用としてグラフ上での場の理論が考えられる。

ヒッグスレス理論だけでなく、グラフ上で様々な場の理論を考えることができ、重力理論にも応用できる。

「デモクラティックスリーサイトモデル」

デモクラティック条件を課したスリーサイトモデルを考えた。この理論をデモクラティックスリーサイトモデルと呼ぶことにした。デモクラティックという言葉は、全てのゲージ場が同じ性質を持つという意味で用いた。まずは同じ性質をもつ $SU(2)$ ゲージ場を３つ用意した。次に、$[SU(2)]^3$ ゲージ理論がヒッグスメカニズムによって $[SU(2)]^2 \otimes U(1)$ に破れる過程を考えた。このとき、モノポールの配位が得られた。後は、次元脱構築の方法にある手続きを踏んだ。調査の結果、デモクラティック条件を課すと電弱理論についての実験結果との一致が難しいことが分かった。デモクラティックモデルは改良が必要である。

「グラフ上でのボーテックスと超場」

MD を一般のグラフに拡張するという意味で、DD の応用を試みた。グラフ上に超場を配置してボーテックスの存在条件を考えた。超場とは、ボソンとフェルミオンの入れ替えに対する対称性 (超対称性) を持つ場である。超対称性は、ゲージ階層性問題を解決する手法の 1 つとして知られている。頂点にベクトル超場を、辺にカイラル超場をのせた。そして、ボソン項だけを取り出した。すると、頂点にベクトル場 (ゲージ場)、辺にヒッグス場 (スカラー場) を置いたモデルが構成された。理論の持つゲージ対称性が $[U(1)]^p$ (p はグラフの頂点の数) から $U(1)$ に破れるような理論を考えた。ボーテックスの存在条件とグラフの形の関係を調べた。その結果、幾つかの簡単なグラフでボー

テックスが存在することが分かった。将来的には、各々のゲージ場の持つ対称性を $SU(2)$ に拡張することで、電弱統一理論に応用できると考えている。

Acknowledgements

This thesis is based on the collaboration with Kiyoshi Shiraishi. First of all, I express my best gratitude to him. He gave me fruitful discussion and warm advice everyday.

I am grateful to Jun-ichiro Hara, Masami Ashida, Takanao Asahi and Kenta Fujisawa. They encouraged and assisted me over years. Their supports made me possible to complete this thesis.

I am grateful to the members in Elementary Particle Theory and Cosmology Group in Yamaguchi University: Takayuki Suzuki, Syota Jinnouchi, Masato Tanoue, Kazuhiro Yoshimura and Hideto Manjyo for useful conversations and suggestions. I would like to thank Nahomi Kan, Ryo Takakura, Tatsuki Miyoshi, Teruki Hanada, Koichiro Sugiyama, Yasuo Higaki, Kazuhiko Shinoda, Takayuki Hayashino and Yuji Naramoto.

I am most grateful to my parents, Masakazu and Takami, my sister, Chihiro, and my brother, Yuji.

Contents

Chapter 1

Introduction and motivation

We introduce two novel models ("Democratic Three Site Higgsless Model" and "Vortices and Superfields on a Graph") that are based on the technique of Dimensional Deconstruction. The technique of discretizing the (extra-) dimension is called "Dimensional Deconstruction" (DD). We use this technique in the extra-dimension. We supposed the existence of the extra-dimension. In the (dimensionally) deconstructed theory, we use the moose diagram which denotes the theory framework (theory space).

We mention the reason why we consider the field theory in Dimensional Deconstruction and Graph Dimensional Deconstruction. We also mention the relation between the field and the moose diagram (or graph).

Electroweak Unified Theory

From ancient days, many people have been researching Nature. Nowadays, in the (elementary) particle physics, the Glashow-Weinberg-Salam (GWS) Model [1] is well known theory as the Electroweak (Unified) Theory. In this model, the symmetry of the gauge field $SU(2)_L \otimes U(1)_Y$ is spontaneously broken to the electromagnetic symmetry $U(1)_{em}$. In the process of symmetry breaking, some gauge fields become massive and the Higgs particle (a massive scalar particle) is produced. This mechanism is called the Higgs mechanism [2]. The GWS Model symmetry group $SU(2)_L \otimes U(1)_Y$ forms the electroweak gauge sector of the Standard Model (SM) of particle physics. The SM is the very successful theory, as decades of experiments have confirmed it predictions to a high level accuracy. Nevertheless there are some questions that have not been answered. We introduce two of them.

One is the missing Higgs particle problem. This is the problem that the existence of the Higgs particle has never observed. Therefore the Higgs particle is the missing piece of the GWS Model.

The other is the gauge hierarchy problem. As the further unification, there is the Grand Unified Theory (GUT). GUT (for example $SU(5)$ GUT) unifies both Electroweak Theory and Quantum Chromodynamics (the fundamental theory of the strong interactions). The unification energy scale of the GUT is about 10^{14} GeV. On the other hand, the unification energy scale of the Electroweak Theory is about 100 GeV. The gap of the order between these two unification energy scale is about 12. This large gap of the energy scale is enormous hierarchy. The gauge hierarchy problem is that what the origin of this enormous hierarchy is. Saying another way, why there is no physical object between these unification scale.

To solve these two problems, we introduce the extra-dimensional gauge theory of the Electroweak Theory. The extra-dimensional theory is known as Kaluza-Klein (KK) theory. We suppose the existence of the unobservable extra-dimension in this theory. The existence of the extra-dimension is the origin of the mass of particles. Imposing some boundary conditions on the extra-dimension, theories have the KK mode of the infinite mass spectrum. In this thesis, we have an interest in the five-dimensional gauge theory. The fifth-component of the gauge fields plays the role of the Higgs particle and the KK mode of the four-dimensional gauge fields explains the gauge hierarchy problem. The Electroweak Theory which does not need the Higgs mechanism, is called Higgsless Theory.

We are interested in the low energy scale physics, near the electroweak unified energy scale. We focus on the Higgsless Theory of the deconstructed five-dimensional gauge theory, especially Three Site Models of the highly deconstructed model.

In any case, the Large Hadron Collider (LHC) at CERN, as a proton-proton collider with center-of-mass energies up to 14 TeV, is designed to reach the energy scale of the electroweak symmetry breaking in hard proton scattering process. Thus the underlying dynamics are proved at the LHC.

Solitons

We are also interested in (topological) solitons, such as monopole and vortex. Soliton is studied by many authors [5]. Soliton means a solitary particle. Solitons are the particular classical solutions of the non-linear field equations. An important characteristic of soliton solutions is that they are localized and have finite-energy with a localized, non-dispersive energy density. Generally, they will travel undistorted in shape, with some uniform velocity. In that they are non-dispersive localized packets of energy moving uniformly, solitons resemble extended particles, even though they are solutions of non-linear wave equations. Elementary particles in nature are also localized packets of energy, and are furthermore believed to be described by some relativistic field theory. The field theories describ-

ing elementary particles are quantum theories, whereas the solitons are, to start with, solutions of classical field equations.

In 1974, G. 't Hooft [6] and A. M. Polyakov [7] showed the monopole which had the properties of the soliton. In the $SU(5)$ GUT, the monopole mass is $M \sim 10^{16}$ GeV. This is an enormous mass: therefore magnetic monopoles cannot be produced at any accelerators.

It is well known that the vortex solution can be found in the Abelian-Higgs model [8]. In many papers, the solution is used as a simple model for a cosmic string [9].

We think that topological configurations are a key ingredient in recent studies in theoretical physics.

Field Theory on a Graph - from a moose diagram to a graph

We have an interest in the application of the moose diagram. We try to generalize DD with the help of Graph Theory.

The moose diagram is a figure which consists of sites and links. In the Higgsless Theory (of the deconstructed extra-dimensional gauge theory), gauge fields live in each site and scalar fields live in each link. A connection between sites and links shows the interactions between fields. Therefore the shape of the moose diagram represents the theory space.

We generalize the relation between gauge fields and scalar fields in the context of graph theory. In the language of the graph theory, site corresponds to vertex and link corresponds to edge. Introducing the orientated edge, we have some variations of the connections between vertices. We can express the relation between gauge fields and scalar fields in a graph, which is just a complex moose. We wish to call this theory based on a graph as "Graph Dimensional Deconstruction" (GDD). The idea of GDD has already been published as [10] [11].

Many interesting results on graph theory have been found in the mathematical literature [12]. We introduce graph theoretical methods into DD. Especially, we find that Spectral Graph Theory analytically clarifies the theoretical structure of DD and mathematical theorems on a graph restrict physical quantity on deconstructed theories. We expect that rich and extensive content of Graph Theory produces useful results on DD.

Outline

We have four parts. The first part includes a review of the (dimensionally) deconstructed theory. The second part includes the three site model. The third part includes field theory on a graph. The last part includes summary, perspective and conclusion in this thesis.

In chapter 2 of part 1, we show the review of the deconstructed five-dimensional gauge theories.

Part 2 consists of two chapters, chapter 3 and chapter 4. In chapter 3, we review "the Original Three Site Higgsless Model". In chapter 4, we show "Democratic Three Site Higgsless Model".

In chapter 5 of part 3, we show "Vortices and Superfields on a Graph".

In chapter 6 of part 4, we mention summary, perspective and conclusion in this thesis.

In addition, in appendix A and B, we show some supplements.

Part I

Deconstructed Theory

Chapter 2

Dimensionally deconstructed theory

In this chapter, we show the deconstructed five-dimensional gauge theories. Dimensional Deconstruction (DD) is the technique of discretizing the dimension, this technique was introduced by Harvard group [3] and Fermi lab group [4] independently.

DD is based on the extra-dimensional theory which is imposed any boundary condition (or symmetry) on the extra-dimension. This extra-dimensional theory has the infinite Kaluza-Klein (KK) mode. DD is the technique of discretizing the (extra-) dimension. Deconstructing the extra-dimensional theory corresponds to introducing the cut-off in the theory. We use the technique of DD, the infinite KK mode becomes finite mode. The higher energy mode is cut off. Therefore we control the cut-off energy scale of the KK mode by DD.

2.1 Kaluza-Klein theory

At first, we suppose the existence of the extra-dimension. It is possible for additional spatial dimensions to be undetected by low energy experiments if the dimensions are curled up into a compact space of small volume. KK theory is the extra-dimensional theory. There are the ordinary three dimensional spaces and the extra-space. The number of dimensions is equal to

$$\text{time (1) + space (3) + unobservable extra-space (?)} = 4 + ?. \tag{2.1.1}$$

We think that the extra dimension is too small to observe as in Figure 2.1.

In the following, we consider the case that the extra space is equal to one. In other words, the following theory is described by the five-dimensional space-time.

There is a particle in the five-dimensional space-time. We denote the five-dimensional momentum p^N

$$p^N = (p^0, p^1, p^2, p^3, p^5), \tag{2.1.2}$$

Figure 2.1: This is the image of the rolled-up unobservable extra-dimension. When we view a line from a distance (the right figure), it looks like it has one dimension (along the length). But when we view the line up close (the left figure), we see that the surface has two dimensions (along the length and around it). We can observe only the right figure, but there is the rolled-up extra-dimension as in the left figure.

where $N = (\mu, 5)$, $\mu = (0, 1, 2, 3)$. For the five-dimensional massless particle, it is satisfied that

$$p_N p^N = p_\mu p^\mu + (p^5)^2 = 0. \tag{2.1.3}$$

This equation corresponds to

$$p_\mu p^\mu = -(p^5)^2. \tag{2.1.4}$$

Therefore the five-dimensional massless particle has the mass $M = |p^5|$ in the observable four-dimensional theory. Because we cannot observe the fifth-dimension, the fifth-dimensional momentum corresponds to the mass of the particle. Therefore the existence of the extra-dimension explains the origin of the mass of the particle. This is the important aspect of the extra-dimensional theory.

Kaluza-Klein mode

There is a field in the five-dimensional space-time. We define the five-dimensional space-time coordinate x^N

$$x^N = (x^0, x^1, x^2, x^3, x^5). \tag{2.1.5}$$

We prepare a five-dimensional field

$$\phi(x^N) = \phi(x^\mu, x^5). \tag{2.1.6}$$

We impose the following periodic boundary condition (as in Figure 2.2)

$$\phi(x^\mu, x^5 + 2\pi R) = \phi(x^\mu, x^5). \tag{2.1.7}$$

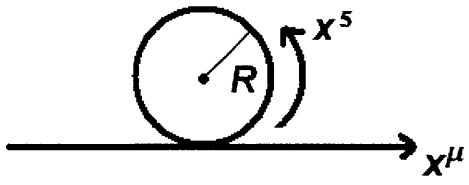

Figure 2.2: The fifth-dimensional space is compactified on a circle of radius R. This boundary condition is called S^1 symmetry.

Therefore the field $\phi(x^N)$ corresponds to

$$\phi(x^N) = \sum_{n=-\infty}^{n=+\infty} \Phi_n(x^\mu) e^{i\frac{n}{R}x^5}. \tag{2.1.8}$$

Each of mode which is identified by the integer number n is called the KK mode. The mass [1] of mode n is

$$M_n = |p^5| = \frac{|n|}{R}. \tag{2.1.9}$$

In the five-dimensional theory, when we impose some fifth-dimensional boundary condition, we get the effective theory. The effective theory is constructed by the four-dimensional theory part and KK mode part. By the fifth-dimensional boundary condition, the massless theory becomes the massive theory in the effective theory. Each mode n has the different mass as in Figure 2.3.

2.2 Five-dimensional gauge theory

We describe the five-dimensional gauge theory. We saw in the above section, the existence of the extra-dimension explains the origin of the mass. In this section, we apply this mechanism to the gauge theory.

We introduce a five-dimensional gauge field A^N,

$$A^N = (A^\mu, A^5). \tag{2.2.1}$$

Using this gauge field, we construct the five-dimensional massless Lagrangian

$$\mathcal{L}_5 = -\frac{1}{2}\mathrm{Tr}\, G_{MN}G^{MN}, \tag{2.2.2}$$

[1] It is satisfied that $(\partial^2 + M_n^2)\phi = 0$.

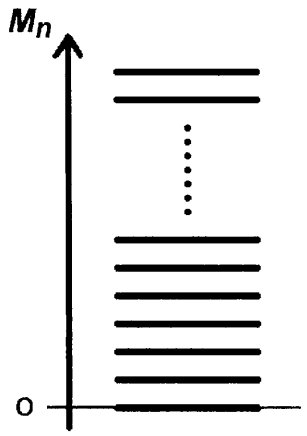

Figure 2.3: The mass is identified by n, $M_n = \frac{|n|}{R}$. The mass has the infinite spectrum.

where G_{MN} is the five-dimensional field strength of the gauge field A^N

$$G_{MN} = \partial_M A_N - \partial_N A_M - ig_5[A_M, A_N]. \tag{2.2.3}$$

g_5 is the coupling constant of the five-dimensional gauge field.

If we impose the some boundary condition, the theory gets the mass of the gauge field. For instance we impose the S^1/Z_2 symmetry (boundary condition) on the fifth-dimension in this theory. Therefore the fifth-dimensional space x^5 is restricted to $-\pi R \leq x^5 \leq \pi R$ and the gauge field satisfies the following conditions

$$\begin{aligned} A^\mu(x^\nu, x^5) &= +A^\mu(x^\nu, -x^5), \\ A^5(x^\nu, x^5) &= -A^5(x^\nu, -x^5). \end{aligned} \tag{2.2.4}$$

We can expand the gauge field as follows

$$\begin{aligned} A^\mu(x^\nu, x^5) &= \frac{1}{\sqrt{2\pi R}} A^{(0),\mu}(x^\nu) + \frac{1}{\sqrt{\pi R}} \sum_{n=1}^{\infty} A^{(n),\mu}(x^\nu) \cos\left(\frac{nx^5}{R}\right), \\ A^5(x^\nu, x^5) &= \frac{1}{\sqrt{\pi R}} \sum_{n=1}^{\infty} A^{(n),5}(x^\nu) \sin\left(\frac{nx^5}{R}\right). \end{aligned} \tag{2.2.5}$$

We separate the fifth-dimensional term from the above five-dimensional La-

grangian (2.2.2),

$$\begin{aligned}\mathcal{L}_5 &= -\frac{1}{2}\left[\mathrm{Tr}\, G_{\mu\nu}G^{\mu\nu} + \mathrm{Tr}\, G_{\mu 5}G^{\mu 5} + \mathrm{Tr}\, G_{5\mu}G^{5\mu} + \mathrm{Tr}\, G_{55}G^{55}\right] \\ &= -\frac{1}{2}\mathrm{Tr}\, G_{\mu\nu}G^{\mu\nu} - \mathrm{Tr}\, G_{\mu 5}G^{\mu 5} \\ &= -\frac{1}{2}\mathrm{Tr}\left\{\partial_\mu A_\nu - \partial_\nu A_\mu - ig_5[A_\mu, A_\nu]\right\}\left\{\partial^\mu A^\nu - \partial^\nu A^\mu - ig_5[A^\mu, A^\nu]\right\} \\ &\quad - \mathrm{Tr}\left\{\partial_\mu A_5 - \partial_5 A_\mu - ig_5[A_\mu, A_5]\right\}\left\{\partial^\mu A^5 - \partial^5 A^\mu - ig_5[A^\mu, A^5]\right\},\end{aligned} \tag{2.2.6}$$

where in the second line we used the anti-symmetric property of the field strength G^{MN}. To consider the kinetic and mass terms of the four-dimensional gauge field, we ignore interacting terms

$$\mathcal{L}_5 \sim -\frac{1}{2}\,\mathrm{Tr}\left\{\partial_\mu A_\nu - \partial_\nu A_\mu\right\}\left\{\partial^\mu A^\nu - \partial^\nu A^\mu\right\} - \mathrm{Tr}\left\{\partial_\mu A_5 - \partial_5 A_\mu\right\}\left\{\partial^\mu A^5 - \partial^5 A^\mu\right\}. \tag{2.2.7}$$

After some calculations we get the following result,

$$\begin{aligned}\mathcal{L}_5 \sim \mathrm{Tr}\Bigg[&\frac{1}{4\pi R}\left(\partial_\mu A_\nu^{(0)} - \partial_\nu A_\mu^{(0)}\right)^2 + \frac{1}{2\pi R}\sum_{n=1}^{\infty}\cos^2\left(\frac{nx^5}{R}\right)\left(\partial_\mu A_\nu^{(n)} - \partial_\nu A_\mu^{(n)}\right)^2 \\ &+ \frac{1}{\pi R}\sum_{n=1}^{\infty}\sin^2\left(\frac{nx^5}{R}\right)\left(\partial_\mu A_5^{(n)} + M_n A_\mu^{(n)}\right)^2\Bigg].\end{aligned} \tag{2.2.8}$$

Here we used the notation, $M_n = n/R$. The four-dimensional effective Lagrangian is obtained by integrating out the fifth-dimensional coordinate,

$$\begin{aligned}\mathcal{L}_{4-effective} &= \int_0^{2\pi R} dx_5 \mathcal{L}_5 \\ &\sim \mathrm{Tr}\left[\frac{1}{2}\left(\partial_\mu A_\nu^{(0)} - \partial_\nu A_\mu^{(0)}\right)^2 + \frac{1}{2}\sum_{n=1}^{\infty}\left(\partial_\mu A_\nu^{(n)} - \partial_\nu A_\mu^{(n)}\right)^2 + \sum_{n=1}^{\infty}\left(\partial_\mu A_5^{(n)} + M_n A_\mu^{(n)}\right)^2\right].\end{aligned} \tag{2.2.9}$$

Therefore the mass term of the four-dimensional gauge field $A_\mu^{(n)}$ is

$$M_n = \frac{n}{R}. \tag{2.2.10}$$

This mass term constructs the mass tower. As the consequence, the existence of the extra fifth-dimension is the origin of the mass.

We considered the five-dimensional gauge theory which has the arbitrary gauge field. For the later description we introduce two examples, $SU(2)_L \otimes SU(2)_R \otimes U(1)_{B-L}$ and $SU(2)$ gauge field theories. We show only boundary conditions in these theories.

The five-dimensional $SU(2)_L \otimes SU(2)_R \otimes U(1)_{B-L}$ gauge theory

The five-dimensional $SU(2)_L \otimes SU(2)_R \otimes U(1)_{B-L}$ gauge theory is showed in [13]. In this theory, the gauge symmetry is broken by boundary conditions. The symmetry breaking pattern and the mass spectrum resemble that in the Electroweak Theory of the SM.

We prepare the three types of the five-dimensional gauge field, $SU(2)_L$, $SU(2)_R$ and $U(1)_{B-L}$ gauge fields. We denote $SU(2)_L$, $SU(2)_R$ and $U(1)_{B-L}$ gauge fields as A_N^L, A_N^R and B_N^{B-L} respectively, in addition the gauge coupling of two $SU(2)$ fields as g_5 and $U(1)$ field $\tilde{g}_5$. We define the following identity,

$$A_N^{\pm} \equiv \frac{1}{\sqrt{2}}\left(A_N^L \pm A_N^R\right). \tag{2.2.11}$$

This five-dimensional $SU(2)_L \otimes SU(2)_R \otimes U(1)_{B-L}$ gauge theory is based on the Randall-Sundrum (RS) model [14]. The fifth-dimensional coordinate x^5 is on the interval $[R, R']$ (as in Figure 2.4). There exist branes in the fifth-dimension, the four-dimensional space exists on each brane. In RS-type models, R is typically $\sim 1/M_{Pl}{}^2$ and R' $\sim$TeV^{-1}. Therefore the brane which lies on $x^5 = R$ is called the Planck brane and $x^5 = R'$ the TeV brane. On the Planck brane, the $SU(2)_L \otimes SU(2)_R \otimes U(1)_{B-L}$ symmetry is broken down to $SU(2)_L \otimes U(1)_Y$ by the following boundary conditions,

$$\begin{aligned} &\partial_5 A_\mu^L = 0, \quad A_\mu^{R,(1,2)} = 0, \\ &\partial_5 \left(g_5 B_\mu + \tilde{g}_5 A_\mu^{R,3}\right) = 0, \\ &\tilde{g}_5 B_\mu - g_5 A_\mu^{R,3} = 0, \\ &A_5^L = 0, \quad A_5^R = 0, \quad B_5 = 0. \end{aligned} \tag{2.2.12}$$

The non zero fields are four-dimensional the $SU(2)_L$ field A_μ^L and the $U(1)_Y$ field $g_5 B_\mu + \tilde{g}_5 A_\mu^{R,3}$, and these two fields do not depend on the fifth-dimensional coordinate. In this brane, the $SU(2)_L \otimes U(1)_Y$ gauge field corresponds to the the gauge field of the GWS model. On the other hand, in the case of TeV brane, the $SU(2)_L \otimes SU(2)_R \otimes U(1)_{B-L}$ symmetry is broken down to $SU(2)_V \otimes U(1)_{B-L}$ by the following boundary conditions.

$$\begin{aligned} &\partial_5 A_\mu^+ = 0, \quad A_\mu^- = 0, \quad \partial_5 B_\mu = 0, \\ &A_5^+ = 0, \quad \partial_5 A_5^- = 0, \quad B_5 = 0. \end{aligned} \tag{2.2.13}$$

The non zero fields are the four-dimensional $SU(2)_V$ field A_μ^+, the $U(1)_{B-L}$ field B_μ and the fifth-dimensional field A_5^-, and these fields also do not depend on fifth-dimensional coordinate.

[2]The Planck mass is $M_{Pl} \sim 10^{19}$ GeV

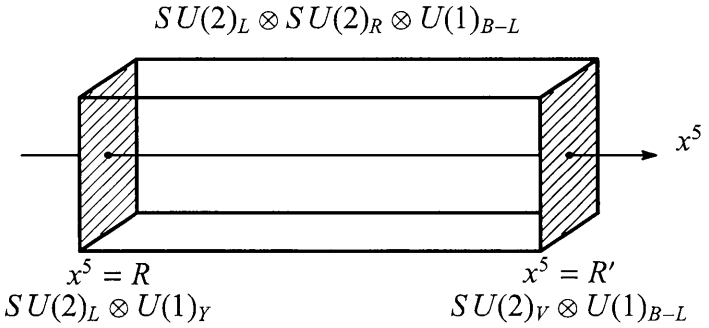

Figure 2.4: This is the shape of the five-dimensional $SU(2)_L \otimes SU(2)_R \otimes U(1)_{B-L}$ gauge theory. There exist branes in the fifth-dimension, the four-dimensional space exists on each brane. The above cuboid is consisted of infinite branes. We denote symmetries of the gauge field in each brane.

The five-dimensional $SU(2)$ gauge theory

We consider the five-dimensional $SU(2)$ gauge theory (as in Figure 2.5). As the boundary conditions we impose

$$\begin{aligned} &\partial_5 A_\mu^a = 0, \\ &A_5^a = 0, \end{aligned} \tag{2.2.14}$$

in the one brane ($x^5 = R$). In another brane ($x^5 = R'$), we impose

$$\begin{aligned} &A_\mu^{1,2} = 0, \\ &\partial_5 A_\mu^3, \\ &\partial_5 A_5^{1,2} = 0, \\ &A_5^3 = 0. \end{aligned} \tag{2.2.15}$$

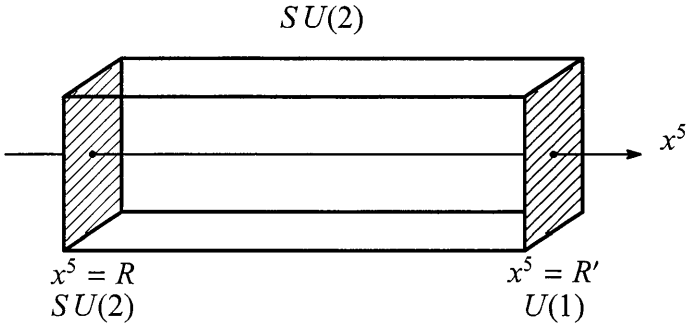

Figure 2.5: This is the shape of the five-dimensional $SU(2)$ gauge theory. This is the same type as Figure 2.4.

2.3 Dimensional Deconstruction

DD is the technique of discretizing the dimension, saying in other words DD is the reduction of the dimension to a finite point lattice (as in Figure 2.6). In five-dimensional theory, deconstructed five-dimensional space corresponds to a moose diagram (as in Figure 2.7). The moose diagram is a graph consisted of sites and links. The four-dimensional space-time (brane) lives in each site and sites are connected by links. From the moose diagram, we know that neighboring sites have interaction through the link.

In the five-dimensional theory, when we impose some boundary conditions on the fifth-dimension, the infinite KK mode appears. We use the technique of DD in this theory, the higher values of the infinite mass spectrum are cut off. The deconstructed theory has the finite mass spectrum (as in Figure 2.8).

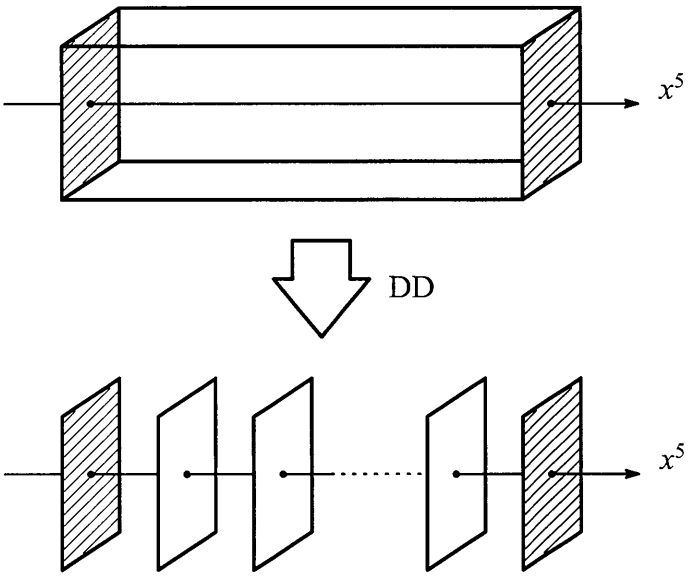

Figure 2.6: DD is the reduction of the dimension to a finite point lattice. Therefore the number of branes becomes finite.

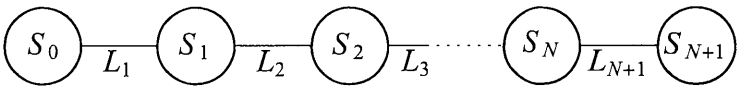

Figure 2.7: This is the moose diagram. S means a site and L means a link. The subscript is the label of each site and link.

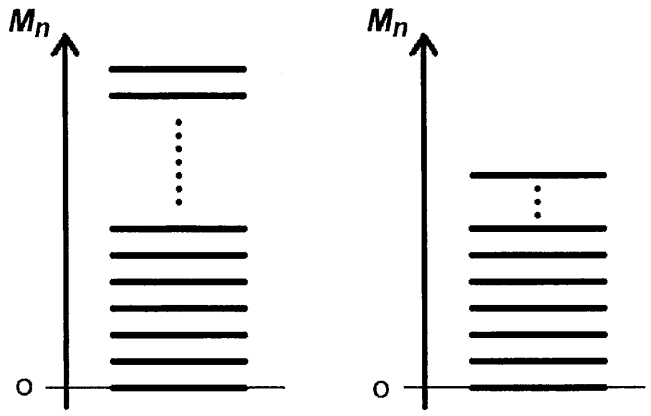

Figure 2.8: The left figure has the infinite mass spectrum and the right figure has the finite mass spectrum. In the right figure, we use the technique of the DD. Therefore the higher values of the infinite mass spectrum are cut off.

2.4 Deconstructed five-dimensional gauge theory

In this thesis, we consider the deconstructed five-dimensional gauge theory. Deconstructing the five-dimensional gauge theory, the fifth-dimension is discretized. Therefore the gauge fields A_μ at each position in the extra-dimension become independent gauge fields of a product gauge group in four-dimensions. The gauge fields that point along the fifth-dimension A_5 are reinterpreted as the Nambu-Goldstone boson fields of a non-linear sigma model, which break the gauge groups at neighboring sites of the discretized extra-dimension down to the diagonal. We represent the discretized model using the moose diagram.

2.4.1 $SU(2) \otimes [SU(2)]^N \otimes U(1)$ model

The discretized fifth-dimensional space corresponds to a moose diagram as in Figure 2.9. This moose diagram denotes the theory framework. This moose diagram is derived from the five-dimensional $SU(2)$ gauge field imposing some boundary conditions. The ordinary four-dimensional gauge fields live in each site (circle vertex), and the Nambu-Goldstone boson fields live in each link. There are the

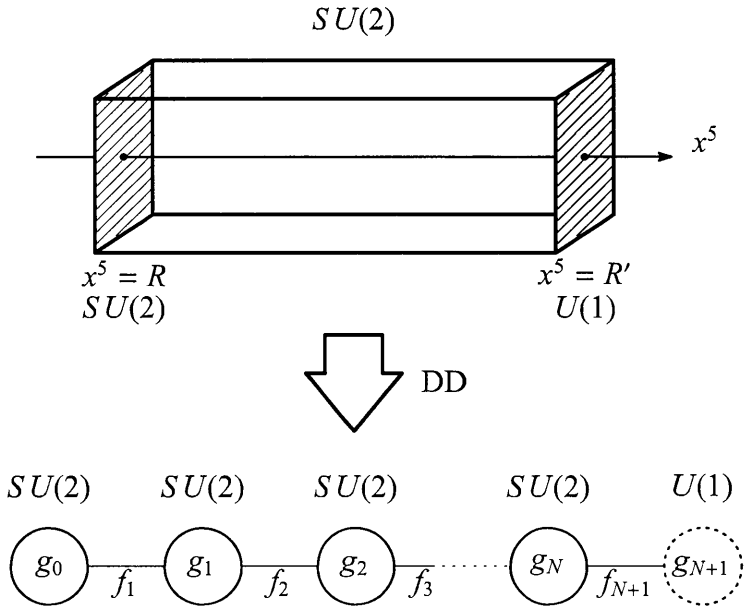

Figure 2.9: This moose diagram is based on the five-dimensional $SU(2)$ gauge theory. $U(1)$ gauge field is derived from $SU(2)$ gauge field which is imposed some boundary conditions.

four-dimensional gauge fields $A_{0\mu}$, $A_{1\mu}$, $\cdots$, $A_{N\mu}$ and B_μ in each site. $A_{I\mu}$ means the $SU(2)$ gauge field and B_μ means the $U(1)$ gauge field. The label I of $A_{I\mu}$ corresponds to the site number I. g_I is the gauge coupling constant of the $SU(2)$ gauge $A_{I\mu}$. Especially, g_{N+1} is the gauge coupling constant of the $U(1)$ gauge B_μ. Therefore the gauge group of this model is $[SU(2)]^{N+1} \otimes U(1)$. There are the Nambu-Goldstone boson fields of a non-linear sigma model Σ_1, Σ_2, $\cdots$, Σ_{N+1} in each link (edge). Σ_I has $(SU(2) \otimes SU(2))/SU(2)$ symmetry, and has the vacuum expectation value (VEV) f_I. For finite N, this model is four-dimensional theory, but for infinite N ($N \to \infty$), this model becomes the five-dimensional theory.

The Lagrangian of $SU(2) \otimes [SU(2)]^N \otimes U(1)$ model is

$$\mathcal{L} = -\frac{1}{2}\sum_{I=0}^{N} \mathrm{Tr}\, G_{I\mu\nu}G_I^{\mu\nu} - \frac{1}{4}F_{\mu\nu}F^{\mu\nu} - \sum_{I=1}^{N+1} \mathrm{Tr}\, \left|D_\mu \Sigma_I\right|^2 . \tag{2.4.1}$$

Here it is satisfied that

$$G_{I\mu\nu} = \partial_\mu A_{I\nu} - \partial_\nu A_{I\mu} - ig_I[A_{I\mu}, A_{I\nu}], \tag{2.4.2}$$

$$F_{\mu\nu} = \partial_\mu B_\nu - \partial_\nu B_\mu. \tag{2.4.3}$$

The non-linear sigma field is

$$\Sigma_I = f_I \exp\left(i\frac{\pi^a T^a}{f_I}\right), \tag{2.4.4}$$

where $\pi = \pi^a T^a$ is the Nambu-Goldstone boson field and T^a ($a = 1, 2, 3$) is the generator of the $SU(2)$ group. The covariant derivative of Σ_I is

$$\begin{aligned} D_\mu \Sigma_I &= \partial_\mu \Sigma_I - ig_{I-1}A_{I-1,\mu}\Sigma_I - ig_I \Sigma_I A_{I,\mu} \quad (1 \le I \le N), \\ D_\mu \Sigma_{N+1} &= \partial_\mu \Sigma_{N+1} - ig_N A_{N,\mu}\Sigma_{N+1} - ig_{N+1}\Sigma_{N+1}B_\mu T^3. \end{aligned} \tag{2.4.5}$$

The mechanism of the symmetry breaking is taking the unitary gauge. Therefore we regard Σ_I as f_I

$$\Sigma_I \to \frac{1}{f_I}{\Sigma_I}^\dagger \Sigma_I = f_I. \tag{2.4.6}$$

The covariant derivative term becomes

$$\begin{aligned}\sum_{I=1}^{N+1} \mathrm{Tr}\,\left|D_\mu \Sigma_I\right|^2 \to \sum_{I=1}^{N} \mathrm{Tr}\,\left(-ig_{I-1}A_{I-1,\mu}f_I - ig_I f_I A_{I,\mu}\right)^2 + \mathrm{Tr}\,\left(-ig_N A_{N,\mu} f_{N+1} - ig_{N+1}f_{N+1}B_\mu T^3\right)^2 \\ = -\frac{1}{2}\sum_{I=1}^{N} {f_I}^2\left(g_{I-1}A^1_{I-1,\mu} + g_I A^1_{I,\mu}\right)^2 - \frac{1}{2}{f_{N+1}}^2 {g_N}^2\left(A^1_{N,\mu}\right)^2 \\ - \frac{1}{2}\sum_{I=1}^{N} {f_I}^2\left(g_{I-1}A^2_{I-1,\mu} + g_I A^2_{I,\mu}\right)^2 - \frac{1}{2}{f_{N+1}}^2 {g_N}^2\left(A^2_{N,\mu}\right)^2 \\ - \frac{1}{2}\sum_{I=1}^{N} {f_I}^2\left(g_{I-1}A^3_{I-1,\mu} + g_I A^3_{I,\mu}\right)^2 - \frac{1}{2}{f_{N+1}}^2\left(g_N A^3_{N,\mu} - g_{N+1}B_\mu\right)^2 .\end{aligned} \tag{2.4.7}$$

This term involves the mass term of the gauge fields. We rewrite this mass term. In the $a = 1, 2$ case, we find

$$\begin{aligned}&\mathcal{L}_{mass\ term\ a=1,2} \\ &= -\frac{1}{2}\sum_{I=1}^{N} {f_I}^2\left(g_{I-1}A^{1,2}_{I-1,\mu} + g_I A^{1,2}_{I,\mu}\right)^2 - \frac{1}{2}{f_{N+1}}^2 {g_N}^2\left(A^{1,2}_{N,\mu}\right)^2 \\ &= -\frac{1}{2}\boldsymbol{A}^{1,2^T}(mass^{1,2})^2\boldsymbol{A}^{1,2},\end{aligned} \tag{2.4.8}$$

where it is satisfied that

$$\boldsymbol{A}^{1,2} = \begin{pmatrix} A^{1,2}_{0\mu} \\ A^{1,2}_{1\mu} \\ \vdots \\ A^{1,2}_{N-1,\mu} \\ A^{1,2}_{N,\mu} \end{pmatrix},$$

$$(mass^{1,2})^2 = \begin{pmatrix} {f_1}^2{g_0}^2 & -{f_1}^2 g_0 g_1 & & & & \\ -{f_1}^2 g_0 g_1 & ({f_1}^2 + {f_2}^2){g_1}^2 & -{f_2}^2 g_1 g_2 & & & \\ & & \ddots & & & \\ & & & -{f_{N-1}}^2 g_{N-2} g_{N-1} & ({f_{N-1}}^2 + {f_N}^2){g_{N-1}}^2 & -{f_N}^2 g_{N-1} g_N \\ & & & & -{f_N}^2 g_{N-1} g_N & ({f_N}^2 + {f_{N+1}}^2){g_N}^2 \end{pmatrix} \tag{2.4.9}$$

In the $a = 3$ case, we find

$$\begin{aligned}
&\mathcal{L}_{mass\ term\ a=3} \\
&= -\frac{1}{2}\sum_{I=1}^{N} f_I{}^2 \left(g_{I-1}A^3_{I-1,\mu} + g_I A^3_{I,\mu}\right)^2 - \frac{1}{2} f_{N+1}{}^2 \left(g_N A^3_{N,\mu} - g_{N+1}B_\mu\right)^2 \\
&= -\frac{1}{2} A^{3T} (mass^3)^2 A^3,
\end{aligned} \tag{2.4.10}$$

where it is satisfied that

$$A^3 = \begin{pmatrix} A^3_{0\mu} \\ A^3_{1\mu} \\ \vdots \\ A^3_{N-1,\mu} \\ A^3_{N,\mu} \\ B_\mu \end{pmatrix},$$

$$(mass^3)^2 = \begin{pmatrix} f_1{}^2 g_0{}^2 & -f_1{}^2 g_0 g_1 & & & & & \\ -f_1{}^2 g_0 g_1 & (f_1{}^2 + f_2{}^2) g_1{}^2 & -f_2{}^2 g_1 g_2 & & & & \\ & \ddots & & & & & \\ & & & -f_{N-1}{}^2 g_{N-2} g_{N-1} & (f_{N-1}{}^2 + f_N{}^2) g_{N-1}{}^2 & -f_N{}^2 g_{N-1} g_N & \\ & & & & -f_N{}^2 g_{N-1} g_N & (f_N{}^2 + f_{N+1}{}^2) g_N{}^2 & -f_{N+1}{}^2 g_N g_{N+1} \\ & & & & & -f_{N+1}{}^2 g_N g_{N+1} & f_{N+1}{}^2 g_{N+1}{}^2 \end{pmatrix}. \tag{2.4.11}$$

Here we call $(mass)^2$ the mass-squared matrix of the gauge field. We calculate the eigenvalue problem in this matrix. As the result, we get the mass-squared value and the state of the gauge fields. This mass is equal to the energy of the gauge field. Because we know $E = mc^2$ and use $c = 1$ of the natural units.

For simplicity, we examine the case

$$\begin{aligned} g_0 &= g_1 = \cdots = g_{N+1} = g, \\ f_1 &= f_2 = \cdots = f_{N+1} = f. \end{aligned} \tag{2.4.12}$$

Therefore the mass-squared matrix of $a = 1, 2$ becomes

$$(mass^{1,2})^2 = f^2 g^2 \begin{pmatrix} 1 & -1 & & & & \\ -1 & 2 & -1 & & & \\ & & \ddots & & & \\ & & & -1 & 2 & -1 \\ & & & & -1 & 2 \end{pmatrix}. \tag{2.4.13}$$

We define the matrix $(M^{1,2})^2$ as

$$(M^{1,2})^2 \equiv \frac{(mass^{1,2})^2}{g^2 f^2}. \tag{2.4.14}$$

We consider the eigenvalue of this $(N+1)\times(N+1)$ matrix. After some calculations, we get the eigenvalue

$$(E^{1,2})^2 = 4\sin^2\left(\frac{(2n+1)}{2(2N+3)}\pi\right), \quad (n = 0, 1, \cdots, N). \tag{2.4.15}$$

We consider the $a = 3$ case in the same way. The mass-squared matrix of $a = 3$ becomes

$$(mass^3)^2 = f^2g^2\begin{pmatrix} 1 & -1 & & & & & \\ -1 & 2 & -1 & & & & \\ & & \ddots & & & & \\ & & & -1 & 2 & -1 & \\ & & & & -1 & 2 & -1 \\ & & & & & -1 & 1 \end{pmatrix}. \tag{2.4.16}$$

We define the matrix $(M^3)^2$ as

$$(M^3)^2 \equiv \frac{(mass^3)^2}{g^2f^2}. \tag{2.4.17}$$

We consider the eigenvalue of this $(N+2)\times(N+2)$ matrix. After some calculations, we get the eigenvalue

$$(E^3)^2 = 4\sin^2\left(\frac{n\pi}{2(N+2)}\right), \quad (n = 0, 1, \cdots, N+1). \tag{2.4.18}$$

A Three Site Model - $SU(2)\otimes SU(2)\otimes U(1)$ model

Since we were interested in the low-energy scale physics, we consider A Three Site Model $N = 1$.

The mass-squared matrix of $a = 1, 2$ becomes

$$(mass^{1,2})^2 = f^2g^2\begin{pmatrix} 1 & -1 \\ -1 & 2 \end{pmatrix}. \tag{2.4.19}$$

We denote the matrix $(M^{1,2})^2$ as

$$(M^{1,2})^2 = \frac{(mass^{1,2})^2}{g^2f^2}. \tag{2.4.20}$$

We consider the eigenvalue of this 2×2 matrix. After some calculations, we get the eigenvalue

$$(E^{1,2})^2 = 4\sin^2\left(\frac{(2n+1)}{10}\pi\right), \quad (n = 0, 1). \tag{2.4.21}$$

The mass-squared matrix of $a = 3$ becomes

$$(mass^3)^2 = f^2 g^2 \begin{pmatrix} 1 & -1 & \\ -1 & 2 & -1 \\ & -1 & 1 \end{pmatrix}. \tag{2.4.22}$$

We denote the matrix $(M^3)^2$ as

$$(M^3)^2 = \frac{(mass^3)^2}{g^2 f^2}. \tag{2.4.23}$$

We consider the eigenvalue of this 3×3 matrix. After some calculations, we get the eigenvalue

$$(E^3)^2 = 4 \sin^2 \left(\frac{n\pi}{6} \right), \quad (n = 0, 1, 2). \tag{2.4.24}$$

2.5 Summary

We made mention of the (dimensionally) deconstructed five-dimensional gauge theories. The central content of this chapter was the mass terms of fields. The existence of the extra-dimensions is the origin of the mass of particles.

At first we studied the five-dimensional theory (section 2.1 and 2.2). We supposed the existence of the unobservable fifth-dimension. We imposed some boundary conditions on the fifth-dimension, the theory had KK mode which had the infinite mass spectrum.

DD is the technique of discretizing the dimension. In this thesis, we consider the deconstructed fifth-dimension. As in Figure 2.8, we introduced the cut-off in the infinite mass spectrum. Therefore we ignore the higher energy physics which is above the cut-off energy scale. This is the effect of DD.

In the deconstructed model, the moose diagram represents the theory framework. The moose diagram is a figure which consists of sites and links. In the Higgsless Theory, gauge fields (vector bosons) live in each site and scalar fields live in each link. A connection between sites and links shows the interactions between fields.

In section 2.4, we introduced the technique of DD to five-dimensional $SU(2)$ gauge theory. For simplicity, we examined the condition (2.4.12), the spectrum includes a massless state and many massive states. But under some appropriate conditions, the spectrum should include states identified with the photon (γ), W and Z bosons, and also finite tower of additional massive vector bosons (the higher KK excitations). Since we were interested in the low-energy scale physics, we focused on A Three Site Model.

Part II

Three Site Model

Chapter 3

The Original Three Site Higgsless Model

Recently, "Higgsless Theories" are eagerly studied by many authors. Higgsless Theory is the Electroweak Theory which does not include Higgs mechanism. In this chapter, we review "the Original Three Site Higgsless Model".

3.1 The Original Three Site Higgsless Model

We call the theory based on [15] "the Original Three Site Higgsless Model". This theory is the highly deconstructed model of the five-dimensional $SU(2)_L \otimes SU(2)_R \otimes U(1)_{B-L}$ gauge theory. Arbitrary deconstructed model of the five-dimensional $SU(2)_L \otimes SU(2)_R \otimes U(1)_{B-L}$ gauge theory is represented by the four-dimensional $SU(2)_L \otimes U(1)_Y \otimes [SU(2)_L \otimes SU(2)_R \otimes U(1)_{B-L}]^N \otimes SU(2)_V \otimes U(1)_{B-L}$ gauge theory, where N represents the ratio of the DD. In Figure 3.1, we show the moose diagram of this model. As the highly deconstructed model, there is the Original Three Site Higgsless Model $SU(2)_L \otimes SU(2)_V \otimes U(1)_Y$. In Figure 3.2, we show the moose diagram of this Three Site Model. This model is the low energy effective model of the five-dimensional $SU(2)_L \otimes SU(2)_R \otimes U(1)_{B-L}$ gauge theory. In the paper [15], "the Ideal Fermion Delocalization" is considered as the fermionic part.

3.1.1 The basic structure

The basic structure of the Original Three Site Model is the following. The moose diagram of this model is illustrated in Figure 3.3. This moose diagram is basically same as Figure 3.2 in the bosonic part. The gauge symmetry is $SU(2)_L \otimes SU(2)_V \otimes U(1)_Y$.

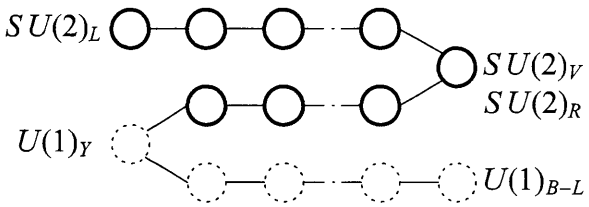

Figure 3.1: This is the moose diagram of the $SU(2)_L \otimes U(1)_Y \otimes [SU(2)_L \otimes SU(2)_R \otimes U(1)_{B-L}]^N \otimes SU(2)_V \otimes U(1)_{B-L}$ gauge theory.

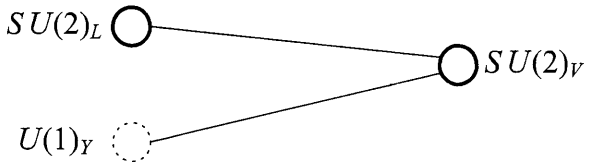

Figure 3.2: Reducing the lattice points (KK mode) as much as possible. Because we think it is enough to 1st KK mode for low energy physics.

The Lagrangian of the bosonic term is

$$\mathcal{L}_b = -\frac{1}{2}\mathrm{Tr}\, G_{0,\mu\nu}G_0^{\mu\nu} - \frac{1}{2}\mathrm{Tr}\, G_{1,\mu\nu}G_1^{\mu\nu} - \frac{1}{4}F_{\mu\nu}F^{\mu\nu} - \mathrm{Tr}\,|D_\mu\Sigma_1|^2 - \mathrm{Tr}\,|D_\mu\Sigma_2|^2. \quad (3.1.1)$$

Here it is satisfied that

$$G_{I\mu\nu} = \partial_\mu A_{I\nu} - \partial_\nu A_{I\mu} - ig_I[A_{I\mu}, A_{I\nu}], \quad (3.1.2)$$

$$F_{\mu\nu} = \partial_\mu B_\nu - \partial_\nu B_\mu. \quad (3.1.3)$$

The non-linear sigma field which connects neighboring gauge fields is

$$\Sigma_I = f_I \exp\left(i\frac{\pi^a T^a}{f_I}\right), \quad (3.1.4)$$

where $\pi = \pi^a T^a$ is the Nambu-Goldstone boson field. This sigma field Σ_I has $(SU(2) \otimes SU(2))/SU(2)$ symmetry. The covariant derivative of Σ_I is

$$\begin{aligned} D_\mu\Sigma_1 &= \partial_\mu\Sigma_1 - ig_0 A_{0,\mu}\Sigma_1 + ig_1\Sigma_1 A_{1,\mu}, \\ D_\mu\Sigma_2 &= \partial_\mu\Sigma_2 - ig_1 A_{1,\mu}\Sigma_2 + ig_2\Sigma_2 B_\mu T^3. \end{aligned} \quad (3.1.5)$$

The fermionic term includes three terms. They are the kinetic term, the Yukawa

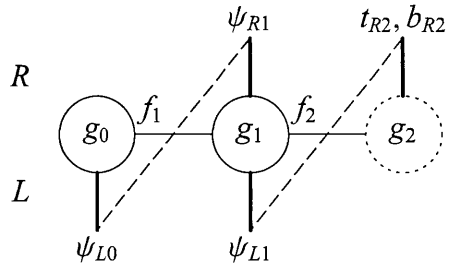

Figure 3.3: This is the moose diagram of the Original Three Site Higgsless Model. The solid circles represent $SU(2)$ gauge groups, with coupling constants g_0 and g_1, and the dashed circle is a $U(1)$ gauge group with coupling g_2. The left-handed fermions, denoted by the lower vertical lines, are located at sites 0 and 1, and the right-handed fermions, denoted by the upper vertical lines, at sites 1 and 2. The dashed lines correspond to Yukawa couplings, as described in the text. As discussed below, we will take $f_1 = f_2 = \sqrt{2}v$, and take $g_1 \gg g_0, g_1$.

coupling term and the Dirac mass term,

$$\begin{aligned}\mathcal{L}_f &= i\bar{\psi}_{L0}\not{D}_0\psi_{L0} + i\bar{\psi}_{L1}\not{D}_1\psi_{L1} + i\bar{\psi}_{R1}\not{D}_1\psi_{R1} + i\begin{pmatrix}\bar{u}_{R2} & \bar{d}_{R2}\end{pmatrix}\not{D}_2\begin{pmatrix}u_{R2}\\ d_{R2}\end{pmatrix} \\ &- \sqrt{2}v_1\lambda_1\left(\bar{\psi}_{R1}\psi_{L1} + \bar{\psi}_{L1}\psi_{R1}\right) - \lambda_{01}\left(\bar{\psi}_{L0}\Sigma_1\psi_{R1} + \bar{\psi}_{R1}\Sigma_1\psi_{L0}\right) \\ &- \left\{\bar{\psi}_{L1}\Sigma_2\begin{pmatrix}\lambda_u & \\ & \lambda_d\end{pmatrix}\begin{pmatrix}u_{R2}\\ d_{R2}\end{pmatrix} + \begin{pmatrix}\bar{u}_{R2} & \bar{d}_{R2}\end{pmatrix}\begin{pmatrix}\lambda_u & \\ & \lambda_d\end{pmatrix}\Sigma_2\psi_{L1}\right\}.\end{aligned} \tag{3.1.6}$$

Here it is satisfied that $\not{D} = \gamma^\mu D_\mu$,

$$\begin{aligned}D_{L0,\mu} &= \partial_\mu - ig_0A_{0,\mu} - ig_2Y_{0,f}B_\mu T^3, \\ D_{(LorR)1,\mu} &= \partial_\mu - ig_1A_{1,\mu} - ig_2Y_{1,f}B_\mu T^3, \\ D_{R2,\mu} &= \partial_\mu - ig_2Y_{2,f}B_\mu T^3.\end{aligned} \tag{3.1.7}$$

$Y_{I,f}$ is $U(1)$ charges of each site fermions. I denotes the site number $I = 0, 1, 2$ and f the fermion type. $Y_{(0or1),Q} = 1/6$, $Y_{(0or1),L} = -1/2$, $Y_{2,u} = 2/3$, $Y_{2,d} = -1/3$, $Y_{2,e} = -1$.

We take the VEV of two sigma fields as

$$f_1 = f_2 = \sqrt{2}v. \tag{3.1.8}$$

We impose the Ansatz on the gauge couplings

$$g_1 \gg g_0, g_2. \tag{3.1.9}$$

We define the ratio of the gauge coupling as following

$$\begin{aligned} x &\equiv g_0/g_1 \ll 1, \\ y &\equiv g_2/g_1 \ll 1. \end{aligned} \tag{3.1.10}$$

g_0 and g_2 are approximately equal to the SM-like $SU(2)_L$ and $U(1)_Y$ couplings. We define an angle θ

$$\frac{g_2}{g_0} = \frac{\sin\theta}{\cos\theta} = \tan\theta \equiv t. \tag{3.1.11}$$

In the fermionic mass contribution term, the Dirac mass contribution is much larger than the Yukawa coupling mass contributions

$$\lambda_1 \gg \lambda_{01}, \lambda_u, \lambda_d. \tag{3.1.12}$$

We define the ratio of the λ coupling constant as following

$$\begin{aligned} \varepsilon_L &\equiv \lambda_{01}/\lambda_1 = O(x) \ll 1, \\ \varepsilon_{uR,dR} &\equiv \lambda_{u,d}/\lambda_1 = O(x) \ll 1. \end{aligned} \tag{3.1.13}$$

Finally note that, treating the link fields as non-linear sigma models, the model as described here is properly considered a low-energy effective theory valid below a mass scale of order $4\pi\sqrt{2}v \simeq 4.3$ TeV. Another way of saying, the cut-off Λ should satisfy

$$\Lambda \lesssim 4\pi f_1 = 4\pi f_2 = 4\pi\sqrt{2}v = 4.3 \text{ TeV}. \tag{3.1.14}$$

3.1.2 The mass of the bosonic term

We choose the unitary gauge to fix the gauge, $\Sigma_I \to \sqrt{2}v$. Therefore the covariant derivative of Σ_I fields becomes

$$\begin{aligned} D_\mu\Sigma_1 &\to -ig_0A_{0,\mu}\sqrt{2}v + ig_1\sqrt{2}vA_{1,\mu} = -i\sqrt{2}vg_1\left(xA_{0,\mu} - A_{1,\mu}\right), \\ D_\mu\Sigma_2 &\to -ig_1A_{1,\mu}\sqrt{2}v + ig_2\sqrt{2}vB_\mu T^3 = -i\sqrt{2}vg_1\left(A_{1,\mu} - yB_\mu T^3\right). \end{aligned} \tag{3.1.15}$$

The mass term of the gauge field involved in the covariant derivative term of the Σ_I fields is

$$\begin{aligned} -\text{Tr}\,|D_\mu\Sigma_1|^2 - \text{Tr}\,|D_\mu\Sigma_2|^2 \to -\text{Tr}\,&\left|-i\sqrt{2}vg_1\left(xA_{0,\mu} - A_{1,\mu}\right)\right|^2 - \text{Tr}\,\left|-i\sqrt{2}vg_1\left(A_{1,\mu} - yB_\mu T^3\right)\right|^2 \\ &= -\frac{1}{2}2v^2{g_1}^2\left\{\left(xA^1_{0,\mu} - A^1_{1,\mu}\right)^2 + \left(A^1_{1,\mu}\right)^2\right\} \\ &\quad -\frac{1}{2}2v^2{g_1}^2\left\{\left(xA^2_{0,\mu} - A^2_{1,\mu}\right)^2 + \left(A^2_{1,\mu}\right)^2\right\} \\ &\quad -\frac{1}{2}2v^2{g_1}^2\left\{\left(xA^3_{0,\mu} - A^3_{1,\mu}\right)^2 + \left(A^3_{1,\mu} + yB_\mu\right)^2\right\}, \end{aligned} \tag{3.1.16}$$

where we separated the terms about the internal space $a = 1, 2, 3$. Rewriting these terms, we find

$$\mathcal{L}_{b,\ mass\ a=1,2} = -\frac{1}{2}\boldsymbol{A}^{1,2^T}(mass^{1,2})^2\boldsymbol{A}^{1,2}, \tag{3.1.17}$$

$$\mathcal{L}_{b,\ mass\ a=3} = -\frac{1}{2}\boldsymbol{A}^{3^T}(mass^{3})^2\boldsymbol{A}^{3}, \tag{3.1.18}$$

where it is satisfied that

$$\boldsymbol{A}^{1,2} = \begin{pmatrix} A^{1,2}_{0,\mu} \\ A^{1,2}_{1,\mu} \end{pmatrix}, \quad (mass^{1,2})^2 = 2v^2{g_1}^2\begin{pmatrix} x^2 & -x \\ -x & 2 \end{pmatrix}, \tag{3.1.19}$$

$$\boldsymbol{A}^{3} = \begin{pmatrix} A^{3}_{0,\mu} \\ A^{3}_{1,\mu} \\ B_{\mu} \end{pmatrix}, \quad (mass^{3})^2 = 2v^2{g_1}^2\begin{pmatrix} x^2 & -x & 0 \\ -x & 2 & -y \\ 0 & -y & y^2 \end{pmatrix}. \tag{3.1.20}$$

The mass of the charged bosons

The eq.(3.1.19) is related to charged gauge bosons. At first we will obtain the eigen value of the mass-squared matrix $(mass^{1,2})^2$ to get the mass values of these gauge fields. The eigen value of the matrix

$$M^{1,2} \equiv (mass^{1,2})^2/2v^2{g_1}^2 \tag{3.1.21}$$

is

$$\left(E^{1,2}\right)^2 = \frac{2 + x^2 \pm \sqrt{4 + x^2}}{2}. \tag{3.1.22}$$

The corresponding eigen states are $W^{1,2}_{\mu}$ and $W'^{1,2}_{\mu}$ which are elements of $\boldsymbol{W}^{1,2}$

$$\begin{aligned} \boldsymbol{W}^{1,2} &= \begin{pmatrix} W'^{1,2}_{\mu} \\ W^{1,2}_{\mu} \end{pmatrix} \\ &= \begin{pmatrix} v_{W',A^{1,2}_0} & v_{W',A^{1,2}_1} \\ v_{W,A^{1,2}_0} & v_{W,A^{1,2}_1} \end{pmatrix} \boldsymbol{A}^{1,2}, \end{aligned} \tag{3.1.23}$$

where $W'^{1,2}_{\mu}$ corresponds the eigen state of higher eigenvalue, and $W^{1,2}_{\mu}$ lower one. The squared mass of the gauge fields is

$$\left(m^{1,2}_{W,W'}\right)^2 = 2v^2{g_1}^2\left(E^{1,2}\right)^2. \tag{3.1.24}$$

We insert the eq.(3.1.22) into this equation and we expand for small x.

$$\begin{aligned} \left(m^{1,2}_{W}\right)^2 &= v^2{g_0}^2\left(1 - \frac{x^2}{4} + \frac{x^6}{64} + O(x^7)\right), \\ \left(m^{1,2}_{W'}\right)^2 &= 4v^2{g_1}^2\left(1 + \frac{x^2}{4} + \frac{x^4}{16} + O(x^7)\right). \end{aligned} \tag{3.1.25}$$

We define the N_W and $N_{W'}$ used in the normalization of the eigenstate,

$$\begin{aligned} N_W &= \left\{\left(-\frac{-2+x^2-\sqrt{4+x^4}}{2x}\right)^2+1^2\right\}^{1/2}, \\ N_{W'} &= \left\{\left(-\frac{-2+x^2+\sqrt{4+x^4}}{2x}\right)^2+1^2\right\}^{1/2}. \end{aligned} \tag{3.1.26}$$

The corresponding eigenstate of the W boson is

$$\begin{aligned} W_\mu^{1,2} &= \frac{1}{N_W}\left(-\frac{-2+x^2-\sqrt{4+x^4}}{2x}\right)A_{0,\mu}^{1,2}+\frac{1}{N_W}A_{1,\mu}^{1,2} \\ &= \left(1-\frac{x^2}{8}-\frac{5x^4}{128}+\frac{11x^6}{1024}+O(x^7)\right)A_{0,\mu}^{1,2}+\left(\frac{x}{2}+\frac{x^3}{16}-\frac{9x^5}{256}+O(x^7)\right)A_{1,\mu}^{1,2}. \end{aligned} \tag{3.1.27}$$

The corresponding eigenstate of the W' boson is

$$\begin{aligned} W_\mu'^{1,2} &= \frac{1}{N_{W'}}\left(-\frac{-2+x^2+\sqrt{4+x^4}}{2x}\right)A_{0,\mu}^{1,2}+\frac{1}{N_{W'}}A_{1,\mu}^{1,2} \\ &= \left(-\frac{x}{2}-\frac{x^3}{16}+\frac{9x^5}{256}+O(x^7)\right)A_{0,\mu}^{1,2}+\left(1-\frac{x^2}{8}-\frac{5x^4}{128}+\frac{11x^6}{1024}+O(x^7)\right)A_{1,\mu}^{1,2}. \end{aligned} \tag{3.1.28}$$

Primarily, the W boson state consists of the gauge boson at site 0 and the W' boson state consists of the gauge boson at site 1. It is satisfied that

$$\begin{aligned} \begin{pmatrix} v_{W',A_0^{1,2}} & v_{W',A_1^{1,2}} \\ v_{W,A_0^{1,2}} & v_{W,A_1^{1,2}} \end{pmatrix} &= \begin{pmatrix} \frac{1}{N_{W'}}\left(-\frac{-2+x^2+\sqrt{4+x^4}}{2x}\right) & \frac{1}{N_{W'}} \\ \frac{1}{N_W}\left(-\frac{-2+x^2-\sqrt{4+x^4}}{2x}\right) & \frac{1}{N_W} \end{pmatrix} \\ &= \begin{pmatrix} -\frac{x}{2}-\frac{x^3}{16}+\frac{9x^5}{256}+O(x^7) & 1-\frac{x^2}{8}-\frac{5x^4}{128}+\frac{11x^6}{1024}+O(x^7) \\ 1-\frac{x^2}{8}-\frac{5x^4}{128}+\frac{11x^6}{1024}+O(x^7) & \frac{x}{2}+\frac{x^3}{16}-\frac{9x^5}{256}+O(x^7) \end{pmatrix}. \end{aligned} \tag{3.1.29}$$

Comparing weak boson's masses $\left(m_{W,W'}^{1,2}\right)^2$ in eqs.(3.1.25), we find

$$\begin{aligned} \left(m_W^{1,2}\right)^2 / \left(m_{W'}^{1,2}\right)^2 &= \left(\frac{2+x^2-\sqrt{4+x^4}}{2}\right) \Big/ \left(\frac{2+x^2+\sqrt{4+x^4}}{2}\right) \\ &= \frac{x^2}{4}-\frac{x^4}{8}+\frac{x^6}{64}+O(x^7). \end{aligned} \tag{3.1.30}$$

The mass of the neutral bosons

The eq.(3.1.20) is related to neutral gauge bosons. This mass squared matrix contains two small parameters x, y. Therefore we use the t $(= y/x)$ parameter to expand about only small x parameter. Same as the case of charged gauge bosons, we will obtain the eigen value of the mass-squared matrix $(mass^3)^2$. The eigen value of the matrix

$$M^3 \equiv (mass^3)^2/2v^2{g_1}^2 = \begin{pmatrix} x^2 & -x & 0 \\ -x & 2 & -tx \\ 0 & -tx & t^2x^2 \end{pmatrix} \tag{3.1.31}$$

is

$$\left(E^3\right)^2 = 0, \quad \frac{2 + x^2 + t^2x^2 \pm \sqrt{4 + x^4 - 2t^2x^4 + t^4x^4}}{2}. \tag{3.1.32}$$

The corresponding eigen states are γ_μ, Z_μ and Z'_μ, are elements of $\boldsymbol{Z}$

$$\begin{aligned} \boldsymbol{Z} &= \begin{pmatrix} Z'_\mu \\ Z_\mu \\ \gamma_\mu \end{pmatrix} \\ &= \begin{pmatrix} v_{Z',A_0^3} & v_{Z',A_1^3} & v_{Z',B} \\ v_{Z,A_0^3} & v_{Z,A_1^3} & v_{Z,B} \\ v_{\gamma,A_0^3} & v_{\gamma,A_1^3} & v_{\gamma,B} \end{pmatrix} \boldsymbol{A}^3, \end{aligned} \tag{3.1.33}$$

where γ_μ corresponds the eigen state of the lowest eigen value, Z_μ middle one and Z'_μ the highest one. The squared mass of the neutral gauge field is

$$\left(m^3_{\gamma,Z,Z'}\right)^2 = 2v^2{g_1}^2\left(E^3\right)^2. \tag{3.1.34}$$

At first we show about the γ gauge boson. The γ gauge boson represents the massless photon which mediates the $U(1)_{em}$ electromagnetic force. The squared mass of the γ gauge boson is

$$\left(m^3_\gamma\right)^2 = 0. \tag{3.1.35}$$

The corresponding eigen state is

$$\gamma_\mu = \frac{t}{N_\gamma}A^3_{0,\mu} + \frac{tx}{N_\gamma}A^3_{1,\mu} + \frac{1}{N_\gamma}B_\mu, \tag{3.1.36}$$

where N_γ satisfies

$$N_\gamma = \left\{t^2 + t^2x^2 + 1^2\right\}^{1/2}. \tag{3.1.37}$$

We rewrite γ_μ as

$$\gamma_\mu = \frac{e}{g_0} A^3_{0,\mu} + \frac{e}{g_1} A^3_{1,\mu} + \frac{e}{g_2} B_\mu. \tag{3.1.38}$$

The electric charge e satisfies

$$\frac{1}{e^2} = \frac{1}{{g_0}^2} + \frac{1}{{g_1}^2} + \frac{1}{{g_2}^2}. \tag{3.1.39}$$

We show the mass and state about Z and Z' gauge bosons. These gauge bosons represent the massive weak bosons which mediate the weak forces. The squared mass of the Z and Z' gauge bosons are

$$\begin{aligned}
\left(m^3_Z\right)^2 &= 2v^2{g_0}^2\left(\frac{g_1}{g_0}\right)^2 \frac{2 + x^2 + t^2x^2 - \sqrt{4 + x^4 - 2t^2x^4 + t^4x^4}}{2} \\
&= v^2{g_0}^2 \frac{2 + x^2 + t^2x^2 - \sqrt{4 + x^4 - 2t^2x^4 + t^4x^4}}{x^2} \\
&= v^2{g_0}^2 \left\{\left(1 + t^2\right) - \frac{1}{4}\left(1 - t^2\right)^2 x^4 + \frac{1}{64}\left(1 - t^2\right)^4 x^6 + O(x^7)\right\} \\
&= \frac{v^2{g_0}^2}{c^2}\left\{1 - \frac{c^2\left(1 - t^2\right)^2}{4}x^4 + \frac{c^2\left(1 - t^2\right)^4}{64}x^6 + O(x^7)\right\} \\
&= \frac{v^2{g_0}^2}{c^2}\left\{1 - \frac{\left(c^2 - s^2\right)^2}{4c^2}x^4 + \frac{\left(c^2 - s^2\right)^4}{64c^6}x^6 + O(x^7)\right\},
\end{aligned} \tag{3.1.40}$$

$$\begin{aligned}
\left(m^3_{Z'}\right)^2 &= 2v^2{g_1}^2 \frac{2 + x^2 + t^2x^2 + \sqrt{4 + x^4 - 2t^2x^4 + t^4x^4}}{2} \\
&= v^2{g_1}^2\left\{4 + \left(1 + t^2\right)x^2 + \frac{1}{4}\left(1 - t^2\right)^2 x^4 + O(x^7)\right\} \\
&= 4v^2{g_1}^2\left\{1 + \frac{1}{4c^2}x^2 + \frac{\left(1 - t^2\right)^2}{16}x^4 + O(x^7)\right\}.
\end{aligned} \tag{3.1.41}$$

The corresponding eigen states of Z and Z' are

$$Z_\mu = v_{Z,A^3_0} A^3_{0,\mu} + v_{Z,A^3_1} A^3_{1,\mu} + v_{Z,B} B_\mu, \tag{3.1.42}$$

$$Z'_\mu = v_{Z',A^3_0} A^3_{0,\mu} + v_{Z',A^3_1} A^3_{1,\mu} + v_{Z',B} B_\mu. \tag{3.1.43}$$

Here it is satisfied that

$$\begin{aligned} v_{Z,A_0^3} &= a_Z/N_Z,\ \ v_{Z,A_1^3} = b_Z/N_Z,\ \ v_{Z,B} = c_Z/N_Z, \\ N_Z &= \left(a_Z{}^2 + b_Z{}^2 + c_Z{}^2\right)^{1/2}, \\ a_Z &= -\frac{-x^2 + t^2x^2 + \sqrt{4 + x^4 - 2t^2x^4 + t^4x^4}}{2t}, \\ b_Z &= -\frac{2 + x^2 - t^2x^2 - \sqrt{4 + x^4 - 2t^2x^4 + t^4x^4}}{2tx}, \\ c_Z &= 1, \end{aligned} \tag{3.1.44}$$

and

$$\begin{aligned} v_{Z',A_0^3} &= a_{Z'}/N_{Z'},\ \ v_{Z',A_1^3} = b_{Z'}/N_{Z'},\ \ v_{Z',B} = c_{Z'}/N_{Z'}, \\ N_{Z'} &= \left(a_{Z'}{}^2 + b_{Z'}{}^2 + c_{Z'}{}^2\right)^{1/2}, \\ a_{Z'} &= -\frac{-x^2 + t^2x^2 - \sqrt{4 + x^4 - 2t^2x^4 + t^4x^4}}{2t}, \\ b_{Z'} &= -\frac{2 + x^2 - t^2x^2 + \sqrt{4 + x^4 - 2t^2x^4 + t^4x^4}}{2tx}, \\ c_{Z'} &= 1. \end{aligned} \tag{3.1.45}$$

We expand coefficients $v_{Z,A_0^3}, \cdots, v_{Z',B}$ about x, we use the following notation $t = s/c \equiv \sin\theta/\cos\theta$.

$$\begin{aligned} v_{Z,A_0^3} &= -c + O(x^2), \\ v_{Z,A_1^3} &= \frac{c(-1 + t^2)}{2}x + O(x^3), \\ v_{Z,B} &= s - \frac{sc^2(-3 + 2t^2 + t^4)}{8}x^2 + O(x^4), \\ v_{Z',A_0^3} &= \frac{x}{2} + \frac{1 - 3t^2}{16}x^3 + O(x^5), \\ v_{Z',A_1^3} &= -1 + \frac{1 + t^2}{8}x^2 + O(x^4), \\ v_{Z',B} &= \frac{t}{2}x - \frac{(3 - t^2)t}{16}x^3 + O(x^5). \end{aligned} \tag{3.1.46}$$

3.1.3 The mass of the fermionic term

We rewrite the fermionic term in the Lagrangian.

$$\begin{aligned}\mathcal{L}_f = {} & i\begin{pmatrix}\bar{\psi}_{L0} & \bar{\psi}_{L1}\end{pmatrix}\begin{pmatrix}\not{D}_0 & \\ & \not{D}_1\end{pmatrix}\begin{pmatrix}\psi_{L0}\\ \psi_{L1}\end{pmatrix} + i\begin{pmatrix}\bar{\psi}_{R1}\\ \bar{\psi}_{uR,dR}\end{pmatrix}\begin{pmatrix}\not{D}_1 & \\ & \not{D}_2\end{pmatrix}\begin{pmatrix}\psi_{R1}\\ \psi_{uR,dR}\end{pmatrix} \\ & - \sqrt{2}v\lambda_1\begin{pmatrix}\bar{\psi}_{L0} & \bar{\psi}_{L1}\end{pmatrix}\begin{pmatrix}\frac{\varepsilon_L\Sigma_1}{\sqrt{2}v} & 0\\ 1 & \frac{\varepsilon_{uR,dR}\Sigma_2}{\sqrt{2}v}\end{pmatrix}\begin{pmatrix}\psi_{R1}\\ \psi_{uR,dR}\end{pmatrix} - \sqrt{2}v\lambda_1\begin{pmatrix}\bar{\psi}_{R1} & \bar{\psi}_{uR,dR}\end{pmatrix}\begin{pmatrix}\frac{\varepsilon_L\Sigma_1}{\sqrt{2}v} & 1\\ 0 & \frac{\varepsilon_{uR,dR}\Sigma_2}{\sqrt{2}v}\end{pmatrix}\begin{pmatrix}\psi_{L0}\\ \psi_{L1}\end{pmatrix},\end{aligned} \tag{3.1.47}$$

where we use the following notation

$$\psi_{uR,dR} \equiv \begin{pmatrix}u_{R2}\\ d_{R2}\end{pmatrix}, \quad \varepsilon_{uR,dR} \equiv \begin{pmatrix}\varepsilon_{uR} & \\ & \varepsilon_{dR}\end{pmatrix}. \tag{3.1.48}$$

We use the useful notation

$$\begin{aligned}&\psi_L \equiv \begin{pmatrix}\psi_{L0}\\ \psi_{L1}\end{pmatrix}, \quad \psi_R \equiv \begin{pmatrix}\psi_{R1}\\ \psi_{uR,dR}\end{pmatrix}, \\ &\not{D}_{01} \equiv \begin{pmatrix}\not{D}_0 & \\ & \not{D}_1\end{pmatrix}, \quad \not{D}_{12} \equiv \begin{pmatrix}\not{D}_1 & \\ & \not{D}_2\end{pmatrix}, \quad M_{u,d,\Sigma_{1,2}} \equiv \sqrt{2}v\lambda_1\begin{pmatrix}\frac{\varepsilon_L\Sigma_1}{\sqrt{2}v} & 0\\ 1 & \frac{\varepsilon_{uR,dR}\Sigma_2}{\sqrt{2}v}\end{pmatrix}.\end{aligned} \tag{3.1.49}$$

Therefore the fermionic term becomes

$$\mathcal{L}_f = i\bar{\psi}_L\not{D}_{01}\psi_L + \bar{\psi}_R\not{D}_{12}\psi_R - \bar{\psi}_L M_{u,d,\Sigma_{1,2}}\psi_R - \bar{\psi}_R M^{\dagger}_{u,d,\Sigma_{1,2}}\psi_L. \tag{3.1.50}$$

We take the VEV of the $\Sigma_{1,2}$ fields, $\Sigma_{1,2} \to \sqrt{2}v$. Therefore the matrix becomes $M_{u,d,\Sigma_{1,2}} \to M_{u,d}$, where it is satisfied that

$$M_{u,d} = \sqrt{2}v\lambda_1\begin{pmatrix}\varepsilon_L & 0\\ 1 & \varepsilon_{uR,dR}\end{pmatrix} \equiv \begin{pmatrix}m_L & 0\\ m & m_{uR,dR}\end{pmatrix}. \tag{3.1.51}$$

After some calculations about the fermionic part of the Lagrangian, we get the two Klein-Gordon type equations

$$\begin{aligned}\left(\partial^2 + M_{u,d}M^{\dagger}_{u,d}\right)\psi_L = 0,\\ \left(\partial^2 + M^{\dagger}_{u,d}M_{u,d}\right)\psi_R = 0,\end{aligned} \tag{3.1.52}$$

where we neglected the interaction terms included in the covariant derivatives. We obtain the mass squared values as the eigen values of the matrices $M_{u,d}M^{\dagger}_{u,d}$ and $M^{\dagger}_{u,d}M_{u,d}$.

In the case of the matrix $M_{u,d}M_{u,d}^{\dagger}$, the eigen value is

$$\left(m_{fL}\right)^2 = \frac{{m_L}^2 + m^2 + {m_{uR,dR}}^2 \pm \sqrt{-4{m_L}^2{m_{uR,dR}}^2 + \left({m_L}^2 + m^2 + {m_{uR,dR}}^2\right)^2}}{2}. \tag{3.1.53}$$

The corresponding eigen states of light and heavy left-handed fermions ψ_{Lfl} and ψ_{Lfh} are

$$\begin{aligned} \psi_{Lfl} &= v_{Lfl,L0}\psi_{L0} + v_{Lfl,L1}\psi_{L1}, \\ \psi_{Lfh} &= v_{Lfh,L0}\psi_{L0} + v_{Lfh,L1}\psi_{L1}. \end{aligned} \tag{3.1.54}$$

Here it is satisfied that

$$\begin{aligned} &v_{Lfl,L0} = a_{Lfl}/N_{Lfl}, \quad v_{Lfl,L1} = b_{Lfl}/N_{Lfl}, \\ &N_{Lfl} = \left({a_{Lfl}}^2 + {b_{Lfl}}^2\right)^{1/2}, \\ &a_{Lfl} = -\frac{-{m_L}^2 + m^2 + {m_{uR,dR}}^2 + \sqrt{-4{m_L}^2{m_{uR,dR}}^2 + \left({m_L}^2 + m^2 + {m_{uR,dR}}^2\right)^2}}{2m_L m}, \\ &b_{Lfl} = 1, \end{aligned} \tag{3.1.55}$$

and

$$\begin{aligned} &v_{Lfh,L0} = a_{Lfh}/N_{Lfh}, \quad v_{Lfh,L1} = b_{Lfh}/N_{Lfh}, \\ &N_{Lfh} = \left({a_{Lfh}}^2 + {b_{Lfh}}^2\right)^{1/2}, \\ &a_{Lfh} = -\frac{-{m_L}^2 + m^2 + {m_{uR,dR}}^2 - \sqrt{-4{m_L}^2{m_{uR,dR}}^2 + \left({m_L}^2 + m^2 + {m_{uR,dR}}^2\right)^2}}{2m_L m}, \\ &b_{Lfh} = 1. \end{aligned} \tag{3.1.56}$$

In the case of the matrix $M_{u,d}^{\dagger}M_{u,d}$, the eigen value is

$$\left(m_{fR}\right)^2 = \frac{{m_L}^2 + m^2 + {m_{uR,dR}}^2 \pm \sqrt{-4{m_L}^2{m_{uR,dR}}^2 + \left({m_L}^2 + m^2 + {m_{uR,dR}}^2\right)^2}}{2}. \tag{3.1.57}$$

The corresponding eigen states of light and heavy right-handed fermions ψ_{Lfl} and ψ_{Lfh} are

$$\begin{aligned} \psi_{Rfl} &= v_{Rfl,R1}\psi_{R1} + v_{Rfl,R2}\psi_{R2}, \\ \psi_{Rfh} &= v_{Rfh,R1}\psi_{R1} + v_{Rfh,R2}\psi_{R2}. \end{aligned} \tag{3.1.58}$$

Here it is satisfied that

$$\begin{aligned} v_{Rfl,R1} &= a_{Rfl}/N_{Rfl}, \quad v_{Rfl,R2} = b_{Rfl}/N_{Rfl}, \\ N_{Rfl} &= \left(a_{Rfl}{}^2 + b_{Rfl}{}^2\right)^{1/2}, \\ a_{Rfl} &= -\frac{-m_L{}^2 - m^2 + m_{uR,dR}{}^2 + \sqrt{-4m_L{}^2 m_{uR,dR}{}^2 + (m_L{}^2 + m^2 + m_{uR,dR}{}^2)^2}}{2mm_{uR,dR}}, \\ b_{Rfl} &= 1, \end{aligned} \tag{3.1.59}$$

and

$$\begin{aligned} v_{Rfh,R1} &= a_{Rfh}/N_{Rfh}, \quad v_{Rfh,R2} = b_{Rfh}/N_{Rfh}, \\ N_{Rfh} &= \left(a_{Rfh}{}^2 + b_{Rfh}{}^2\right)^{1/2}, \\ a_{Rfh} &= -\frac{-m_L{}^2 - m^2 + m_{uR,dR}{}^2 - \sqrt{-4m_L{}^2 m_{uR,dR}{}^2 + (m_L{}^2 + m^2 + m_{uR,dR}{}^2)^2}}{2mm_{uR,dR}}, \\ b_{Rfh} &= 1. \end{aligned} \tag{3.1.60}$$

The Ideal Fermion Delocalization

The idea of the Ideal Fermion Delocalization is discussed in [16]. The main point of this idea is that it is possible to minimize precision electroweak corrections due to the light fermions by appropriate (" Ideal ") Delocalization of the light fermions along the moose. At site $I = 0, 1$, for the left-handed light fermion, we require the couplings and eigenstates of the ideally delocalized fermion and the W boson to be related as

$$\begin{aligned} g_0(v_{Lfl,L0})^2 &= g_W v_{W,A_0^{1,2}}, \\ g_1(v_{Lfl,L1})^2 &= g_W v_{W,A_1^{1,2}}. \end{aligned} \tag{3.1.61}$$

Therefore the following condition is imposed,

$$\frac{g_0(v_{Lfl,L0})^2}{g_1(v_{Lfl,L1})^2} = \frac{v_{W,A_0^{1,2}}}{v_{W,A_1^{1,2}}}. \tag{3.1.62}$$

3.2 Summary

We reviewed the Original Three Site Higgsless Model in section 3.1. This theory is highly deconstructed model of the five-dimensional $SU(2)_L \otimes SU(2)_R \otimes U(1)_{B-L}$ gauge theory. For the bosonic part, this model includes the photon, the nearly-standard light W and Z, the heavier W' and Z'. For the fermionic part, includes a set of SM-like fermions and heavy copies of those fermions. We implemented the Ideal Delocalization for light fermions.

Chapter 4

Democratic Three Site Higgsless Model

We are interested in the Three Site Model which has $[SU(2)]^2 \otimes U(1)$ gauge symmetry. In this chapter, we consider $[SU(2)]^2 \otimes U(1)$ symmetric gauge it is taken from $[SU(2)]^3$ broken by [effective] adjoint scalar. In general, "Democratic" means "having or supporting equality for all members". We use this word "Democratic" as the following that each $SU(2)$ gauge field is equivalent in the $[SU(2)]^3$ symmetric Three Site Model. We call the "Democratic Condition" that each gauge field has same coupling constant.

4.1 Model building

4.1.1 The basic structure

The basic structure of the Democratic Three Site Higgsless Model is the following. The moose diagram of this model is illustrated in Figure 4.1.

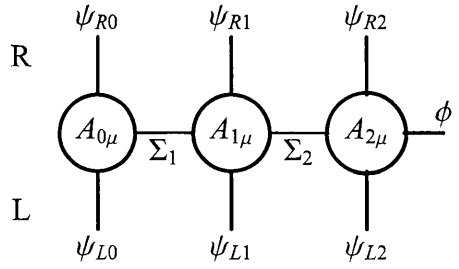

Figure 4.1: This is the moose diagram of the Democratic Three Site Higgsless Model. The solid circles represent $SU(2)$ gauge groups, with coupling constants g_0, g_1 and g_2. The left-handed fermions, denoted by the lower vertical lines, and the right-handed fermions, denoted by the upper vertical lines, at sites 0, 1 and 2. We omit the dashed lines of Yukawa couplings to avoid becoming complex. The rightmost parallel line is the scalar field of the Higgs field which relates to the site 2.

For simplicity, we show the bosonic part of the moose diagram in Figure 4.2. In the beginning, we prepare the $[SU(2)]^3$ symmetric gauge. If the $SU(2)$ gauge symmetry is spontaneously broken to $U(1)$ by the Higgs mechanism, then there are monopole solutions. Therefore $[SU(2)]^3$ gauge symmetry is spontaneously broken to $[SU(2)]^2 \otimes U(1)$, there are monopole solutions in the Three Site Higgsless Model. We have some difference points between Original Three Site Higgsless Model and this model. The bosonic part of given Lagrangian is

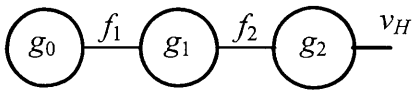

Figure 4.2: This moose diagram is the bosonic part of the Democratic Three Site Model.

$$\mathcal{L}_b = -\frac{1}{2}\sum_{I=0}^{2} \mathrm{Tr}\, G_{I\mu\nu}G_I^{\mu\nu} - \sum_{I=1}^{2} \mathrm{Tr}\left(D_\mu \Sigma_I\right)^\dagger (D^\mu \Sigma_I) - \mathrm{Tr}\left(D_\mu \phi\right)^\dagger (D^\mu \phi) - U(\phi), \tag{4.1.1}$$

where they are satisfied that

$$G_{I\mu\nu} \equiv \partial_\mu A_{I\nu} - \partial_\nu A_{I\mu} - ig_I \left[A_{I\mu}, A_{I\nu}\right], \tag{4.1.2}$$

$$D_\mu \Sigma_I \equiv \partial_\mu \Sigma_I - ig_{I-1} A_{I-1,\mu} \Sigma_I + ig_I \Sigma A_{I,\mu}, \tag{4.1.3}$$

$$D_\mu \phi \equiv \partial_\mu \phi - ig_2 \left[A_{2\mu}, \phi\right]. \tag{4.1.4}$$

The gauge field $A_{I\mu}$ exists on the site S_I ($I = 0, 1, 2$). The field strength of the gauge field $A_{I\mu}$ is $G_{I\mu\nu}$. The non-linear sigma field Σ_J exists on the link L_J ($J = 1, 2$). This sigma field connects the gauge fields at neighboring sites. The covariant derivative of this sigma field is $D_\mu \Sigma_I$. The Higgs field ϕ exists on the site v_2. This field is coupled to the gauge field $A_{I=2,\mu}$.

$$U(\phi) \equiv \frac{1}{4}\lambda \left(2\,\mathrm{Tr}\phi\phi - {v_H}^2\right)^2 \tag{4.1.5}$$

is the scalar potential in this model.

We denote the fermionic term using the doublet of quarks and leptons,

$$\psi = \begin{pmatrix} q_u \\ q_d \end{pmatrix}, \quad \text{or} \quad \psi = \begin{pmatrix} \nu_e \\ e \end{pmatrix}. \tag{4.1.6}$$

There are six types of fermions, the left-handed fermions are ψ_{L0}, ψ_{L1} and ψ_{L2}, the right-handed fermions are ψ_{R0}, ψ_{R1} and ψ_{R2}. The kinetic term of the fermion is

$$\mathcal{L}_{f-k} = i\bar{\psi}_{L0}\not{D}_0\psi_{L0} + i\bar{\psi}_{R0}\not{D}_0\psi_{R0} + i\bar{\psi}_{L1}\not{D}_1\psi_{L1} + i\bar{\psi}_{R1}\not{D}_1\psi_{R1} + i\bar{\psi}_{L2}\not{D}_2\psi_{L2} + i\bar{\psi}_{R2}\not{D}_2\psi_{R2}. \tag{4.1.7}$$

Here we used the notation $\not{D} = \gamma^\mu D_\mu$,

$$\begin{aligned} D_{0,\mu} &= \partial_\mu - ig_0 A_{0\mu} - ig_2 Y_{0,f} B_\mu T^3, \\ D_{1,\mu} &= \partial_\mu - ig_1 A_{1\mu} - ig_2 Y_{1,f} B_\mu T^3, \\ D_{2,\mu} &= \partial_\mu - ig_2 Y_{2,f} B_\mu T^3. \end{aligned} \tag{4.1.8}$$

Here $Y_{I,f}$[1] is $U(1)$ charges of each site fermion. I means the site number $I = 0, 1, 2$ and f means the fermion type. Rewriting the kinetic term, we find

$$\mathcal{L}_{f-k} = i\begin{pmatrix} \bar{\psi}_{L0} & \bar{\psi}_{L1} & \bar{\psi}_{L2} \end{pmatrix}\begin{pmatrix} \not{D}_{L0} & 0 & 0 \\ 0 & \not{D}_{L1} & 0 \\ 0 & 0 & \not{D}_{L2} \end{pmatrix}\begin{pmatrix} \psi_{L0} \\ \psi_{L1} \\ \psi_{L2} \end{pmatrix} + i\begin{pmatrix} \bar{\psi}_{R0} & \bar{\psi}_{R1} & \bar{\psi}_{R2} \end{pmatrix}\begin{pmatrix} \not{D}_{R0} & 0 & 0 \\ 0 & \not{D}_{R1} & 0 \\ 0 & 0 & \not{D}_{R2} \end{pmatrix}\begin{pmatrix} \psi_{R0} \\ \psi_{R1} \\ \psi_{R2} \end{pmatrix}. \tag{4.1.9}$$

[1]For reference, in the case of the Original Three Site Higgsless Model, it is satisfied that $Y_{(0or1),Q} = 1/6$, $Y_{(0or1),L} = -1/2$, $Y_{2,u} = 2/3$, $Y_{2,d} = -1/3$, $Y_{2,e} = -1$.

This Lagrangian includes the coupling of the fermion. At first, we consider the Yukawa coupling in same site.

$$\mathcal{L}_{f-ms} = -\sqrt{2}v_0\lambda_0\,(\bar{\psi}_{R0}\psi_{L0} + \bar{\psi}_{L0}\psi_{R0}) - \sqrt{2}v_1\lambda_1\,(\bar{\psi}_{R1}\psi_{L1} + \bar{\psi}_{L1}\psi_{R1}) - \lambda_2\,(\bar{\psi}_{R2}\phi\psi_{L2} + \bar{\psi}_{L2}\phi\psi_{R2})\,. \tag{4.1.10}$$

Secondly, we consider the coupling between another site fermions. We show in Figure.4.3, 4.4 and 4.5. Therefore the interaction term is

$$\begin{aligned}\mathcal{L}_{f-m} = &-\begin{pmatrix}\bar{\psi}_{L0} & \bar{\psi}_{L1} & \bar{\psi}_{L2}\end{pmatrix}\begin{pmatrix}\sqrt{2}v_0\lambda_0 & \lambda_{01}\Sigma_1 & f_3\lambda'_{20}\\ \lambda'_{01}\Sigma_1 & \sqrt{2}v_1\lambda_1 & \lambda_{12}\Sigma_2\\ f_3\lambda_{20} & \lambda'_{12}\Sigma_2 & \lambda_2\phi\end{pmatrix}\begin{pmatrix}\psi_{R0}\\ \psi_{R1}\\ \psi_{R2}\end{pmatrix}\\ &-\begin{pmatrix}\bar{\psi}_{R0} & \bar{\psi}_{R1} & \bar{\psi}_{R2}\end{pmatrix}\begin{pmatrix}\sqrt{2}v_0\lambda_0 & \lambda'_{01}\Sigma_1 & f_3\lambda_{20}\\ \lambda_{01}\Sigma_1 & \sqrt{2}v_1\lambda_1 & \lambda'_{12}\Sigma_2\\ f_3\lambda'_{20} & \lambda_{12}\Sigma_2 & v_H\lambda_2\end{pmatrix}\begin{pmatrix}\psi_{L0}\\ \psi_{L1}\\ \psi_{L2}\end{pmatrix}.\end{aligned} \tag{4.1.11}$$

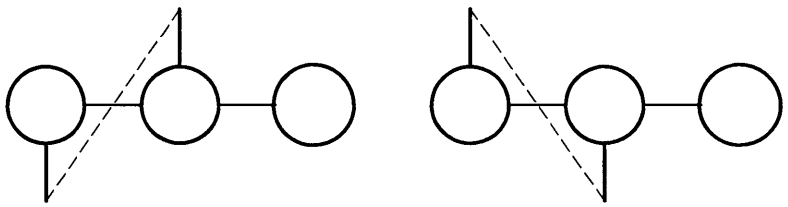

Figure 4.3: The left diagram denote the $L0$ and $R1$ coupling term $-\lambda_{01}\,(\bar{\psi}_{L0}\Sigma_1\psi_{R1} + \bar{\psi}_{R1}\Sigma_1\psi_{L0})$. The right diagram denote the $R0$ and $L1$ coupling term $-\lambda'_{01}\,(\bar{\psi}_{R0}\Sigma_1\psi_{L1} + \bar{\psi}_{L1}\Sigma_1\psi_{R0})$.

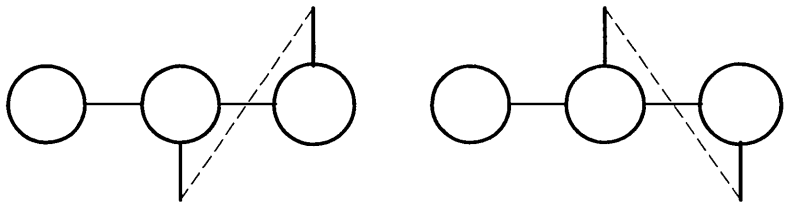

Figure 4.4: The left diagram denote the $L1$ and $R2$ coupling term $-\lambda_{12}\,(\bar{\psi}_{L1}\Sigma_2\psi_{R2} + \bar{\psi}_{R2}\Sigma_2\psi_{L1})$. The right diagram denote the $R1$ and $L2$ coupling term $-\lambda'_{12}\,(\bar{\psi}_{R1}\Sigma_2\psi_{L2} + \bar{\psi}_{L2}\Sigma_2\psi_{R1})$.

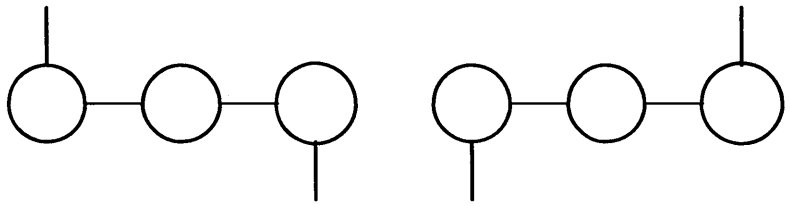

Figure 4.5: The left diagram denote the $L2$ and $R0$ coupling term $-\lambda_{20} f_3 \left(\underline{\psi}_{L2}\psi_{R0} + \underline{\psi}_{R0}\psi_{L2}\right)$. The right diagram denote the $R2$ and $L0$ coupling term $-\lambda'_{20} f_3 \left(\psi_{R2}\psi_{L0} + \psi_{L0}\psi_{R2}\right)$. We omit the dashed lines of Yukawa couplings to avoid becoming complex.

4.1.2 The mass of the bosonic term

After using the Higgs mechanism the bosonic part of the Lagrangian becomes

$$\begin{aligned}\mathcal{L}_b \sim & -\frac{1}{4}\sum_{I=0}^{2} G^a_{I\mu\nu} G_I^{a\mu\nu} - \frac{1}{2}\sum_{I=1}^{2} \left(D_\mu \Sigma_I\right)^{a\dagger} \left(D^\mu \Sigma_I\right)^a \\ & -\frac{1}{2}(g_2 v)^2 B^2_\mu B^{2\mu} - \frac{1}{2}(g_2 v)^2 B^1_\mu B^{1\mu} - \frac{1}{2}\partial_\mu\varphi\partial^\mu\varphi - \frac{1}{2}\left(\sqrt{2\lambda}v\right)^2 \varphi^2.\end{aligned} \tag{4.1.12}$$

We take the non-linear sigma field $\Sigma_I \to f_I$, therefore the covariant derivative of the fields becomes

$$\mathrm{Tr}\left(D_\mu \Sigma_I\right)^\dagger \left(D^\mu \Sigma_I\right) \to \frac{1}{2} f_I^2 \begin{pmatrix} A^a_{I-1,\mu} & A^a_{I,\mu} \end{pmatrix} \begin{pmatrix} g^2_{I-1} & -g_{I-1}g_I \\ -g_{I-1}g_I & g_I^2 \end{pmatrix} \begin{pmatrix} A^a_{I-1,\mu} \\ A^a_{I,\mu} \end{pmatrix}. \tag{4.1.13}$$

It is satisfied that

$$\sum_{I=1}^{2} \mathrm{Tr}\left(D_\mu \Sigma_I\right)^\dagger \left(D^\mu \Sigma_I\right) \to \frac{1}{2} \begin{pmatrix} A^a_{0,\mu} & A^a_{1,\mu} & A^a_{2,\mu} \end{pmatrix} \begin{pmatrix} f_1^2 g_0^2 & -f_1^2 g_0 g_1 & 0 \\ -f_1^2 g_0 g_1 & (f_1^2 + f_2^2) g_1^2 & -f_2^2 g_1 g_2 \\ 0 & -f_2^2 g_1 g_2 & f_2^2 g_2^2 \end{pmatrix} \begin{pmatrix} A^a_{0,\mu} \\ A^a_{1,\mu} \\ A^a_{2,\mu} \end{pmatrix}. \tag{4.1.14}$$

The mass of the charged bosons

When $a = 1, 2$, the mass matrix of the gauge boson becomes

$$\frac{1}{2} \begin{pmatrix} A^a_{0,\mu} & A^a_{1,\mu} & A^a_{2,\mu} \end{pmatrix} \begin{pmatrix} f_1^2 g_0^2 & -f_1^2 g_0 g_1 & 0 \\ -f_1^2 g_0 g_1 & (f_1^2 + f_2^2) g_1^2 & -f_2^2 g_1 g_2 \\ 0 & -f_2^2 g_1 g_2 & (f_2^2 + v^2) g_2^2 \end{pmatrix} \begin{pmatrix} A^a_{0,\mu} \\ A^a_{1,\mu} \\ A^a_{2,\mu} \end{pmatrix}. \tag{4.1.15}$$

We define the matrix M^a that the mass-squared matrix of the gauge field is divided by $g_1^2 f_1^2$,

$$M^{1,2} \equiv \frac{1}{g_1^2 f_1^2}\begin{pmatrix} f_1^2 g_0^2 & -f_1^2 g_0 g_1 & 0 \\ -f_1^2 g_0 g_1 & (f_1^2+f_2^2)g_1^2 & -f_2^2 g_1 g_2 \\ 0 & -f_2^2 g_1 g_2 & (f_2^2+v^2)g_2^2 \end{pmatrix}, \tag{4.1.16}$$

We impose that $x = \frac{g_0}{g_1}, y = \frac{g_2}{g_1}, f = \frac{f_2}{f_1}, v_f = \frac{v_H}{f_1}$. Therefore it is satisfied that

$$M^{1,2} = \begin{pmatrix} x^2 & -x & 0 \\ -x & 1+f^2 & -f^2 y \\ 0 & -f^2 y & (f^2+v_f^2)y^2 \end{pmatrix}, \tag{4.1.17}$$

The eigen value becomes $(E_b^{1,2})^2$, and its eigen state becomes

$$A_\mu^{'1,2} = v_{b0}^{1,2} A_{0,\mu}^{1,2} + v_{b1}^{1,2} A_{1,\mu}^{1,2} + v_{b2}^{1,2} A_{2,\mu}^{1,2}. \tag{4.1.18}$$

The mass of the gauge field $A_\mu^{'1,2}$ is

$$m_b^{1,2} = g_1 f_1 E_b^{1,2}. \tag{4.1.19}$$

The mass of the neutral bosons

We define the matrix M^a,

$$M^3 = \begin{pmatrix} x^2 & -x & 0 \\ -x & 1+f^2 & -f^2 y \\ 0 & -f^2 y & f^2 y^2 \end{pmatrix}. \tag{4.1.20}$$

Similarly to $M^{1,2}$, the eigen value becomes $(E_b^3)^2$, and its eigen state becomes

$$A_\mu^{'3} = v_{b0}^3 A_{0,\mu}^3 + v_{b1}^3 A_{1,\mu}^3 + v_{b2}^3 A_{2,\mu}^3. \tag{4.1.21}$$

The mass of the gauge field $A_\mu^{'3}$ is

$$m_b^3 = g_1 f_1 E_b^3. \tag{4.1.22}$$

4.1.3 The mass of the fermionic term

This Lagrangian includes the mass term of the fermion. At first, we consider the Yukawa coupling in same site.

$$\mathcal{L}_{f-ms} = -\sqrt{2}v_0\lambda_0(\bar{\psi}_{R0}\psi_{L0} + \bar{\psi}_{L0}\psi_{R0}) - \sqrt{2}v_1\lambda_1(\bar{\psi}_{R1}\psi_{L1} + \bar{\psi}_{L1}\psi_{R1}) - \sqrt{2}v_H\lambda_2(\bar{\psi}_{R2}\psi_{L2} + \bar{\psi}_{L2}\psi_{R2}). \tag{4.1.23}$$

Secondly, we consider the coupling between another site fermions. We show in Figure.4.3, 4.4 and 4.5. Therefore the mass term of the fermionic part is

$$\begin{aligned}\mathcal{L}_{f-m} = &-\left(\bar{\psi}_{L0} \quad \bar{\psi}_{L1} \quad \bar{\psi}_{L2}\right)\begin{pmatrix} \sqrt{2}v_0\lambda_0 & f_1\lambda_{01} & f_3\lambda'_{20} \\ f_1\lambda'_{01} & \sqrt{2}v_1\lambda_1 & f_2\lambda_{12} \\ f_3\lambda_{20} & f_2\lambda'_{12} & v_H\lambda_2 \end{pmatrix}\begin{pmatrix}\psi_{R0}\\ \psi_{R1}\\ \psi_{R2}\end{pmatrix} \\ &-\left(\bar{\psi}_{R0} \quad \bar{\psi}_{R1} \quad \bar{\psi}_{R2}\right)\begin{pmatrix} \sqrt{2}v_0\lambda_0 & f_1\lambda'_{01} & f_3\lambda_{20} \\ f_1\lambda_{01} & \sqrt{2}v_1\lambda_1 & f_2\lambda'_{12} \\ f_3\lambda'_{20} & f_2\lambda_{12} & v_H\lambda_2 \end{pmatrix}\begin{pmatrix}\psi_{L0}\\ \psi_{L1}\\ \psi_{L2}\end{pmatrix}.\end{aligned} \tag{4.1.24}$$

We use following notations

$$\begin{aligned} m_0 &= \sqrt{2}v_0\lambda_0, \quad m_{01} = f_1\lambda_{01}, \quad m'_{01} = f_1\lambda'_{01}, \\ m_1 &= \sqrt{2}v_1\lambda_1, \quad m_{12} = f_2\lambda_{12}, \quad m'_{12} = f_2\lambda'_{12}, \\ m_H &= v_H\lambda_2, \quad m_{20} = f_3\lambda_{20}, \quad m'_{20} = f_3\lambda'_{20}, \end{aligned} \tag{4.1.25}$$

$$M = \begin{pmatrix} m_0 & m_{01} & m'_{20} \\ m'_{01} & m_1 & m_{12} \\ m_{20} & m'_{12} & m_H \end{pmatrix}, \quad M^\dagger = \begin{pmatrix} m_0 & m'_{01} & m_{20} \\ m_{01} & m_1 & m'_{12} \\ m'_{20} & m_{12} & m_H \end{pmatrix}. \tag{4.1.26}$$

We construct λ_{matrix} and f_{matrix} matrices.

$$\lambda_{matrix} = \begin{pmatrix} \lambda_{00} & \lambda_{01} & \lambda'_{20} \\ \lambda'_{01} & \lambda_{11} & \lambda_{12} \\ \lambda_{20} & \lambda'_{12} & \lambda_{22} \end{pmatrix}, \tag{4.1.27}$$

$$f_{matrix} = \begin{pmatrix} \sqrt{2}v_0 & f_1 & f_3 \\ f_1 & \sqrt{2}v_1 & f_2 \\ f_3 & f_2 & v_H \end{pmatrix} = \begin{pmatrix} f_{00} & f_{01} & f_{20} \\ f_{01} & f_{11} & f_{12} \\ f_{20} & f_{12} & f_{22} \end{pmatrix}. \tag{4.1.28}$$

The component of the matrix M^{IJ} is

$$M^{IJ} = f^{IJ}\lambda^{IJ} \text{ (no sum)}, \tag{4.1.29}$$

where $I, J = 0, 1, 2$.

Therefore the mass-squared matrix of the left- and right-handed fermionic fields are $MM^\dagger$ and $M^\dagger M$ respectively. We consider the left-handed one $MM^\dagger$.

$$\begin{aligned} MM^\dagger &= \begin{pmatrix} m_0 & m_{01} & m'_{20} \\ m'_{01} & m_1 & m_{12} \\ m_{20} & m'_{12} & m_H \end{pmatrix}\begin{pmatrix} m_0 & m'_{01} & m_{20} \\ m_{01} & m_1 & m'_{12} \\ m'_{20} & m_{12} & m_H \end{pmatrix} \\ &= \begin{pmatrix} m_0^2 + m_{01}^2 + m'^2_{20} & m_0m'_{01} + m_{01}m_1 + m'_{20}m_{12} & m_0m_{20} + m_{01}m'_{12} + m'_{20}m_H \\ m'_{01}m_0 + m_1m_{01} + m_{12}m'_{20} & m'^2_{01} + m_1^2 + m_{12}^2 & m'_{01}m_{20} + m_1m'_{12} + m_{12}m_H \\ m_{20}m_0 + m'_{12}m_{01} + m_Hm'_{20} & m_{20}m'_{01} + m'_{12}m_1 + m_Hm_{12} & m_{20}^2 + m'^2_{12} + m_H^2 \end{pmatrix}. \end{aligned} \tag{4.1.30}$$

We define that

$$n = \frac{m}{m_{01}}. \tag{4.1.31}$$

Therefore it is satisfied that

$$\begin{aligned} NN^{\dagger} &= \frac{1}{{m_{01}}^2} MM^{\dagger} \\ &= \begin{pmatrix} {n_0}^2 + 1 + {n'_{20}}^2 & n_0 n'_{01} + n_1 + n'_{20} n_{12} & n_0 n_{20} + n'_{12} + n'_{20} n_H \\ n'_{01} n_0 + n_1 + n_{12} n'_{20} & {n'_{01}}^2 + {n_1}^2 + {n_{12}}^2 & n'_{01} n_{20} + n_1 n'_{12} + n_{12} n_H \\ n_{20} n_0 + n'_{12} + n_H n'_{20} & n_{20} n'_{01} + n'_{12} n_1 + n_H n_{12} & {n_{20}}^2 + {n'_{12}}^2 + {n_H}^2 \end{pmatrix}. \end{aligned} \tag{4.1.32}$$

The eigen value becomes $(E_{f,L})^2$, and its eigen state becomes

$$\psi'_L = v_{f,L0}\psi_{L0} + v_{f,L1}\psi_{L1} + v_{f,L2}\psi_{L2}. \tag{4.1.33}$$

The mass of the fermionic field ψ'_L is

$$m_{f,L} = m_{01} E_{f,L}. \tag{4.1.34}$$

Similarly, for right-handed fermion, the mass-squared matrix is $M^{\dagger}M$. Therefore we define the matrix

$$\begin{aligned} N^{\dagger}N &= \frac{1}{{m_{01}}^2} M^{\dagger}M \\ &= \begin{pmatrix} {n_0}^2 + {n'_{01}}^2 + {n_{20}}^2 & n_0 + n'_{01} n_1 + n_{20} n'_{12} & n_0 n'_{20} + n'_{01} n_{12} + n_{20} n_H \\ n_0 + n_1 n'_{01} + n'_{12} n_{20} & 1 + {n_1}^2 + {n'_{12}}^2 & n'_{20} + n_1 n_{12} + n'_{12} n_H \\ n'_{20} n_0 + n_{12} n'_{01} + n_H n_{20} & n'_{20} + n_{12} n_1 + n_H n'_{12} & {n'_{20}}^2 + {n_{12}}^2 + {n_H}^2 \end{pmatrix}. \end{aligned} \tag{4.1.35}$$

The eigen value $(E_{f,R})^2$ is same as the left-handed one $(E_{f,L})^2$, and its eigen state becomes

$$\psi'_R = v_{f,R0}\psi_{R0} + v_{f,R1}\psi_{R1} + v_{f,R2}\psi_{R2}. \tag{4.1.36}$$

The mass of the fermionic field ψ'_R is

$$m_{f,R} = m_{01} E_{f,R}. \tag{4.1.37}$$

4.1.4 Interaction term

From

$$\begin{aligned} &\mathcal{L}_{f-k} = i\bar{\psi}_{L0}\not{D}_0\psi_{L0} + i\bar{\psi}_{R0}\not{D}_0\psi_{R0} + i\bar{\psi}_{L1}\not{D}_1\psi_{L1} + i\bar{\psi}_{R1}\not{D}_1\psi_{R1} + i\bar{\psi}_{L2}\not{D}_2\psi_{L2} + i\bar{\psi}_{R2}\not{D}_2\psi_{R2}, \\ &D_{0,\mu} = \partial_\mu - ig_0 A_{0\mu} - ig_2 Y_{0,f} B_\mu T^3, \\ &D_{1,\mu} = \partial_\mu - ig_1 A_{1\mu} - ig_2 Y_{1,f} B_\mu T^3, \\ &D_{2,\mu} = \partial_\mu - ig_2 Y_{2,f} B_\mu T^3, \end{aligned} \tag{4.1.38}$$

we find the interacting between the electron and bosons. For example

$$i\bar{\psi}_{L0}\not{D}_0\psi_{L0} = ii\bar{\psi}_{L0}\not{\partial}\psi_{L0} + \bar{\psi}_{L0}\left(g_0\not{A}_0 + g_2 Y_{0,f}\not{B}T^3\right)\psi_{L0}, \tag{4.1.39}$$

in this equation the second term of the left-hand side is interaction term. Therefore, the interaction term is

$$\begin{aligned}
\mathcal{L}_{f-k} =& \bar{\psi}_{L0}\left(g_0\not{A}_0 + g_2 Y_{0,f}\not{B}T^3\right)\psi_{L0} + \bar{\psi}_{R0}\left(g_0\not{A}_0 + g_2 Y_{0,f}\not{B}T^3\right)\psi_{R0} \\
&+ \bar{\psi}_{L1}\left(g_1\not{A}_1 + g_2 Y_{1,f}\not{B}T^3\right)\psi_{L1} + \bar{\psi}_{R1}\left(g_1\not{A}_1 + g_2 Y_{1,f}\not{B}T^3\right)\psi_{R1} \\
&+ \bar{\psi}_{L2}\left(g_2 Y_{2,f}B_\mu T^3\right)\psi_{L2} + \bar{\psi}_{R2}\left(g_2 Y_{2,f}B_\mu T^3\right)\psi_{R2} \\
=& \bar{\psi}_{L0}\left(g_0\not{A}_0^{1,2}\right)T^{1,2}\psi_{L0} + \bar{\psi}_{R0}\left(g_0\not{A}_0^{1,2}\right)T^{1,2}\psi_{R0} \\
&+ \bar{\psi}_{L1}\left(g_1\not{A}_1^{1,2}\right)T^{1,2}\psi_{L1} + \bar{\psi}_{R1}\left(g_1\not{A}_1^{1,2}\right)T^{1,2}\psi_{R1} \\
+& \bar{\psi}_{L0}\left(g_0\not{A}_0^3 + g_2 Y_{0,f}\not{B}\right)T^3\psi_{L0} + \bar{\psi}_{R0}\left(g_0\not{A}_0^3 + g_2 Y_{0,f}\not{B}\right)T^3\psi_{R0} \\
&+ \bar{\psi}_{L1}\left(g_1\not{A}_1^3 + g_2 Y_{1,f}\not{B}\right)T^3\psi_{L1} + \bar{\psi}_{R1}\left(g_1\not{A}_1^3 + g_2 Y_{1,f}\not{B}\right)T^3\psi_{R1} \\
&+ \bar{\psi}_{L2}\left(g_2 Y_{2,f}\not{B}\right)T^3\psi_{L2} + \bar{\psi}_{R2}\left(g_2 Y_{2,f}\not{B}\right)T^3\psi_{R2}.
\end{aligned} \tag{4.1.40}$$

4.2 Parameter fitting

4.2.1 Some Democratic parameter fittings - The ratio of the gauge boson masses

From the experimental result, it is well known that the ratio of the weak boson masses is

$$\frac{(m_W)^2}{(m_Z)^2} \simeq 0.77. \tag{4.2.1}$$

To realize this mass term's relation, we choose appropriate parameter values

$$g_0, g_1, g_2, f_1, f_2, v_H. \tag{4.2.2}$$

We consider some parameter fittings. The idea of "Democratic Model" is that all $SU(2)$ gauge fields is equivalent. Democratic Condition means that all gauge fields have same gauge coupling constants ($g_0 = g_1 = g_2$).

We consider the threes cases of coupling constants g, f in the following.

Ideally Democratic case

At first, we consider Ideally Democratic case,

$$\begin{aligned} g_0 &= g_1 = g_2, \\ f_1 &= f_2. \end{aligned} \tag{4.2.3}$$

In this case, the VEV of the sigma fields also have same values. Therefore v_H is independent of f_1. In this case the ratio of the weak boson masses has upper bound

$$\frac{(m_W)^2}{(m_Z)^2} \lesssim 0.38. \tag{4.2.4}$$

We show $\frac{(M_W)^2}{(M_Z)^2}$ - $\frac{v_H}{f_1}$ graph in Figure 4.6.

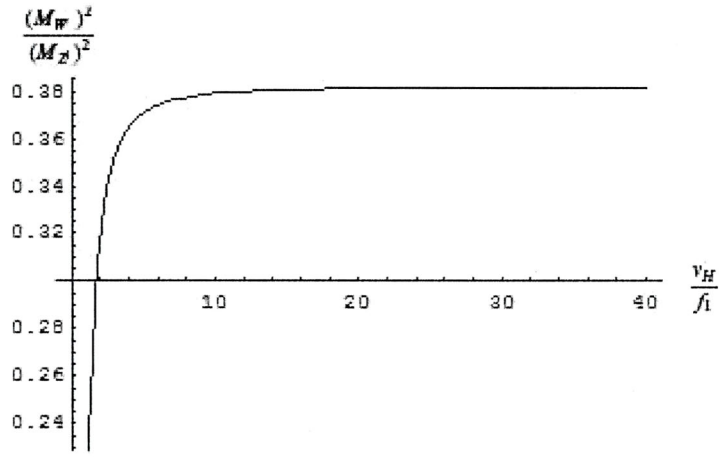

Figure 4.6: This is the $\frac{(M_W)^2}{(M_Z)^2}$ - $\frac{v_H}{f_1}$ graph.

Democratic case

We consider Democratic case,

$$g_0 = g_1 = g_2. \tag{4.2.5}$$

Therefore f_1, f_2 and v_H are independent parameters. In this case the ratio of the weak boson masses also has upper bound

$$\frac{(m_W)^2}{(m_Z)^2} \lesssim 2/3. \tag{4.2.6}$$

We show The contour plot of the ratio of the weak boson masses $\frac{(M_W)^2}{(M_Z)^2}$ in Figure 4.7.

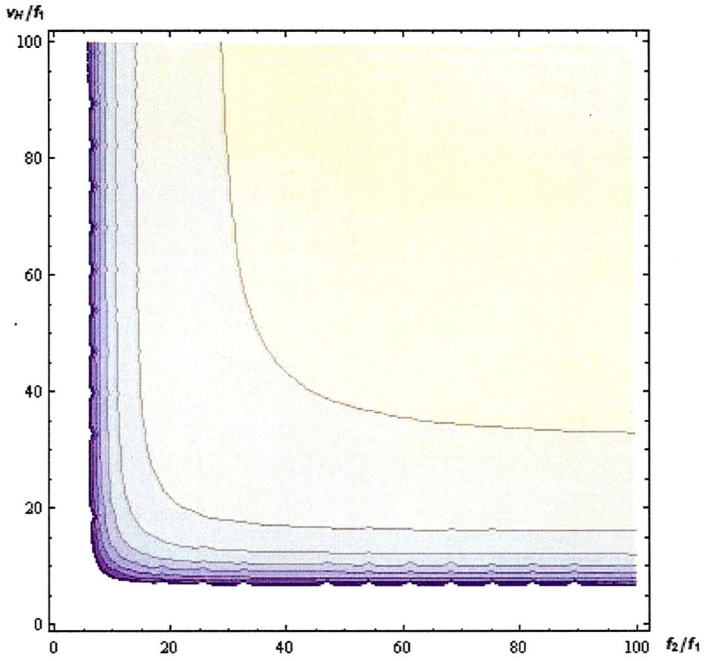

Figure 4.7: The contour plot of the ratio of the weak boson masses $\frac{(M_W)^2}{(M_Z)^2}$. The horizontal axis indicates f_2/f_1 while the vertical axis indicates v_H/f_1. The more the color becomes light, the more the value becomes the upper boound.

Nearly Democratic case

Under the Democratic Condition, the ratio of the gauge boson masses did not have experimental value (4.2.1). Therefore we guess the condition of the gauge coupling that nearly satisfies the Democratic Condition. In their parameters, constraint from the democratic idea, x and y are nearly 1. We suggest (or propose) the condition

$$\begin{aligned} x &= g_0/g_1 = 1.2, \\ y &= g_2/g_1 = 0.8, \\ f_2/f_1 &= 6, \\ v_H/f_1 &\gtrsim 60. \end{aligned} \tag{4.2.7}$$

In this case the ratio of the weak boson masses becomes

$$\frac{(m_W)^2}{(m_Z)^2} \simeq 0.77. \tag{4.2.8}$$

This parameter condition is the one of the parameter choices.

Some comments about g and f values

As the result, we found that the ratio of the weak boson masses did not realize the experimental value in the Democratic Condition. The Nearly Democratic case is based on the Democratic Condition. In this case, the ratio of the weak boson masses corresponded to the experimental value.

In the Original Three Site Higgsless Model, it were satisfied that

$$\begin{aligned} &g_1 \gg g_0, g_2, \\ &f_1 = f_2 \end{aligned} \tag{4.2.9}$$

and g_0 and g_2 was approximately equal to the SM-like $SU(2)_L$ and $U(1)_Y$ couplings. We call this condition "Original Condition". In this condition, our Three Site Higgsless Model realizes the experimental value (of the ratio of the weak boson masses). In addition, if we ignore Democratic Condition, there are many choices of g and f values which realize the experimantal value.

4.2.2 The ratio of the fermion masses

We consider the Nearly Democratic case. We choose parameters as in Figure 4.8. Therefore the eigen value of the fermion mass-squared matrix becomes

$$\left(\frac{m_f}{\lambda_f f_1}\right)^2 = 2.6\times 10^{14}, 3.8\times 10^{13}, 1.00, \tag{4.2.10}$$

and its eigen state is

$$\begin{pmatrix}\psi_{heavy}\\ \psi_{middle}\\ \psi_{light}\end{pmatrix} = \begin{pmatrix}0.53 & 0 & 0.85\\ -0.85 & 0 & 0.53\\ 0 & -1 & 0\end{pmatrix}\begin{pmatrix}\psi_0\\ \psi_1\\ \psi_2\end{pmatrix}. \tag{4.2.11}$$

f and g coupling constants

$$\lambda_{matrix} = \begin{pmatrix}\lambda_f & \lambda_f & \lambda_f\\ \lambda_f & \lambda_f & \lambda_f\\ \lambda_f & \lambda_f & \lambda_f\end{pmatrix}, \tag{4.2.12}$$

$$f_{matrix} = \begin{pmatrix}f_{00} & f_{01} & f_{20}\\ f_{01} & f_{11} & f_{12}\\ f_{20} & f_{12} & f_{22}\end{pmatrix} = \begin{pmatrix}f_1 & f_1 & 10^7 f_1\\ f_1 & f_1 & 6f_1\\ 10^7 f_1 & 6f_1 & 10^7 f_1\end{pmatrix}. \tag{4.2.13}$$

Figure 4.8: This is the one of the example of the λ and f couplings.

To decide the parameter value of f_H, we use the following ration of mass

$$\frac{(mass_{f,middle})^2}{(mass_{f,light})^2} > 10^{11}, \tag{4.2.14}$$

because we know the following condition

$$\left(\frac{mass_{top}}{mass_{electron}}\right)^2 = \left(\frac{1.74\times 10^5}{0.5}\right)^2 \sim 10^{11}. \tag{4.2.15}$$

4.2.3 The gauge coupling ratio of weak and electromagnetic gauge

We consider the some coupling constants as in 4.2.2. It is satisfied that

$$\begin{pmatrix} A^{1,2}_{0,\mu} \\ A^{1,2}_{1,\mu} \\ A^{1,2}_{2,\mu} \end{pmatrix} = \begin{pmatrix} 0 & -0.03 & 0.99 \\ 0 & 0.99 & 0.03 \\ 1 & 0 & 0 \end{pmatrix} \begin{pmatrix} W''_{\mu} \\ W'_{\mu} \\ W_{\mu} \end{pmatrix}, \tag{4.2.16}$$

$$\begin{pmatrix} A^{3}_{0,\mu} \\ A^{3}_{1,\mu} \\ A^{3}_{2,\mu} \end{pmatrix} = \begin{pmatrix} -0.02 & 0.89 & 0.46 \\ 0.78 & -0.27 & 0.55 \\ -0.62 & -0.37 & 0.69 \end{pmatrix} \begin{pmatrix} Z'_{\mu} \\ Z_{\mu} \\ A^{\gamma}_{\mu} \end{pmatrix}, \tag{4.2.17}$$

$$\begin{pmatrix} \psi_0 \\ \psi_1 \\ \psi_2 \end{pmatrix} = \begin{pmatrix} 0.53 & -0.85 & 0 \\ 0 & 0 & -1 \\ 0.85 & 0.53 & 0 \end{pmatrix} \begin{pmatrix} \psi_{heavy} \\ \psi_{middle} \\ \psi_{light} \end{pmatrix}. \tag{4.2.18}$$

We need the ground state, therefore it becomes that

$$\begin{pmatrix} A^{1,2}_{0,\mu} \\ A^{1,2}_{1,\mu} \\ A^{1,2}_{2,\mu} \end{pmatrix} \to \begin{pmatrix} 0.99 \cdot W_{\mu} \\ 0.03 \cdot W_{\mu} \\ 0 \cdot W_{\mu} \end{pmatrix}, \tag{4.2.19}$$

$$\begin{pmatrix} A^{3}_{0,\mu} \\ A^{3}_{1,\mu} \\ A^{3}_{2,\mu} \end{pmatrix} \to \begin{pmatrix} 0.46 \cdot A^{\gamma}_{\mu} \\ 0.55 \cdot A^{\gamma}_{\mu} \\ 0.69 \cdot A^{\gamma}_{\mu} \end{pmatrix}, \tag{4.2.20}$$

$$\begin{pmatrix} \psi_0 \\ \psi_1 \\ \psi_2 \end{pmatrix} \to \begin{pmatrix} 0 \cdot \psi_{light} \\ -1 \cdot \psi_{light} \\ 0 \cdot \psi_{light} \end{pmatrix}. \tag{4.2.21}$$

Therefore the interaction term becomes

$$\begin{aligned} &\mathcal{L}_{f-k} \\ &= \bar{\psi}_{L,light} \left(g_1 0.03 \cdot \not{W}^{\pm}\right) T^{1,2} \psi_{L,light} + \bar{\psi}_{R,light} \left(g_1 0.03 \cdot \not{W}^{\pm}\right) T^{1,2} \psi_{R,light} \\ &+ \bar{\psi}_{L,light} \left(g_1 0.55 \cdot \not{A}^{\gamma} + 0.8 \cdot g_1 Y_{1,f} 0.69 \cdot \not{A}^{\gamma}\right) T^{3} \psi_{L,light} + \bar{\psi}_{R,light} \left(g_1 0.55 \cdot \not{A}^{\gamma} + 0.8 \cdot g_1 Y_{1,f} 0.69 \cdot \not{A}^{\gamma}\right) T^{3} \psi_{R,light} \\ &= 0.03 \cdot g_1 \bar{\psi}_{L,light} \not{W}^{\pm} T^{1,2} \psi_{L,light} + 0.03 \cdot g_1 \bar{\psi}_{R,light} \not{W}^{\pm} T^{1,2} \psi_{R,light} \\ &+ \left(0.55 \cdot g_1 + 0.55 \cdot g_1 Y_{1,f}\right) \bar{\psi}_{L,light} \not{A}^{\gamma} T^{3} \psi_{L,light} + \left(0.55 \cdot g_1 + 0.55 \cdot g_1 Y_{1,f}\right) \bar{\psi}_{R,light} \not{A}^{\gamma} T^{3} \psi_{R,light}. \end{aligned} \tag{4.2.22}$$

It is satisfied that

$$\begin{aligned} g_{A^{\gamma}} &= 0.55 \cdot g_1 \left(1 + Y_{1,f}\right), \\ g_{W^{\pm}} &= 0.03 \cdot g_1. \end{aligned} \tag{4.2.23}$$

Therefore it is satisfied that

$$\left(\frac{g_{A^\gamma}}{g_{W^\pm}}\right)^2 = \left(\frac{0.55 \cdot g_1\left(1 + Y_{1,f}\right)}{0.03 \cdot g_1}\right)^2 = \left(\frac{0.55\left(1 + Y_{1,f}\right)}{0.03}\right)^2 . \tag{4.2.24}$$

The experimental value is $\left(\frac{g_{A^\gamma}}{g_W}\right)^2 \sim 0.22$.

4.2.4 Some parameter fitting

We show the detail of parameters, eigenstates and eigenvalues in two cases. One is the Ideally Democratic case and the other is the Nearly Democratic case.

Case.1 Ideally Democratic case

The gauge coupling condition is

$$g_0 = g_1 = g_2. \tag{4.2.25}$$

The VEV of the scalar fields satisfies

$$f_{matrix} = \begin{pmatrix} f_{00} & f_{01} & f_{20} \\ f_{01} & f_{11} & f_{12} \\ f_{20} & f_{12} & f_{22}(=v_H) \end{pmatrix} = \begin{pmatrix} f_1 & f_1 & f_1 \\ f_1 & f_1 & f_1 \\ f_1 & f_1 & 10^2 f_1 \end{pmatrix}. \tag{4.2.26}$$

The coupling constant of fermions is

$$\lambda_{matrix} = \begin{pmatrix} \lambda_{00} & \lambda_{01} & \lambda'_{20} \\ \lambda'_{01} & \lambda_{11} & \lambda_{12} \\ \lambda_{20} & \lambda'_{12} & \lambda_{22} \end{pmatrix} = \begin{pmatrix} \lambda_f & \lambda_f & \lambda_f \\ \lambda_f & \lambda_f & \lambda_f \\ \lambda_f & \lambda_f & \lambda_f \end{pmatrix}. \tag{4.2.27}$$

The mass of bosons and fermions is the following.

boson type	$(\text{mass})^2/(g_1^2 f_1^2)$
W''	1.00×10^4
W'	2.62
W	0.382
Z'	3
Z	1
γ	0

fermion type	$(\text{mass})^2/(\lambda_f^2 f_1^2)$
ψ_{heavy}	1.00×10^4
ψ_{middle}	3.92
ψ_{light}	0

The state of bosons and fermions is

$$\begin{pmatrix} W''_\mu \\ W'_\mu \\ W_\mu \end{pmatrix} = \begin{pmatrix} 0 & 0 & 1 \\ -0.53 & 0.85 & 0 \\ 0.85 & 0.53 & 0 \end{pmatrix} \begin{pmatrix} A^{1,2}_{0,\mu} \\ A^{1,2}_{1,\mu} \\ A^{1,2}_{2,\mu} \end{pmatrix}, \quad \begin{pmatrix} A^{1,2}_{0,\mu} \\ A^{1,2}_{1,\mu} \\ A^{1,2}_{2,\mu} \end{pmatrix} = \begin{pmatrix} 0 & -0.53 & 0.85 \\ 0 & 0.85 & 0.53 \\ 1 & 0 & 0 \end{pmatrix} \begin{pmatrix} W''_\mu \\ W'_\mu \\ W_\mu \end{pmatrix}, \tag{4.2.28}$$

$$\begin{pmatrix} Z'_\mu \\ Z_\mu \\ \gamma_\mu \end{pmatrix} = \begin{pmatrix} 0.41 & -0.82 & 0.41 \\ -0.71 & -0.71 & 0.01 \\ -0.71 & 0.71 & 0 \end{pmatrix} \begin{pmatrix} A^3_{0,\mu} \\ A^3_{1,\mu} \\ A^3_{2,\mu} \end{pmatrix}, \quad \begin{pmatrix} A^3_{0,\mu} \\ A^3_{1,\mu} \\ A^3_{2,\mu} \end{pmatrix} = \begin{pmatrix} 0.01 & -0.71 & -0.71 \\ 0.01 & -0.71 & 0.71 \\ 0.99 & 0.01 & 0 \end{pmatrix} \begin{pmatrix} Z'_\mu \\ Z_\mu \\ \gamma_\mu \end{pmatrix}, \tag{4.2.29}$$

$$\begin{pmatrix}\psi_{heavy}\\ \psi_{middle}\\ \psi_{light}\end{pmatrix}=\begin{pmatrix}0.01 & -0.70 & -0.70\\ 0.01 & -0.70 & 0.70\\ 0.99 & 0.01 & 0\end{pmatrix}\begin{pmatrix}\psi_0\\ \psi_1\\ \psi_2\end{pmatrix},\quad \begin{pmatrix}\psi_0\\ \psi_1\\ \psi_2\end{pmatrix}=\begin{pmatrix}0.01 & 0.01 & 0.99\\ -0.70 & -0.70 & 0.01\\ -0.70 & 0.70 & 0\end{pmatrix}\begin{pmatrix}\psi_{heavy}\\ \psi_{middle}\\ \psi_{light}\end{pmatrix}. \tag{4.2.30}$$

The interaction term becomes

$$\begin{aligned}\mathcal{L}_{f-k} =&\bar{\psi}_{L0}\left(g_0 \not{A}_0^{1,2}\right) T^{1,2}\psi_{L0}+\bar{\psi}_{R0}\left(g_0 \not{A}_0^{1,2}\right) T^{1,2}\psi_{R0}\\ &+\bar{\psi}_{L1}\left(g_1 \not{A}_1^{1,2}\right) T^{1,2}\psi_{L1}+\bar{\psi}_{R1}\left(g_1 \not{A}_1^{1,2}\right) T^{1,2}\psi_{R1}\\ &+\bar{\psi}_{L0}\left(g_0 \not{A}_0^{3}+g_2 Y_{0,f}\not{B}\right) T^{3}\psi_{L0}+\bar{\psi}_{R0}\left(g_0 \not{A}_0^{3}+g_2 Y_{0,f}\not{B}\right) T^{3}\psi_{R0}\\ &+\bar{\psi}_{L1}\left(g_1 \not{A}_1^{3}+g_2 Y_{1,f}\not{B}\right) T^{3}\psi_{L1}+\bar{\psi}_{R1}\left(g_1 \not{A}_1^{3}+g_2 Y_{1,f}\not{B}\right) T^{3}\psi_{R1}\\ &+\bar{\psi}_{L2}\left(g_2 Y_{2,f} B_\mu\right) T^{3}\psi_{L2}+\bar{\psi}_{R2}\left(g_2 Y_{2,f} B_\mu\right) T^{3}\psi_{R2}\\ &\to 0.83\cdot g_1\bar{\psi}_{light}\not{W}T^{1,2}\psi_{light}-0.69\cdot g_1\bar{\psi}_{light}\not{\gamma}T^{3}\psi_{light}\end{aligned} \tag{4.2.31}$$

Here it is satisfied that

$$\begin{aligned} g_{A'_\gamma} &= -0.69 g_1,\\ g_{A_W} &= 0.83 g_1. \end{aligned} \tag{4.2.32}$$

Therefore we find

$$\left(\frac{g_{A'_\gamma}}{g_{A_W}}\right)^2=\left(\frac{0.69}{0.83}\right)^2\sim 0.69 \tag{4.2.33}$$

We show two values.

$\frac{(M_W)^2}{(M_Z)^2}$	$\frac{(g_{A'_\gamma})^2}{(g_{A_W})^2}$
0.38	0.69

Case.2 - Nearly Democratic case

The gauge coupling condition is

$$\frac{g_0}{g_1} = 1.2, \frac{g_2}{g_1} = 0.8. \tag{4.2.34}$$

The VEV of the scalar fields satisfies

$$f_{matrix} = \begin{pmatrix} f_{00} & f_{01} & f_{20} \\ f_{01} & f_{11} & f_{12} \\ f_{20} & f_{12} & f_{22}(=v_H) \end{pmatrix} = \begin{pmatrix} f_1 & f_1 & 10^7 f_1 \\ f_1 & f_1 & 6f_1 \\ 10^7 f_1 & 6f_1 & 10^7 f_1 \end{pmatrix}. \tag{4.2.35}$$

The coupling constant of fermions is

$$\lambda_{matrix} = \begin{pmatrix} \lambda_{00} & \lambda_{01} & \lambda'_{20} \\ \lambda'_{01} & \lambda_{11} & \lambda_{12} \\ \lambda_{20} & \lambda'_{12} & \lambda_{22} \end{pmatrix} = \begin{pmatrix} \lambda_f & \lambda_f & \lambda_f \\ \lambda_f & \lambda_f & \lambda_f \\ \lambda_f & \lambda_f & \lambda_f \end{pmatrix}. \tag{4.2.36}$$

The mass of bosons and fermions is the following.

boson type	$(\text{mass})^2/(g_1^2 f_1^2)$
W''	6.40×10^{13}
W'	37.0
W	1.40
Z'	59.7
Z	1.81
γ	~ 0.00

fermion type	$(\text{mass})^2/(\lambda_f^2 f_1^2)$
ψ_{heavy}	2.6×10^{14}
ψ_{middle}	3.8×10^{13}
ψ_{light}	1.00

The state of bosons and fermions is

$$\begin{pmatrix} W''_\mu \\ W'_\mu \\ W_\mu \end{pmatrix} = \begin{pmatrix} 0 & 0 & 1 \\ -0.03 & 0.99 & 0 \\ 0.99 & 0.03 & 0 \end{pmatrix} \begin{pmatrix} A^{1,2}_{0,\mu} \\ A^{1,2}_{1,\mu} \\ A^{1,2}_{2,\mu} \end{pmatrix}, \quad \begin{pmatrix} A^{1,2}_{0,\mu} \\ A^{1,2}_{1,\mu} \\ A^{1,2}_{2,\mu} \end{pmatrix} = \begin{pmatrix} 0 & -0.03 & 0.99 \\ 0 & 0.99 & 0.03 \\ 1 & 0 & 0 \end{pmatrix} \begin{pmatrix} W''_\mu \\ W'_\mu \\ W_\mu \end{pmatrix}, \tag{4.2.37}$$

$$\begin{pmatrix} Z'_\mu \\ Z_\mu \\ \gamma_\mu \end{pmatrix} = \begin{pmatrix} -0.01 & 0.79 & -0.62 \\ 0.89 & -0.27 & -0.37 \\ 0.46 & 0.55 & 0.69 \end{pmatrix} \begin{pmatrix} A^3_{0,\mu} \\ A^3_{1,\mu} \\ A^3_{2,\mu} \end{pmatrix}, \quad \begin{pmatrix} A^3_{0,\mu} \\ A^3_{1,\mu} \\ A^3_{2,\mu} \end{pmatrix} = \begin{pmatrix} -0.02 & 0.89 & 0.46 \\ 0.78 & -0.27 & 0.55 \\ -0.62 & -0.37 & 0.69 \end{pmatrix} \begin{pmatrix} Z'_\mu \\ Z_\mu \\ \gamma_\mu \end{pmatrix}, \tag{4.2.38}$$

$$\begin{pmatrix} \psi_{heavy} \\ \psi_{middle} \\ \psi_{light} \end{pmatrix} = \begin{pmatrix} 0.53 & 0 & 0.85 \\ -0.85 & 0 & 0.53 \\ 0 & -1 & 0 \end{pmatrix} \begin{pmatrix} \psi_0 \\ \psi_1 \\ \psi_2 \end{pmatrix}, \quad \begin{pmatrix} \psi_0 \\ \psi_1 \\ \psi_2 \end{pmatrix} = \begin{pmatrix} 0.53 & -0.85 & 0 \\ 0 & 0 & -1 \\ 0.85 & 0.53 & 0 \end{pmatrix} \begin{pmatrix} \psi_{heavy} \\ \psi_{middle} \\ \psi_{light} \end{pmatrix}. \tag{4.2.39}$$

The interaction term becomes

$$\begin{aligned}\mathcal{L}_{f-k} =& \bar{\psi}_{L0}\left(g_0 \not{A}_0^{1,2}\right) T^{1,2}\psi_{L0} + \bar{\psi}_{R0}\left(g_0 \not{A}_0^{1,2}\right) T^{1,2}\psi_{R0} \\ &+ \bar{\psi}_{L1}\left(g_1 \not{A}_1^{1,2}\right) T^{1,2}\psi_{L1} + \bar{\psi}_{R1}\left(g_1 \not{A}_1^{1,2}\right) T^{1,2}\psi_{R1} \\ &+ \bar{\psi}_{L0}\left(g_0 \not{A}_0^{3} + g_2 Y_{0,f} \not{B}\right) T^{3}\psi_{L0} + \bar{\psi}_{R0}\left(g_0 \not{A}_0^{3} + g_2 Y_{0,f} \not{B}\right) T^{3}\psi_{R0} \\ &+ \bar{\psi}_{L1}\left(g_1 \not{A}_1^{3} + g_2 Y_{1,f} \not{B}\right) T^{3}\psi_{L1} + \bar{\psi}_{R1}\left(g_1 \not{A}_1^{3} + g_2 Y_{1,f} \not{B}\right) T^{3}\psi_{R1} \\ &+ \bar{\psi}_{L2}\left(g_2 Y_{2,f} B_\mu\right) T^{3}\psi_{L2} + \bar{\psi}_{R2}\left(g_2 Y_{2,f} B_\mu\right) T^{3}\psi_{R2} \\ &= 0.03 \cdot g_1 \bar{\psi}_{light} \not{W} T^{1,2}\psi_{light} + \left(0.55 \cdot g_1 + 0.55 \cdot g_1 Y_{1,f}\right) \bar{\psi}_{light} \not{\gamma} T^{3}\psi_{light}.\end{aligned} \tag{4.2.40}$$

Here it is satisfied that

$$\begin{aligned} g_{A'_\gamma} &= 0.55 \cdot g_1\left(1 + Y_{1,f}\right), \\ g_{A_W} &= 0.03 \cdot g_1. \end{aligned} \tag{4.2.41}$$

Therefore we find

$$\begin{aligned}\left(\frac{g_{A'_\gamma}}{g_{A_W}}\right)^2 &= \left(\frac{0.55 \cdot g_1\left(1 + Y_{1,f}\right)}{0.03 \cdot g_1}\right)^2 \\ &= \left(\frac{0.55\left(1 + Y_{1,f}\right)}{0.03}\right)^2.\end{aligned} \tag{4.2.42}$$

We show two values.

$\frac{(M_W)^2}{(M_Z)^2}$	$\frac{(g_{A'_\gamma})^2}{(g_{A_W})^2}$
0.77	$\left(\frac{0.55\left(1 + Y_{1,f}\right)}{0.03}\right)^2$

4.3 The aspect of the monopole

We considered the Three Site Higgless Model which included the novel monopole. The mass of heavy weak bosons W'' is extremely heavier than the mass of other bosons. Therefore the mass of the monopole is the same order of the mass of the heavy weak bosons. The mass of the heavy weak bosons consists of parameters v_H and f_1. In this model, parameters v_H and f_1 are highly correlated with the mass of the monopole. The ratio v_H/f_1 is limited to $v_H/f_1 \gtrsim 60$. Therefore the mass of the monopole has the lower limit.

We think that the monopole mixture exists as the dark matter in the universe. We hope that the scale of the scalar VEV is the 10 TeV. The mass of the monopole mixture is 100 TeV. This scale is smaller than that of GUT scale 10^{15} GeV. The GUT monopole is considered to be produced in the Inflation. But this novel monopole is produced in the later period.

4.4 Conclusion and Outlook

The idea of "Democratic Model" is that each $SU(2)$ gauge field has equivalent property. Saying this another way, all $SU(2)$ gauge fields have same gauge couplings. From the bosonic part, the condition of the Democratic gauge coupling $g_0 = g_1 = g_2$ does not satisfy the ratio of the gauge boson masses (4.2.1). Therefore we guessed (or proposed) the condition of the gauge coupling that nearly satisfied the Democratic Condition. In this condition we realized the experimental value. This value depended on the VEV of the sigma field and the Higgs field. The former could not choose any values, but the latter could choose the rang of value $v_H/f_1 \gtrsim 60$. This parameter condition is the one of the parameter choices. In fact, there are any parameter conditions that satisfy the experimental value of the gauge boson masses. Including the result of the fermionic part, the ratio of g_{A^γ}/g_W (4.2.24) showed that above condition did not satisfy the experimental value $(g_{A^\gamma}/g_W)^2 \sim 0.22$.

We mentioned the monopole. The mass of heavy weak bosons W'' is extremely heavier than the mass of other bosons. Therefore the mass of the monopole is the same order of the mass of the heavy weak bosons. The mass of the heavy weak bosons consists of parameters v_H and f_1. In this model, parameters v_H and f_1 are highly correlated with the mass of the monopole. The ratio v_H/f_1 is limited to $v_H/f_1 \gtrsim 60$. Therefore the mass of the monopole has the lower limit.

As in Figure 4.8, the Democratic Three Site Model has many parameters which are chosen by hand. The number of λ and f parameters is 18. The parameter of λ (λ_f) has each value for each type of fermion. The mass of each fermion is controlled by the λ_f parameter.

The Democratic Model includes many difficulties to realize the real phenomenology. We need to improve the Democratic Three Site Higgsless Model.

Part III

Field theory on a Graph

Chapter 5

Vortices and Superfields on a Graph

The moose diagram like Figure 2.9 naturally leads to the Lagrangian of the model. This moose diagram indicates a relation between gauge fields and scalar fields. We will generalize this relation in the context of graph theory. We can express the relation between gauge fields and scalar fields in a graph, which is just a complex moose. We wish to call this theory based on a graph as "Graph Dimensional Deconstruction" (GDD). The idea of GDD has already been published as [10].

In the present work, we propose another idea of using superfields to introduce supersymmetry (SUSY) into the model. We assign vector superfields to vertices and chiral superfields to edges of a graph. This is another extension of the DD.

In the beginning, both DD and SUSY are to provide the mechanism of solving the gauge hierarchy problem. The motivations of including SUSY are, nevertheless, claimed as follows. First of all, we should think that every field theory has SUSY at very high energy, because the correct or controlled UV behaviors are believed, or because of superstring theory or M-theory. The second motivation comes from the necessity of more symmetries. Because DD and GDD are basically the mechanism of controlling the mass spectrum of field theory, we need more symmetry to determine the (self-) interaction of fields. Thus we consider the supersymmetric extension of the GDD model here.

In this GDD, we consider only the Abelian theory. For notation, please consult [10].

5.1 A review of field theory on a graph (or graph dimensional deconstruction)

A graph $G(V, E)$ consists of a set of vertices V and a set of edges E. A vertex is connected with another one by an edge. We let the number of the vertices be p,

$p \equiv \#V$, and the number of the edges be q, $q \equiv \#E$. In Figure 5.1, we show the simplest graph with $p = 2$ and $q = 1$, constructed by two vertices and an edge.

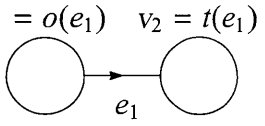

Figure 5.1: The simplest graph, constructed by two vertices and an edge. A vertex v_i is identified by i, where i is a label for each vertex. In the same way, an edge e_i is identified by i, where i is a label for each edges. The arrow means a direction of the edge. This edge is called an oriented edge. In terms of the oriented edge, the original vertex v_1 is $v_1 = o(e_1)$ and the terminal vertex v_2 is $v_2 = t(e_1)$. This oriented graph corresponds to the generalized moose diagram.

We consider a simple Abelian theory. Abelian gauge fields reside at vertices and scalar fields reside at edges. The $U(1)$ transformation is defined at each vertex. The Lagrangian density is

$$\mathcal{L} = -\frac{1}{4}\sum_{v\in V} F^{\mathrm{v}}_{\mu\nu}F^{\mu\nu}_{\mathrm{v}} - \sum_{e\in E}(\mathcal{D}_\mu U_e)^\dagger(\mathcal{D}^\mu U_e)\,, \tag{5.1.1}$$

where the covariant derivative is

$$\mathcal{D}^\mu U_e = (\partial^\mu + igA^\mu_{t(e)} - igA^\mu_{o(e)})U_e\,, \tag{5.1.2}$$

with $|U_e|^2 = f^2$.

If we rewrite U_e as $U_e = fe^{ia_e}$, the real scalar fields a_e act as the Stueckelberg fields. The number of physical massless scalar fields is $q - p + 1$, or the number of closed circuits involved in the graph, because $p - 1$ scalar degrees of freedom are absorbed by the to-be massive vector fields. If and only if the graph is *tree* (or absent from closed circuits), the scalar fields disappear from the physical spectrum.

The $(mass)^2$ matrix of vector fields M_A^2 is given by $2g^2f^2\Delta$, where the (p,p) matrix

$$\Delta \equiv EE^T \tag{5.1.3}$$

is called as the graph Laplacian and the (p,q) matrix E is the incidence matrix [1] defined as

$$(E)_{ve} = \begin{cases} 1 & \text{if } v = o(e) \\ -1 & \text{if } v = t(e) \\ 0 & \text{otherwise} \end{cases}\,. \tag{5.1.4}$$

[1] Unfortunately, the symbol E is used for the incidence matrix and for the set of edges. Please do not confuse them.

Here $v = o(e)$ means that the vertex v is the origin of the edge e and $v = t(e)$ means that the vertex v is the terminus of the edge e. The (q, p) matrix E^T is the transposed matrix of E.

For more general cases, one might consider individual coupling constants for vertices as

$$\mathcal{D}^\mu U_e = (\partial^\mu + ig_{t(e)}A^\mu_{t(e)} - ig_{o(e)}A^\mu_{o(e)})U_e\,, \tag{5.1.5}$$

and $|U_e|^2 = f_e^2$ for each edge. In this case the mass matrix becomes

$$M_A^2 = 2GEF^2E^TG = 2(GEF)(GEF)^T, \tag{5.1.6}$$

where the diagonal matrices G and F are given by

$$(G)_{vv'} = \begin{cases} g_v & \text{if } v = v' \\ 0 & \text{otherwise} \end{cases}, \quad (F)_{ee'} = \begin{cases} f_e & \text{if } e = e' \\ 0 & \text{otherwise} \end{cases}, \tag{5.1.7}$$

respectively.

To summarize this section: In the GDD model, the mass spectrum is given by eigenvalues of the graph Laplacian or the related matrix constructed from the incidence matrix of the graph.

5.2 The use of the Stueckelberg superfield

Next we incorporate SUSY into the GDD model. We use superfields [17] to this end.

In this thesis, we consider that vector superfields $\{V_v\}$ exist on vertices. We still impose the $U(1)$ transformation on $\{V_v\}$ at each vertex as

$$V_v \to V_v + i(\Lambda_v - \overline{\Lambda}_v)\,, \tag{5.2.1}$$

where Λ_v is a chiral superfield. Then the invariant superfield is defined as usual [17]:

$$W_\alpha^v = -\frac{1}{4}\overline{D}\,\overline{D}\,D_\alpha V_v\,. \tag{5.2.2}$$

The kinetic term of the vector field can be created from this for each vertex.

Further we introduce a chiral superfield S_e at each edge. The superfield S_e is assumed to be transformed as

$$S_e \to S_e - i\Lambda_{t(e)} + i\Lambda_{o(e)}\,. \tag{5.2.3}$$

Then we can write the Stueckelberg term [18]

$$(V_{t(e)} - V_{o(e)} + S_e + \overline{S}_e)^2, \tag{5.2.4}$$

and a gauge invariant term for the interaction with scalars

$$\mathcal{L} = \sum_{v\in V}\frac{1}{4g_v^2}\left(W_v^\alpha W_{v\alpha}\big|_{\theta\theta} + \overline{W}_v^{\dot\alpha}\overline{W}_{v\dot\alpha}\big|_{\bar\theta\bar\theta}\right) \tag{5.2.5}$$

$$+\sum_{e\in E} 2f_e^2(V_{t(e)} - V_{o(e)} + S_e + \overline{S}_e)^2\big|_{\theta\theta\bar\theta\bar\theta}. \tag{5.2.6}$$

The bosonic part of the theory is found to be

$$\mathcal{L}_b = -\sum_{v\in V}\frac{1}{4g_v^2}F^v_{\mu\nu}F_v^{\mu\nu} - \sum_{e\in E}\frac{2f_e^2}{2}(A^\mu_{t(e)} - A^\mu_{o(e)} + \partial^\mu a_e)^2 - \frac{1}{2}\sum_{e\in E}2f_e^2(\partial^\mu\rho_e)^2$$
$$+\sum_{v\in V}\frac{1}{2g_v^2}D_v^2 + 2\sum_{e\in E}2f_e^2|F_{Se}|^2 + \sum_{e\in E}2f_e^2(D_{t(e)} - D_{o(e)})\rho_e\,, \tag{5.2.7}$$

where the notation of component field is rather standard one and is gathered in Appendix B.1.

Eliminating the auxiliary fields F_{Se} and rescaling ρ_e, gauge fields and D_v to have canonical kinetic terms we get

$$\mathcal{L}_b = -\frac{1}{4}\sum_{v\in V}F^v_{\mu\nu}F_v^{\mu\nu} - \sum_{e\in E}\frac{2f_e^2}{2}(g_{t(e)}A^\mu_{t(e)} - g_{o(e)}A^\mu_{o(e)} + \partial^\mu a_e)^2$$
$$-\frac{1}{2}\sum_{e\in E}(\partial^\mu\rho_e)^2 - \sum_{e,e'\in E}\sum_{v\in V}f_e\rho_e(E^T)_{ev}g_v^2(E)_{ve'}f_{e'}\rho_{e'}$$
$$+\frac{1}{2}\sum_{v\in V}\left\{D_v - \frac{\sqrt{2}}{2}g_v\sum_{e\in E}(E)_{ve}f_e\rho_e\right\}^2. \tag{5.2.8}$$

Now one can easily find the mass matrices for vectors and scalars:

$$M_A^2 = 2GEF^2E^TG = 2(GEF)(GEF)^T\,,\quad M_\rho^2 = 2FE^TG^2EF = 2(GEF)^T(GEF)\,, \tag{5.2.9}$$

where E is defined as (5.1.4) while G and F are given by (5.1.7). Massless scalar fields are absent if and only if the graph is a tree graph. The mass spectrum of the scalar fields is the same as the one for the vector fields except for zero modes.[2]

The fermionic part of the theory is found to be

$$\mathcal{L}_f = -i\sum_{v\in V}\frac{1}{g_v^2}\lambda_v\sigma^\mu\partial_\mu\bar\lambda_v - i\sum_{e\in E}2f_e^2\chi_e\sigma^\mu\partial_\mu\bar\chi_e$$
$$+\sum_{e\in E}2f_e^2\left[\chi_e(\lambda_{t(e)} - \lambda_{o(e)}) + h.c.\right], \tag{5.2.10}$$

[2]It is well known that two square matrices AB and BA have the same eigenvalues up to zero modes. See Appendix B.2.

and can be rescaled as

$$\begin{aligned}\mathcal{L}_f &= -i\sum_{v\in V}\lambda_v\sigma^\mu\partial_\mu\bar{\lambda}_v - i\sum_{e\in E}\chi_e\sigma^\mu\partial_\mu\bar{\chi}_e \\ &\quad -\sum_{e\in E}\sum_{v\in V}\sqrt{2}\left[f_e\chi_e(E^T)_{ev}g_v\lambda_v + h.c.\right]. \end{aligned} \tag{5.2.11}$$

Here λ_v and χ_e are Weyl spinor fields contained in V_v and S_e, respectively.

One will find the mass matrices for fermions after rescaling the fields:

$$M_\lambda^2 = 2GEF^2E^TG = 2(GEF)(GEF)^T\,, \quad M_\chi^2 = 2FE^TG^2EF = 2(GEF)^T(GEF). \tag{5.2.12}$$

Note that the fermions λ and χ form Dirac fields for massive modes. Also note that all field contents are neutral as well as free from interactions.

5.3 Multi-vector, multi-Higgs model

5.3.1 General construction

We will construct the model that the symmetry $[U(1)]^p$ is *spontaneously* broken to $U(1)$. Therefore we will not use the Stueckelberg fields but the Higgs fields.

As the model in the previous section, we consider vector superfields on vertices and suppose the $U(1)$ transformation is defined at each vertex. Moreover in the present case, we introduce a "bicharged" scalar field Σ on each edge, which is transformed under two $U(1)$ symmetries as as [3],

$$\Sigma_e \to e^{-2i\Lambda_{t(e)}}\Sigma_e\, e^{2i\Lambda_{o(e)}}\,. \tag{5.3.1}$$

Now we get the $[U(1)]^p$ invariant supersymmetric multi-vector, multi-Higgs model on a graph governed by the following Lagrangian:

$$\begin{aligned}\mathcal{L} &= \frac{1}{4}\sum_{v\in V}\left(W_v^\alpha W_\alpha^v\big|_{\theta\theta} + \overline{W}_{\dot\alpha}^v\overline{W}_v^{\dot\alpha}\big|_{\overline{\theta\theta}}\right) + \sum_{e\in E}\overline{\Sigma}_e\, e^{2gV_{t(e)}}\Sigma_e\, e^{-2gV_{o(e)}}\big|_{\theta\theta\overline{\theta\theta}} \\ &\quad - 2g\sum_{e\in V}\zeta_e(V_{t(e)} - V_{o(e)})\big|_{\theta\theta\overline{\theta\theta}}\,, \end{aligned} \tag{5.3.2}$$

where we rescale the gauge coupling constant to be seen explicitly. The Fayet-Illiopoulos (FI) terms are chosen so that they are similar to those in the model of the previous section, when $\zeta_e \approx f_e^2$.[4] This thesis will not go into the issue about anomaly and will deal with only classical aspects of the model.

[3] Note that the transformation law for Σ_e is the same as that for e^{2S_e} in the previous section.

[4] In most general cases, we can choose the Fayet-Illiopoulos (FI) terms as $\sim \sum_v \zeta_v V_v$. We would like to study aspects of (gauge and/or super-) symmetry breakdown with the general FI terms elsewhere.

The bosonic part of the Lagrangian reads

$$\begin{aligned}\mathcal{L}_b = &-\frac{1}{4}\sum_{v\in V} F^v_{\mu\nu}F_v^{\mu\nu} + \frac{1}{2}\sum_{v\in V} D_v^2 - \sum_{e\in E}(\mathcal{D}_\mu\sigma_e)^\dagger(\mathcal{D}^\mu\sigma_e) \\ &+ \sum_{e\in E} F^\dagger_{\Sigma e}F_{\Sigma e} + g\sum_{e\in E}(D_{t(e)} - D_{o(e)})\sigma_e^\dagger\sigma_e - g\sum_{e\in V}(D_{t(e)} - D_{o(e)})\zeta_e\,,\end{aligned} \tag{5.3.3}$$

where the covariant derivative is

$$\mathcal{D}^\mu\sigma_e = (\partial^\mu + igA^\mu_{t(e)} - igA^\mu_{o(e)})\sigma_e\,. \tag{5.3.4}$$

By use of the incidence matrix of the graph, we rewrite the above Lagrangian as

$$\begin{aligned}\mathcal{L}_b &= -\frac{1}{4}\sum_{v\in V} F^v_{\mu\nu}F_v^{\mu\nu} + \frac{1}{2}\sum_{v\in V} D_v^2 - \sum_{e\in E}(\mathcal{D}_\mu\sigma_e)^\dagger(\mathcal{D}^\mu\sigma_e) \\ &+ \sum_{e\in E} F^\dagger_{\Sigma e}F_{\Sigma e} - g\sum_{e\in E}(\sigma_e^\dagger\sigma_e - \zeta_e)(E^TD)_e\,.\end{aligned} \tag{5.3.5}$$

Substituting the equation of motion for the auxiliary fields

$$F_{\Sigma e} = 0 \quad \text{and} \quad D_v = g\sum_{e\in E}(\sigma_e^\dagger\sigma_e - \zeta_e)(E^T)_v\,, \tag{5.3.6}$$

into the bosonic Lagrangian, we obtain

$$\begin{aligned}\mathcal{L}_b &= -\frac{1}{4}\sum_{v\in V} F^v_{\mu\nu}F_v^{\mu\nu} - \sum_{e\in E}(\mathcal{D}_\mu\sigma_e)^\dagger(\mathcal{D}^\mu\sigma_e) \\ &- \frac{g^2}{2}\sum_{e,e'\in E}(\sigma_e^\dagger\sigma_e - \zeta_e)(E^TE)_{ee'}(\sigma_{e'}^\dagger\sigma_{e'} - \zeta_{e'})\,.\end{aligned} \tag{5.3.7}$$

Note that E^TE is a (q,q) matrix.

5.3.2 Example: P_3

The structure of the model depends on the incidence matrix of the graph. For a simple example, let us consider the path graph with three vertices, P_3.

The incidence matrix depends on the orientation of edges. For instance, two cases can be considered as follows:[5]

$$(E_A)_{ve} = \begin{pmatrix} 1 & 0 \\ -1 & 1 \\ 0 & -1 \end{pmatrix}, \quad (E_B)_{ve} = \begin{pmatrix} 1 & 0 \\ -1 & -1 \\ 0 & 1 \end{pmatrix}, \tag{5.3.8}$$

[5]Obviously the overall sign of the incidence matrix is irrelevant.

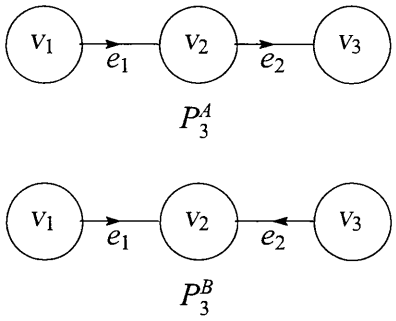

Figure 5.2: P_3: the path graph with three vertices. There are two substantially different graphs. They have the different incidence matrices.

where E_A is the incidence matrix of P_3^A and E_B is the one of P_3^B. The two graphs are shown in Figure 5.2.

Interestingly, the following matrix is independent of the edge orientation:

$$E_A E_A^T = E_B E_B^T = \begin{pmatrix} 1 & -1 & 0 \\ -1 & 2 & -1 \\ 0 & -1 & 1 \end{pmatrix} \equiv \Delta . \tag{5.3.9}$$

This is known as the graph Laplacian.

On the other hand, we find

$$E_A^T E_A = \begin{pmatrix} 2 & -1 \\ -1 & 2 \end{pmatrix}, \quad E_B^T E_B = \begin{pmatrix} 2 & 1 \\ 1 & 2 \end{pmatrix}. \tag{5.3.10}$$

Therefore the shape of the Higgs potential in Eq. (5.3.7) depends on the edge orientation.

Figure 5.3 illustrates the contour plots of the potentials in Eq. (5.3.7) for the graphs P_3^A and P_3^B.

5.3.3 Mass matrices for bosonic and fermionic fields

Individually different gauge coupling constants will also be considered. The consequence of such consideration forces the bosonic part of the Lagrangian to be

$$\begin{aligned} \mathcal{L}_b &= -\frac{1}{4}\sum_{v\in V} F^v_{\mu\nu}F_v^{\mu\nu} - \sum_{e\in E}(\mathcal{D}_\mu\sigma_e)^\dagger(\mathcal{D}^\mu\sigma_e) \\ &\quad - \frac{1}{2}\sum_{e,e'\in E}\sum_{v\in V}(\sigma_e^\dagger\sigma_e - \zeta_e)(E^T)_{ev}g_v^2(E)_{ve'}(\sigma_{e'}^\dagger\sigma_{e'} - \zeta_{e'}), \end{aligned} \tag{5.3.11}$$

with

$$\mathcal{D}^\mu\sigma_e = (\partial^\mu + ig_{t(e)}A^\mu_{t(e)} - ig_{o(e)}A^\mu_{o(e)})\sigma_e . \tag{5.3.12}$$

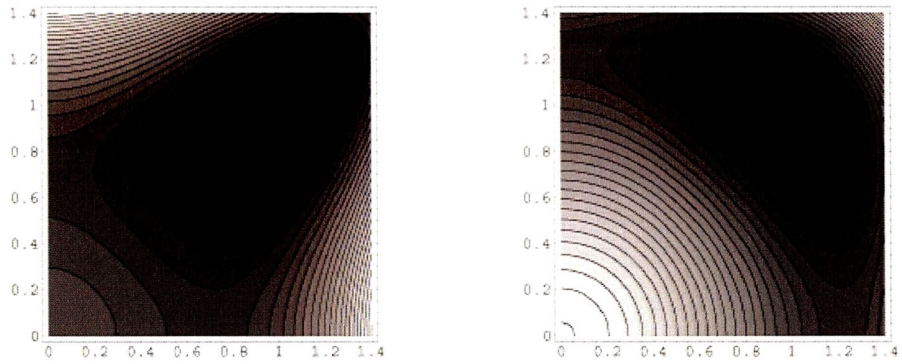

Figure 5.3: Contour plots of scalar potentials for the models based on P_3^A (left) and on P_3^B (right), respectively. In both plots, the horizontal axis indicates $|\sigma_1|/f$ while the vertical axis indicates $|\sigma_2|/f$.

Here we assume that all ζ_e are positive and $\sqrt{\zeta_e} = f_e$. Thus the VEV for $|\sigma_e|$ is f_e and physical scalar fields should be considered as the linear combinations of $|\sigma_e| - f_e$. Each phase part of a to-be massive scalar field is eaten by a vector field through the Higgs mechanism. Then the (mass)^2 matrices M_V^2 for vector fields and M_S^2 for scalar fields in this case are

$$M_V^2 = 2GEF^2E^TG = 2(GEF)(GEF)^T\,, \quad M_S^2 = 2FE^TG^2EF = 2(GEF)^T(GEF)\,, \tag{5.3.13}$$

where the matrices that appeared in the above equations are the same as (5.1.4) and (5.1.7).

Although the shape of the potential with respect to $|\sigma_e|$ depends on the orientation of edges in the graph, the mass spectrum of the scalar fields is the same as the one for the vector fields except for zero modes, similarly to the model in the previous section.

The number of the moduli of the potential is $q - p + 1$ for a general graph. This is equal to the number of independent closed circuits in the graph. [6] For tree graphs, the VEVs of σ_e are determined rigidly if all ζ_e are positive.

The fermionic part of the Lagrangian is

$$\begin{aligned}\mathcal{L}_f &= -i\sum_{v\in V}\lambda_v\sigma^\mu\partial_\mu\bar{\lambda}_v - i\sum_{e\in E}\psi_e\sigma^\mu\mathcal{D}_\mu\bar{\psi}_e \\ &+ i\sqrt{2}\sum_{e\in E}(\sigma_e\bar{\psi}_e(E^T)_{ev}g_v\bar{\lambda}_v - \sigma_e^\dagger\psi_e(E^T)_{ev}g_v\lambda)\,,\end{aligned} \tag{5.3.14}$$

where λ_v and ψ_e are Weyl spinor fields contained in V_v and Σ_e, respectively. The

[6] If $q - p + 1 > 0$, the graph has a closed circuit $C(G)$. It is possible that we add the term like $\sum_{\{e_1,e_2,e_3\}\in C(G)}\Sigma_{e_1}\Sigma_{e_2}\Sigma_{e_3}$ to the Lagrangian to give the scalar masses.

covariant derivative on ψ_e is defined as $\mathcal{D}^\mu\psi_e = (\partial^\mu + ig_{t(e)}A^\mu_{t(e)} - ig_{o(e)}A^\mu_{o(e)})\psi_e$. Substituting the VEVs $\langle\sigma_e\rangle = f_e$, we find

$$M^2_\lambda = 2(GEF)(GEF)^T\,, \quad M^2_\psi = 2(GEF)^T(GEF)\,. \tag{5.3.15}$$

Since SUSY is unbroken, the bosonic and fermionic spectra are the same.

In this thesis, we have considered models with unbroken SUSY. The model with partially broken SUSY is interesting, for some $\zeta_e < 0$. The present analysis will not go into such models.

5.4 Vortex solution

It is well known that the vortex solution can be found in the Abelian-Higgs model [8]. In many papers, the solution is used as a simple model for a cosmic string [9]. We consider the vortex-type solutions in our model described in the previous section.

Although an academic interest in our toy model is an important motivation for the following study, we also think that topological configurations are a key ingredient in recent studies in theoretical physics. A possibility is expected that a similar model provides an example of a complicated brane/string system. In the present thesis, anyway, we study only simple vortex in our theory and their generalizations and possible applications to particle physics and cosmology are left for future work.

Moreover we will consider only tree graphs as the bases of models.

5.4.1 Bogomolnyi equation

In the Abelian-Higgs model, the vortex solution is well known [8]. Moreover, it is known [19] that supersymmetric $U(1)$ theory satisfies the Bogomolnyi condition [20]. Because our model is also supersymmetric, the Bogomolnyi condition can be found. The equations of motion can be reduced to the following two sets of equations:

$$F^{ij}_v = \mp\varepsilon^{ij}g_v\sum_{e\in E}(E)_{ve}(|\sigma_e|^2 - \zeta_e)\,, \tag{5.4.1}$$

and

$$\mathcal{D}^i\sigma_e = \mp i\varepsilon^{ij}\mathcal{D}_j\sigma_e\,, \tag{5.4.2}$$

where i, j denote two spatial directions and ε^{ij} is the antisymmetric tensor.

These equations are the Bogomolnyi equations.

The energy per unit length of a vortex string can be written as

$$\begin{aligned}\mathcal{E} &= \int d^2x \left[\frac{1}{4} \sum_{v\in V} F^v_{ij} F^{ij}_v + \sum_{e\in E} (\mathcal{D}_i \sigma_e)^\dagger (\mathcal{D}^i \sigma_e) \right. \\ &\qquad \left. + \frac{1}{2} \sum_{e,e'\in E} \sum_{v\in V} (|\sigma_e|^2 - \zeta_e)(E^T)_{ev} g_v^2(E)_{ve'} (|\sigma_{e'}|^2 - \zeta_{e'}) \right] \qquad (5.4.3) \\ &= \int d^2x \left[\frac{1}{4} \sum_{v\in V} \left\{ F^{ij}_v \pm \varepsilon^{ij} g_v(E)_{ve} (|\sigma_e|^2 - \zeta_e) \right\}^2 + \frac{1}{2} \sum_{e\in E} \left| \mathcal{D}^i \sigma_e \pm i\varepsilon^{ij} \mathcal{D}_j \sigma_e \right|^2 \right. \\ &\qquad \left. \pm \left\{ \sum_{v\in V} \sum_{e\in E} \frac{1}{2} \varepsilon_{ij} F^{ij}_v g_v(E)_{ve} \zeta_e - i \sum_{e\in E} \varepsilon^{ij} \partial_i (\sigma_e^\dagger \mathcal{D}_j \sigma_e) \right\} \right]. \qquad (5.4.4)\end{aligned}$$

For a solution of finite energy density, $\mathcal{D}_i \sigma_e$ is equal to zero at spatial infinity. If the asymptotic behavior of σ_e is expressed by the azimuthal angle φ and an integer n_e, i.e. $\sigma_e \to \sqrt{\zeta_e} e^{i n_e \varphi}$, the condition tells $(E^T g_v A^v_i)_e \to n_e \partial_i \varphi$, and then $\int d^2x \, (E^T \varepsilon_{ij} g_v F^{ij}_v)_e = 4\pi n_e$. Therefore the energy density becomes

$$\begin{aligned}\mathcal{E} &= \int d^2x \left[\frac{1}{4} \sum_{v\in V} \left\{ F^{ij}_v \pm \varepsilon^{ij} g_v(E)_{ve} (|\sigma_e|^2 - \zeta_e) \right\}^2 + \frac{1}{2} \sum_{e\in E} \left| \mathcal{D}^i \sigma_e \pm i\varepsilon^{ij} \mathcal{D}_j \sigma_e \right|^2 \right] \\ &\quad \pm 2\pi \sum_{e\in E} |n_e| \zeta_e \,. \qquad (5.4.5)\end{aligned}$$

We deal with the lowest bound for the energy density read from this result. The vortex solution satisfying the Bogomolnyi equation (5.4.1) and (5.4.2) has the energy density $2\pi \sum_{e\in E} |n_e| \zeta_e$.[7]

5.4.2 Bogomolnyi vortices and SUSY

It is well known that the SUSY is partially broken in the topological background fields. Here we briefly describe the pattern of SUSY breaking in our model. Notation may be found in [17]. According to SUSY, the variations of the gauginos λ_e are

$$\delta_\epsilon \lambda_v = i\epsilon D_v + \sigma^{\mu\nu} F_{v\mu\nu} \epsilon \,. \qquad (5.4.6)$$

Using the Bogomolnyi equations (5.4.1), and assuming the vortex string lies in the third direction for simplicity, the above variations are rewritten as

$$\delta_\epsilon \lambda_v = \mp i F^{12}_v (1 \pm \sigma^3) \epsilon \,. \qquad (5.4.7)$$

[7]Because of the presence of many fields, non-Bogomolnyi configuration may have lower energy (*i.e.*, the Bogomolnyi solution may correspond to a local minimum).

This means that the half of the SUSY at the vertex is broken in the presence of the central magnetic flux of the vortex.

The variations of partners of σ_e are

$$\delta_\epsilon \psi_e = i\sqrt{2}\bar{\epsilon}\sigma^\mu \mathcal{D}_\mu \sigma_e \,, \tag{5.4.8}$$

where $\mathcal{D}^\mu \psi_e \equiv \partial^\mu \psi_e + i((gA)^\mu_{t(e)} - (gA)^\mu_{o(e)})\psi_e$. If the vortex string lies in the third direction, this reduces when the Bogomolnyi equations (5.4.2) hold,

$$\delta_\epsilon \psi_e = i\sqrt{2}\bar{\epsilon}\left[\sigma^1 \mathcal{D}_1 \psi_e + \sigma^2 \mathcal{D}_2 \psi_e\right] = i\sqrt{2}\bar{\epsilon}(\sigma^1 \pm i\sigma^2)\mathcal{D}_1 \psi_e \,. \tag{5.4.9}$$

We find again that the half of the SUSY at the edge is broken in the presence of the magnetic flux.

5.4.3 Construction of vortices: Ansatz

Next we examine how we can obtain the explicit solutions in our model. For simplicity, we consider a common gauge coupling constant g and a single constant $f = \sqrt{\zeta}$. In other words, we consider the case that $G = gI$ and $F = fI$ (where I is the identity matrix). Although we cannot tell about most general solutions, we take the Ansatz for a simple, physically admissible type of vortex solutions.[8] We impose the axially symmetric Ansatz

$$\sigma_e = \rho_e(r)\, e^{i n_e \varphi} \,, \tag{5.4.10}$$

$$A^v_\varphi = P_v(r) \,, \tag{5.4.11}$$

on Bogomolnyi equations. Here we express the radial coordinate as r and the azimuthal angle as φ. The integers n_e are winding numbers. The detailed calculation is shown in the Appendix B.4. We get the following Bogomolnyi equations,

$$\frac{\rho'_e}{\rho_e} = -\frac{\left(g\left(E^T P\right) - n\right)_e}{r} \,, \tag{5.4.12}$$

$$\frac{P'_v}{r} = -g\sum_{e\in E}(E)_{ve}\left(\rho^2 - f^2\right)_e \,, \tag{5.4.13}$$

where the prime ($'$) denotes the derivative with respect to r. These equations are the special case of the Bogomolnyi equations.

[8] For a reference, we write down the construction of normal vortex solutions in Appendix B.3.

5.4.4 examples of vortex solutions

We show some concrete examples for the vortex solution in our model. To have the vortex solution we restrict the graph structure, or equivalently, the incident matrix E. Here we also consider configurations with the least winding numbers for simplicity and for feasibility in physical systems.

We consider here the cases with the single-centered exact solution similar to the normal vortex. The asymptotic behavior of general cases can be obtained and is shown in Appendix B.5.

Example 1: P_2

The simplest case has two vertices and an edge. This graph is P_2 graph. We show the graph in Figure 5.4.

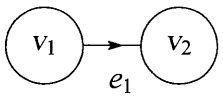

Figure 5.4: P_2: the path graph with two vertices.

In this case, the incidence matrix and its transposed matrix are

$$(E)_{ve} = \begin{pmatrix} 1 \\ -1 \end{pmatrix}, \quad \left(E^T\right)_{ev} = \begin{pmatrix} 1 & -1 \end{pmatrix}. \tag{5.4.14}$$

Then considering the Bogomolnyi equations

$$\frac{P'_v}{r} = -g \sum_{e \in E} (E)_{ve} \left(\rho^2 - f^2\right)_e , \tag{5.4.15}$$

$$\frac{\rho'_e}{\rho_e} = -\frac{\left(g E^T P - n\right)_e}{r} , \tag{5.4.16}$$

the first one becomes

$$\frac{P'_1}{r} = -g\left(\rho^2 - f^2\right) , \tag{5.4.17}$$

$$\frac{P'_2}{r} = +g\left(\rho^2 - f^2\right) . \tag{5.4.18}$$

Therefore it is necessary to find a set of unique equations that we suppose the relation $P_1(r) = -P_2(r)$. On the other hand, in the second equation we notice

$$\sum_v (E^T)_{ev} P_v = \begin{pmatrix} 1 & -1 \end{pmatrix} \begin{pmatrix} 1 \\ -1 \end{pmatrix} P_1 = 2P_1 . \tag{5.4.19}$$

So, we get the following equations

$$\frac{P_1'}{r} = -g\left(\rho^2 - f^2\right), \tag{5.4.20}$$

$$\frac{\rho'}{\rho} = -\frac{2gP_1 - n}{r}. \tag{5.4.21}$$

These equations can be reduced to

$$\frac{\tilde{P}'}{x} = -\left(\tilde{\rho}^2 - 1\right), \tag{5.4.22}$$

$$\frac{\tilde{\rho}'}{\tilde{\rho}} = -\frac{\tilde{P} - n}{x}, \tag{5.4.23}$$

if we rescale the variables so that $\tilde{P}(x) = 2gP_1(r)$, $\tilde{\rho}(x) = \rho(r)/f$, $x = \sqrt{2}gfr$, $n = 1$ and the prime ($'$) is the derivative with respect to x. These equations are precisely same as the normal Bogomolnyi equations. The normal Bogomolnyi equations is referred in Appendix B.3.

The energy per unit length of the straight string is given by $2\pi f^2$ in this case. Generalization to the case with the winding number $n > 1$ is trivial.

Example 2: P_3

We consider the P_3 graph, the three-vertex path graph. In this graph, we consider two patterns of the direction of the edges. We show these in Figure 5.5.

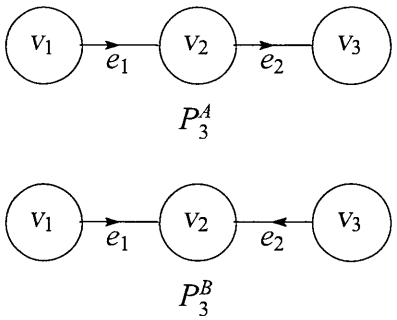

Figure 5.5: The graph P_3^A has edges of the same direction while P_3^B has the edges of the different direction.

The condition to reduce the Bogomolnyi equations in these cases to the normal ones (5.4.22, 5.4.23) with $\rho_1 = \rho_2$ and $n_1 = n_2 = 1$ are $P_1(r) = -P_3(r)$ and $P_2(r) \equiv 0$ in the case with P_3^A while $P_1(r) = P_3(r)$ and $P_2(r) = -2P_1(r)$ in the case with P_3^B. The necessary scaling is that $\tilde{P}(x) = gP_1(r)$ and $x = gfr$ in the case with P_3^A while $\tilde{P}(x) = 3gP_1(r)$ and $x = \sqrt{3}gfr$ in the case with P_3^B. The energy density takes the same value $2\pi f^2(1 + 1) = 4\pi f^2$ in both cases.

Example 3: $K_{1,N}$

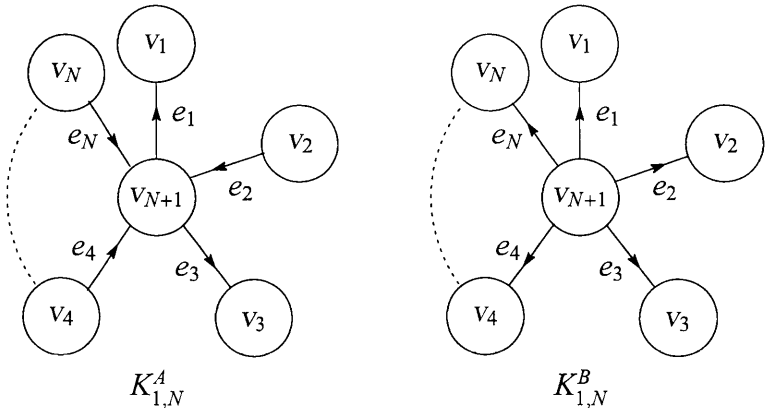

Figure 5.6: The star graphs, $K^A_{1,N}$ and $K^B_{1,N}$.

We consider another tree graph, the star graph $K_{1,N}$. In the star graph, v_{N+1} is adjacent to all the other vertices and no extra edge exists. We recognize two types of edges. One is the edge whose origin is v_{N+1}, another edge is one whose terminus is v_{N+1}. We call the edge of the first type is e_o, the one of the second type is e_t.

We heuristically find the cases that we get the vortex solution similar to the normal one with $\rho_1 = \rho_2 = \cdots = \rho_N = \rho_{N+1}$: Here two cases are shown where the number of edges belonging to two types are

$$K^A_{1,N}: \quad \#e_o = \#e_t = N/2\,, \tag{5.4.24}$$

$$K^B_{1,N}: \quad \#e_o = N \quad \text{and} \quad \#e_t = 0\,, \ \textit{or vice versa}\,, \tag{5.4.25}$$

where, of course, N is considered to be even in the case A. The graphs of two types are shown in Figure 5.6.

The incidence matrix of $K^A_{1,N}$ (where N is even) is $(N+1, N)$ matrix given by

$$(E_A)_{ve} = \begin{pmatrix} -1 & 0 & 0 & \cdots & 0 \\ 0 & 1 & 0 & \cdots & 0 \\ 0 & 0 & -1 & \cdots & 0 \\ \vdots & \vdots & \vdots & \ddots & \vdots \\ 0 & 0 & 0 & \cdots & 1 \\ 1 & -1 & 1 & \cdots & -1 \end{pmatrix}, \tag{5.4.26}$$

while the incidence matrix of $K^B_{1,N}$ is

$$(E_B)_{ve} = \begin{pmatrix} -1 & 0 & 0 & \cdots & 0 \\ 0 & -1 & 0 & \cdots & 0 \\ 0 & 0 & -1 & \cdots & 0 \\ \vdots & \vdots & \vdots & \ddots & \vdots \\ 0 & 0 & 0 & \cdots & -1 \\ 1 & 1 & 1 & \cdots & 1 \end{pmatrix}. \tag{5.4.27}$$

We found these patterns by extending the analysis of getting the vortex solution in the case with P_3 graph shown previously, because $K_{1,2}$ is the same as P_3.

In the first case (5.4.24), we have vortex solutions if $P_{2\ell-1}(r) = -P_{2m}(r)$ (ℓ, m are positive integers and $\ell, m \leq \frac{N}{2}$) and $P_{N+1} \equiv 0$. In the second case (5.4.25), we have the solutions if $P_1(r) = P_2(r) = \cdots = P_N(r)$ and $P_{N+1}(r) = -NP_1(r)$. In both cases the energy density is found to be $2\pi N f^2$ if all the winding numbers are unity.

Inclusion of no winding scalar edge

In the previous two examples, all Higgs scalars have nonzero winding number. Conversely we consider that there is an edge where the assigned scalar has no winding number, thus $\rho_e \equiv f$ at the edge. We use the dashed line to express such an edge, as in Figure 5.7.

Figure 5.7: This dashed line means that $\rho_e \equiv f$ on this edge, no winding scalar edge.

For a constant ρ_e, $P_{o(e)}(r) \equiv P_{t(e)}(r)$ holds everywhere.[9] Suppose that one have already constructed the vortex solution in a certain model with specific graph structure. The one might duplicate the solution and the graph. One may connect the identical vertices of the original and copy of the graph by no winding scalar edge. The number of such connection is arbitrary. This method can be applied to the case with two different models and solutions, if one finds the same functional form of $P_v(r)$ in each model. Of course more than two vertices can be connected if P_v is common at all vertices.

[9]Thus the orientation of the edge is irrelevant (so, there is no arrow assigned to the dashed line).

Example 4: P_4

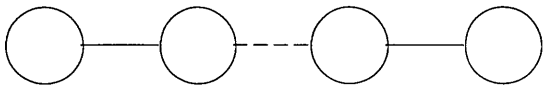

Figure 5.8: P_4 graph consists of two P_2 and an edge.

We consider the P_4 graph. The graph P_4 has two P_2 as subgraphs and is shown in Figure 5.8. We do not show the direction of the edge in this graph. This graph has a left-right symmetry with respect to the dashed edge. This symmetry is connected with the winding number of each vector fields. The vector fields at the both ends of the dashed line must be described by an identical function. For this reason, we should impose the left-right symmetry to the direction of edges. In the P_4 case, we find two types of the edge orientation graph for admitting the normal vortex solutions, shown in Figure 5.9 and Figure 5.10. In the similar way,

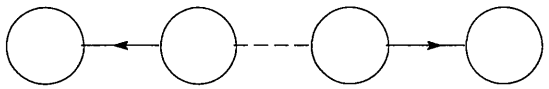

Figure 5.9: P_4 graph whose edge direction is left-right symmetric with respect to the dashed edge. Each of edge directions is outgoing with respect to the dashed edge.

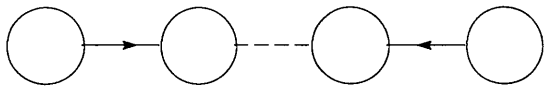

Figure 5.10: P_4 graph. Each of edge direction is incoming with respect to the dashed edge.

we consider the model based on $P_{2\ell}$ with normal vortex solutions.

Example 5: P_6

The graph P_6 has three P_2 as subgraphs. We study the model based on P_6 and their standard solution in the above-mentioned way. In addition, P_6 has two P_3 as subgraphs. Similarly to the case with P_4, we can consider the P_6 graph as two subgraphs connected by an edge. We exhibit the P_6 graph in Figure 5.11. We have the left-right symmetry with respect to the dashed edge also in this case.

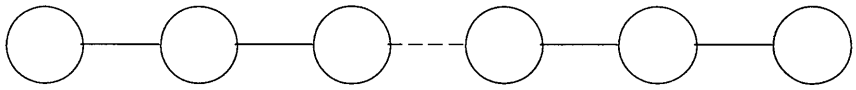

Figure 5.11: P_6 graph, which includes two P_3 as subgraphs.

We classify four types of the graph in terms of the direction of the edges as in Figure 5.12. In the similar way, we can consider the $P_{3\ell}$ graph, and associated

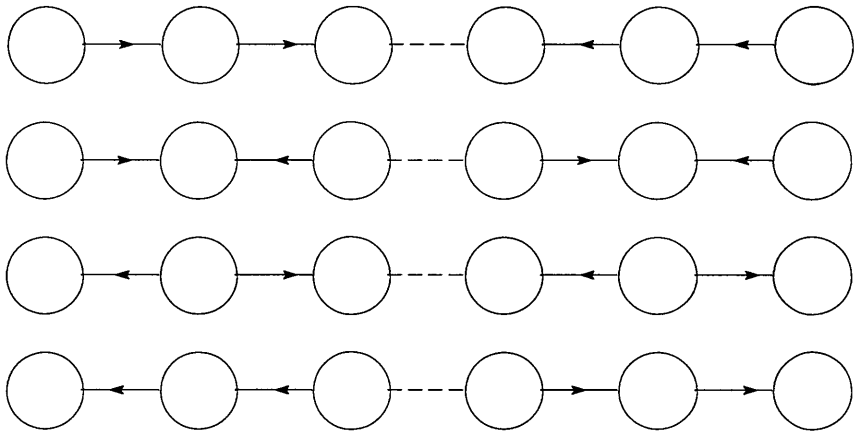

Figure 5.12: There are four types of the P_6 graph consisting of two P_3.

models and solutions.

Example 6

We can connect two $K_{1,N}$ graphs by the dashed edge as in Figure 5.13. As this example, we can find the graph structure admitting the normal vortex solutions.

5.5 Conclusion and Outlook

We have generalized DD into GDD and introduced SUSY to GDD in the Abelian theory. A multi-Abelian-Higgs model has been studied as a further generalization. After getting the Bogomolnyi equations, we explicitly constructed vortex solutions of the normal type. To get the vortex solution, we restricted the graph structure to the special cases shown in the previous section. We showed some examples for the graph which has the normal vortex solution.

We have left the following aspects of the multi-Abelian-Higgs models for future work. First, we discussed single-centered vortex in the present thesis. The

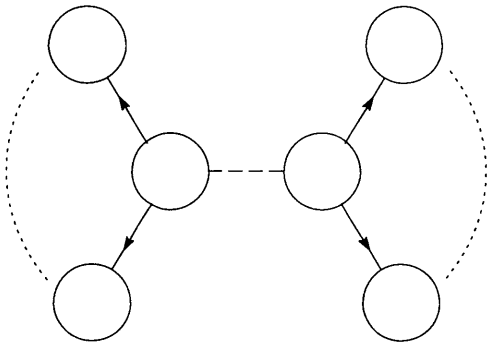

Figure 5.13: The graph consisting of two $K_{1,N}$ connected by the dashed edge.

possibility of multi-vortex solution [21] is an important subject to study. Next, in this thesis, we mainly considered tree graphs. If we take general graph structures as the bases of multi-Abelian-Higgs models, we have scalar potentials with (many) flat direction of the lowest energy. The appearance of moduli is the feature of supersymmetric theories and the vortex solution in such a model is crucial for phenomenological models [22]. At the same time, the quantum corrections might become essential. The generalization of the method in [23] will be useful to investigate the quantum effects about vortices. Finally, because our model contains several fields, the possibility of different types of topological defects, such as rings [24], must be examined.

We considered the Abelian gauge theory in GDD as well as multi-Higgs models. We are also interested in the non-Abelian theory because the Three Site Higgsless model is based on the $[SU(2)]^2 \otimes U(1)$ gauge theory. While we considered vortices in the Abelian gauge theory in this thesis, on the other hand there exist monopoles in the non-Abelian gauge theory. As the future works, we wish to incorporate monopoles, superfields and GDD into non-Abelian theory as some toy models for the Higgsless model.

Part IV

Summary, perspective and conclusion

Chapter 6

Summary, perspective and conclusion

Two novel models

In this thesis we have built two models ("Democratic Three Site Higgsless Model" and "Vortices and Superfield on a Graph") using the technique of DD. These two models are only the mathematical models.

Democratic Three Site Higgsless Model

The idea of "Democratic Model" is that each $SU(2)$ gauge field has equivalent property. Saying this another way, all $SU(2)$ gauge fields have same gauge couplings. From the bosonic part, the condition of the Democratic gauge coupling $g_0 = g_1 = g_2$ does not satisfy the ratio of the gauge boson masses (4.2.1). Therefore we guessed (or proposed) the condition of the gauge coupling that nearly satisfied the Democratic Condition. In this condition we realized the experimental value. This value depended on the VEV of the sigma field and the Higgs field. The former could not choose any values, but the latter could choose the rang of value $v_H/f_1 \gtrsim 60$. This parameter condition is the one of the parameter choices. In fact, there are any parameter conditions that satisfy the experimental value of the gauge boson masses. Including the result of the fermionic part, the ratio of g_{A^γ}/g_W (4.2.24) showed that above condition did not satisfy the experimental value $(g_{A^\gamma}/g_W)^2 \sim 0.22$.

We mentioned the monopole. The mass of heavy weak bosons W'' is extremely heavier than the mass of other bosons. Therefore the mass of the monopole is the same order of the mass of the heavy weak bosons. The mass of the heavy weak bosons consists of parameters v_H and f_1. In this model, parameters v_H and f_1 are highly correlated with the mass of the monopole. The ratio v_H/f_1 is limited to

$v_H/f_1 \gtrsim 60$. Therefore the mass of the monopole has the lower limit.

As in Figure 4.8, the Democratic Three Site Model has many parameters which are chosen by hand. The number of λ and f parameters is 18. The parameter of λ (λ_f) has each value for each type of fermion. The mass of each fermion is controlled by the λ_f parameter.

The Democratic Model includes many difficulties to realize the real phenomenology. We need to improve the Democratic Three Site Higgsless Model.

Vortices and Superfields on a Graph

We generalized the moose diagram in the DD into the directed graph in the graph theory. We considered simple Abelian theory. Abelian gauge fields reside at vertices and scalar fields reside at edges. We have generalized DD into GDD and introduced SUSY to GDD in the Abelian theory. A multi-Abelian-Higgs model has been studied as a further generalization. After getting the Bogomolnyi equations, we explicitly constructed vortex solutions of the normal type. To get the vortex solution, we restricted the graph structure to the special cases shown in this thesis. We showed some examples for the graph which has the normal vortex solution.

We have left the following aspects of the multi-Abelian-Higgs models for future work. First, we discussed single-centered vortex in the present thesis. The possibility of multi-vortex solution [21] is an important subject to study. Next, in this paper, we mainly considered tree graphs. If we take general graph structures as the bases of multi-Abelian-Higgs models, we have scalar potentials with (many) flat direction of the lowest energy. The appearance of moduli is the feature of supersymmetric theories and the vortex solution in such a model is crucial for phenomenological models [22]. At the same time, the quantum corrections might become essential. The generalization of the method in [23] will be useful to investigate the quantum effects about vortices. Finally, because our model contains several fields, the possibility of different types of topological defects, such as "rings" [24], must be examined.

We considered the Abelian gauge theory in GDD as well as multi-Higgs models. We are also interested in the non-Abelian theory because the Three Site Higgsless Model is based on the $[SU(2)]^2 \otimes U(1)$ gauge theory. While we considered vortices in the Abelian gauge theory in this paper, on the other hand there exist monopoles in the non-Abelian gauge theory. As the future works, we wish to incorporate monopoles, superfields and GDD into non-Abelian theory as some toy models for the Higgsless model.

Three kinds of interests

We make some comments about three kinds of interests.

Electroweak (Unified) Theory

In the electroweak energy scale, the dynamics of the symmetry breaking will be proved in the LHC experiment. Higgsless Theory, which is based on the extra-dimensional theory, gives the one of the idea of the symmetry breaking. This is the one of the answers to the gauge hierarchy problem. There exist many heavy weak bosons in Higgsless Theory. We control the cut-off energy scale by DD, three site models are examples of the deconstructed theory. If the heavy weak bosons (W' and Z') are detected, we have an evidence of the existence of the extra-dimension.

Solitons

As the solitonic objects, monopoles and vortices were considered in this thesis.

We considered the novel monopole model which was based on the three site model. We think that the monopole mixture exists as the dark matter in the universe. We guess that the mass of the monopole mixture is 100 TeV.

We considered the vortex solution in multi-Abelian-Higgs model. To get the vortex solution, we restricted the graph structure to the special cases.

We think that topological configurations are a key ingredient in recent studies in theoretical physics.

Field Theory on a Graph

We generalized the moose diagram in the DD into the directed graph in a Graph Theory. GDD and DD are useful techniques not only the Electroweak Theory, but also any other field theories. For examples, Quantum Electrodynamics was considered in [10] and Multi-Gravity theory was considered in [11].

Conclusion as a whole

Based on the (dimensionally) deconstructed theory, we consider two novel theories. It seems that we can search physics in particular "theory space" or "theory framework" by using the moose diagram (DD) on purpose. In fact, we investigated A Three Site Model by controlling the moose diagram (the degree of deconstructing). In this model, they are controlled that the upper limit of the adaptive

energy scale and the relations between fields by the moose diagram. Therefore it is important that the mechanism (or motivation) of determining the moose diagram structure. In the model of "Vortices and Superfields on a Graph", the existence conditions of vertex solutions restricted the graph structure. Therefore the existence of the solitons might be the key point of choosing the "theory space" or "theory framework".

Appendix A

For the Original Three Site Higgsless Model

A.1 The Original Three Site Higgsless Model

We show the process, from the five-dimensional $SU(2)_L \otimes SU(2)_R \otimes U(1)_{B-L}$ gauge theory to the Original Three Site Higgsless Model. In section 3.1, we mentioned that "Arbitrary deconstructed model of the five-dimensional $SU(2)_L \otimes SU(2)_R \otimes U(1)_{B-L}$ gauge theory is represented by the four-dimensional $SU(2)_L \otimes U(1)_Y \otimes [SU(2)_L \otimes SU(2)_R \otimes U(1)_{B-L}]^{N-1} \otimes SU(2)_V \otimes U(1)_{B-L}$ gauge theory, $\cdots$". In this five-dimensional gauge thoery, we imposed the boundary conditions. Therefore we had $U(1)_Y$ and $SU(2)_V$ gauge fields.

In this Appendix, we start from the five-dimensional $SU(2)_L \otimes SU(2)_R \otimes U(1)_{B-L}$ gauge theory which is not imposed any boundary conditions. We show the moose diagram of the deconstructed five-dimensional $SU(2)_L \otimes SU(2)_R \otimes U(1)_{B-L}$ gauge theory in Figure A.1. In Figure A.2, we impose the boundary conditions. Consequently, we have the moose diagram as in Figure A.3. We reduce the lattice points as much as possible in Figure A.4. As the result, we obtain the moose diagram of the Original Three Site Higgsless Model.

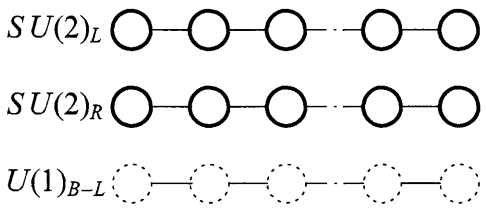

Figure A.1: This is the moose diagram of the discretized five-dimensional $SU(2)_L \otimes SU(2)_R \otimes U(1)_{B-L}$ gauge theory.

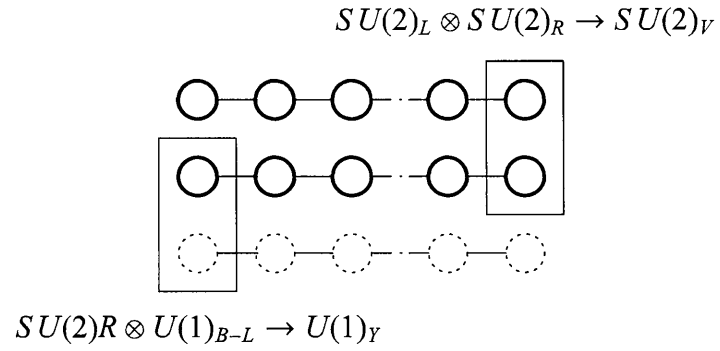

Figure A.2: Imposing the boundary conditions, we find that $SU(2)_R \otimes U(1)_{B-L}$ breaks to $U(1)_Y$ and $SU(2)_L \otimes SU(2)_R$ breaks to $SU(2)_V$.

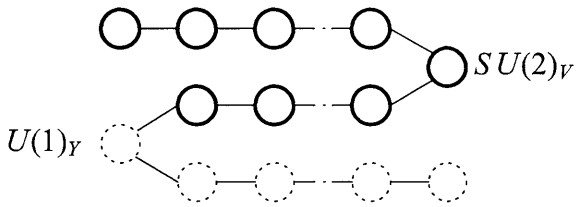

Figure A.3: After breaking to $U(1)_Y$ and $SU(2)_V$, these sites connected to the neighbor sites.

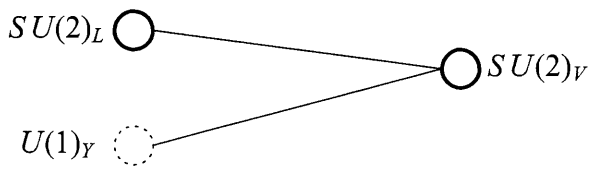

Figure A.4: Reducing the lattice points (KK mode) as much as possible. Because we think it is enough to 1st KK mode for low energy physics.

Appendix B

For Vortices and Superfields on a Graph

B.1 Contents of superfields

In this Appendix, we collect the superfields and their component fields. See the reference [17].

B.1.1 Vector superfield

$$V_v = -\theta\sigma_\mu\bar{\theta}A_v^\mu + i\theta\theta\bar{\theta}\bar{\lambda}_v - i\bar{\theta}\bar{\theta}\theta\lambda_v + \frac{1}{2}\theta\theta\bar{\theta}\bar{\theta}D_v\,. \tag{B.1.1}$$

This satisfies

$$V_v^2 = -\frac{1}{2}\theta\theta\bar{\theta}\bar{\theta}A_\mu^v A_v^\mu\,, \quad V_v^3 = 0\,. \tag{B.1.2}$$

B.1.2 Chiral superfield (Stueckelberg superfield)

$$\begin{aligned} S_e &= \frac{1}{2}(\rho_e + ia_e) + \theta\chi_e + i\theta\sigma^\mu\bar{\theta}\frac{1}{2}(\partial_\mu\rho_e + i\partial_\mu a_e) \\ &\quad + \theta\theta F_{Se} + \frac{i}{2}\theta\theta\bar{\theta}\bar{\sigma}^\mu\partial_\mu\chi_e + \frac{1}{8}\theta\theta\bar{\theta}\bar{\theta}(\rho_e + ia_e)\,, \end{aligned} \tag{B.1.3}$$

$$\begin{aligned} S_e + \bar{S}_e &= \rho_e + \theta\chi_e + \bar{\theta}\bar{\chi}_e - \theta\sigma^\mu\bar{\theta}\partial_\mu a_e + \theta\theta F_{Se} + \bar{\theta}\bar{\theta}F_{Se}^\dagger \\ &\quad + \frac{i}{2}\theta\theta\bar{\theta}\bar{\sigma}^\mu\partial_\mu\chi_e + \frac{i}{2}\bar{\theta}\bar{\theta}\theta\sigma^\mu\partial_\mu\bar{\chi}_e + \frac{1}{4}\theta\theta\bar{\theta}\bar{\theta}\rho_e\,. \end{aligned} \tag{B.1.4}$$

B.1.3 Chiral superfield (Higgs superfield)

$$\begin{aligned}\Sigma_e &= \sigma_e + \sqrt{2}\theta\psi_e + i\theta\sigma^\mu\bar{\theta}\partial_\mu\sigma_e \\ &\quad +\theta\theta F_{\Sigma e} + \frac{i}{\sqrt{2}}\theta\theta\bar{\theta}\bar{\sigma}^\mu\partial_\mu\psi_e + \frac{1}{4}\theta\theta\bar{\theta}\bar{\theta}(\sigma_e)\,. \end{aligned} \tag{B.1.5}$$

B.2 The eigenvalues of matrices AB and BA

Let A be a (p,q) matrix and B be a (q,p) matrix. Then $(p+q, p+q)$ matrices U and V are defined as

$$U = \begin{pmatrix} I_p & A \\ B & xI_q \end{pmatrix}, \quad V = \begin{pmatrix} xI_p & -A \\ 0_{qp} & I_q \end{pmatrix}, \tag{B.2.1}$$

where I_p is the (p,p) identity matrix while 0_{qp} is the (q,p) matrix all of which elements are zero.

The products of two matrices are

$$UV = \begin{pmatrix} xI_p & 0_{pq} \\ xB & xI_q - BA \end{pmatrix}, \quad VU = \begin{pmatrix} xI_p - AB & 0_{pq} \\ B & xI_q \end{pmatrix}. \tag{B.2.2}$$

Because $\det UV = \det VU$, the eigenvalues of AB and BA are equal, except for zero eigenvalues.

B.3 The normal vortex in Abelian-Higgs model

The Ginzburg-Landau theory is used as a macroscopic theory of the superconductivity. That is nonrelativistic theory, and we know an Abelian-Higgs model as the relativistic version of the Ginzburg-Landau theory. This model includes the normal vortex solution. In this paper we distinguish the vortex solution of the Abelian-Higgs model from the vortex solutions of our multi-Abelian-Higgs models, by using the word "normal".

In the Abelian-Higgs model, the Lagrangian density is

$$\mathcal{L} = -\frac{1}{4}F^{\mu\nu}F_{\mu\nu} - \left|D_\mu\sigma\right|^2 - \frac{1}{2}g^2\left(\sigma^2 - f^2\right)^2, \tag{B.3.1}$$

where $F_{\mu\nu} = \partial_\mu A_\nu - \partial_\nu A_\mu$ is a field strength of the Abelian gauge field A_μ, σ is a complex scalar field and f is its vacuum expectation value $\langle\sigma\rangle = f$. $D_\mu\sigma$ is the covariant derivative of the scalar field

$$D_\mu\sigma = \partial_\mu\sigma + igA_\mu\sigma, \tag{B.3.2}$$

where g is the gauge coupling constant to the scalar field σ.

To obtain the classical solution in this theory, we impose the static, axially-symmetric ansatz:

$$\boldsymbol{A} = \boldsymbol{e}_\varphi P(r), \tag{B.3.3}$$

$$\sigma = \rho(r) e^{in\varphi}, \tag{B.3.4}$$

where the integer n is the winding number. We used the circular cylindrical coordinates r, φ, and z.

We use the scale conversion $x \equiv gfr$, $\tilde{P} \equiv gP$ and $\tilde{\rho} \equiv \rho/f$. Therefore the energy density of per unit length of the z axis becomes

$$\mathcal{E} = 2\pi f^2 \int_0^\infty dx\, x \left[\frac{1}{2} \left(\frac{\tilde{P}'}{x} + \tilde{\rho}^2 - 1 \right)^2 + \left(\tilde{\rho}' + \frac{\tilde{P} - n}{x} \tilde{\rho} \right)^2 - \frac{\tilde{P}'}{x} \left(\tilde{\rho}^2 - 1 \right) - 2\tilde{\rho}\tilde{\rho}' \frac{\tilde{P} - n}{x} \right], \tag{B.3.5}$$

where the prime ($'$) denotes the derivative with respect to x. Asymptotic values are as follows: $\tilde{P}(0) = 0$, $\tilde{P}(\infty) = n$, $\tilde{\rho}(0) = 0$ and $\tilde{\rho}(\infty) = 1$. We can write the following inequality for the energy

$$\mathcal{E} \geq 2\pi n f^2 \int_0^\infty \left(\tilde{\rho}^2 \right)' dx = 2\pi n f^2. \tag{B.3.6}$$

This lower bound on the energy is the Bogomolnyi bound and it is saturated when $\tilde{\rho}$ and $\tilde{P}$ satisfy the following equations

$$\frac{\tilde{P}'}{x} = -\left(\tilde{\rho}^2 - 1 \right), \tag{B.3.7}$$

$$\frac{\tilde{\rho}'}{\tilde{\rho}} = -\frac{\tilde{P} - n}{x}. \tag{B.3.8}$$

These equations are the Bogomolnyi equations.

B.4 Action and equation of motion with vortex Ansatz

In this Appendix, we show the details about the Bogomolnyi equations for the vortex configuration. We take the axially symmetric ansatz:

$$\sigma_e = \rho_e(r) e^{in_e\varphi}, \quad A_\varphi^{\mathrm{v}} = P_{\mathrm{v}}(r). \tag{B.4.1}$$

Then we find

$$\mathcal{D}_r \sigma_e = \rho_e' e^{in_e\varphi}, \quad \mathcal{D}_\varphi \sigma_e = i(n_e + (gP)_{t(e)} - (gP)_{o(e)}) \rho_e e^{in_e\varphi}, \tag{B.4.2}$$

where the prime denotes $\frac{d}{dr}$, the derivative with respect to r, and $(gP)_v = g_v P_v$. Thus the kinetic term of the scalar reads

$$|\mathcal{D}_i \sigma_e|^2 = (\rho_e')^2 + \frac{(n_e + (gP)_{t(e)} - (gP)_{o(e)})^2}{r^2}\rho_e^2 , \tag{B.4.3}$$

while the Maxwell term becomes

$$\frac{1}{4}F_v^{ij}F_{ij}^v = \frac{1}{2}\frac{(P_v')^2}{r^2} . \tag{B.4.4}$$

The total action can be rewritten as

$$\begin{aligned}\mathcal{E} \;=\; 2\pi \int_0^\infty dr\, r \Bigg[& \frac{1}{2}\sum_{v\in V}\frac{(P_v')^2}{r^2} + \sum_{e\in E}\left\{(\rho_e')^2 + \frac{((E^T G P)_e - n_e)^2}{r^2}\rho_e^2\right\} \\ & + \frac{1}{2}\sum_{e,e'\in E}(\rho_e^2 - \zeta_e)(E^T G^2 E)_{ee'}(\rho_{e'}^2 - \zeta_{e'})\Bigg] ,\end{aligned} \tag{B.4.5}$$

and this is no other than the energy density per unit length in the present static case.

Varying this, we obtain the following equations of motion:

$$\frac{(r\rho_e')'}{r} \;=\; \frac{((E^T GP)_e - n_e)^2}{r^2}\rho_e + \sum_{e,e'\in E}\rho_e (E^T G^2 E)_{ee'}(\rho_{e'}^2 - \zeta_{e'}) , \tag{B.4.6}$$

$$\left(\frac{P_v'}{r}\right)' \;=\; 2\sum_{e\in E}\frac{((E^T GP)_e - n_e)}{r^2}\rho_e^2 (E^T G)_{ev} . \tag{B.4.7}$$

These second-order simultaneous equations can be reduced to the first-order Bogomolnyi equations:

$$\rho_e' \;=\; \mp\frac{(E^T GP)_e - n_e}{r}\rho_e , \tag{B.4.8}$$

$$\frac{P_v'}{r} \;=\; \mp\sum_{e\in E}(\rho_e^2 - \zeta_e)(E^T G)_{ev} . \tag{B.4.9}$$

B.5 Asymptotic profile of the vortex

We investigate the asymptotic behavior of the solution of (B.4.8,B.4.9) in this Appendix. To this purpose, first we introduce new variables $p_v(r)$ and $R_e(r)$:

$$P_v(r) = a_v - p_v(r) , \quad \rho_e = f_e - R_e(r) , \tag{B.5.1}$$

where the constant a_v satisfies

$$n_e = (E^T G a)_e \,. \tag{B.5.2}$$

Next we prepare p-dimensional eigenvectors $x^{(a)}$ $(a = 1, \cdots, p-1)$ for the $(mass)^2$ mass matrix for vector fields satisfying

$$2(GEF)(GEF)^T x^{(a)} = (m^{(a)})^2 x^{(a)} \,, \quad \text{for nonzero modes} \tag{B.5.3}$$

and q-dimensional eigenvectors $X^{(a)}$ for the $(mass)^2$ mass matrix for scalar fields satisfying

$$2(GEF)^T(GEF)X^{(a)} = (m^{(a)})^2 X^{(a)} \,. \tag{B.5.4}$$

Hereafter we restrict ourselves on the case with tree graphs treated in the text. Thus $q = p - 1$. The zero mode satisfies

$$2(GEF)(GEF)^T x^{(0)} = 0 \,. \tag{B.5.5}$$

The relations of two sets of eigenvectors are

$$X^{(a)} = \frac{\sqrt{2}}{m^{(a)}}(GEF)^T x^{(a)} \,, \quad x^{(a)} = \frac{\sqrt{2}}{m^{(a)}} GEF X^{(a)} \,, \quad (a \neq 0) \tag{B.5.6}$$

and we adopt the normalization convention:

$$x^{(a)T} x^{(a)} = X^{(a)T} X^{(a)} = 1 \,. \tag{B.5.7}$$

Using the eigensystems, we can expand the variables by eigenvectors as

$$p_v(r) = \sum_{(a)} p^{(a)} x_v^{(a)} \,, \quad R_e(r) = \sum_{(a)} R^{(a)} X_e^{(a)} \,, \tag{B.5.8}$$

Noticing $R_e(\infty) = 0$ and $p_v(\infty) = 0$, the equations of motion (B.4.6,B.4.7) becomes at the asymptotic region, $r \to \infty$,

$$R^{(a)\prime\prime} + \frac{1}{r} R^{(a)\prime} - (m^{(a)})^2 R^{(a)} = 0 \,, \tag{B.5.9}$$

$$p^{(a)\prime\prime} - \frac{1}{r} p^{(a)\prime} - (m^{(a)})^2 p^{(a)} = 0 \,, \tag{B.5.10}$$

and the Bogomolnyi equations (B.4.8,B.4.9) become at the asymptotic region, $r \to \infty$,

$$R^{(a)\prime} = -\frac{1}{r} \frac{m^{(a)}}{\sqrt{2}} p^{(a)} \,, \tag{B.5.11}$$

$$\frac{p^{(a)\prime}}{r} = -\sqrt{2} m^{(a)} R^{(a)} \,. \tag{B.5.12}$$

The solution of the above equations is

$$R^{(a)} = C\,K_0(m^{(a)}r)\,, \quad p^{(a)} = \sqrt{2}C\,rK_1(m^{(a)}r)\,. \tag{B.5.13}$$

This result can be derived by using the following formulas for the modified Bessel function of the second type, such as $K_0(z)$ and $K_1(z)$;

$$K_0''(z)+\frac{1}{z}K_0'(z)-K_0(z)=0\,, \qquad K_1''(z)+\frac{1}{z}K_1'(z)-\left(1+\frac{1}{z^2}\right)K_1(z)=0\,, \tag{B.5.14}$$

$$(zK_1(z))''-\frac{1}{z}(zK_1(z))'-(zK_1(z))=0\,, \tag{B.5.15}$$

$$K_0'(z)=-K_1(z)\,, \qquad (zK_1(z))'=-zK_0(z)\,, \tag{B.5.16}$$

where the prime ($'$) means the derivative with respect to z.

More rough estimation can be done with the exponential function because

$$K_\nu(z)\approx\sqrt{\frac{\pi}{2z}}e^{-z}\,, \quad \text{for large } z\,. \tag{B.5.17}$$

Bibliography

[1] S. L. Glashow, "*Partial Symmetries Of Weak Interactions*", Nucl. Phys. **22**, 579 (1961).

S. Weinberg, "*A Model Of Leptons* ", Phys. Rev. Lett. **19**, 1264 (1967).

A. Salam, "*Weak and electromagnetic interactions*", in Elementary Particle Theory, edited by N. Svartholm, 367 (Almqvist and Wiksell, Stockholm,1968).

[2] P. W. Higgs, "*Broken Symmetries And The Masses Of Gauge Bosons*", Phys. Rev. Lett. **13**, 508 (1964).

[3] N. Arkani-Hamed, A. G. Cohen and H. Georgi, Phys. Rev. Lett. **86** (2001) 4757.

N. Arkani-Hamed, A. G. Cohen and H. Georgi, Phys. Lett. **B513** (2001) 232.

N. Arkani-Hamed, A. G. Cohen and H. Georgi,

[arXiv:hep-th/0108089].

[4] C. T. Hill, S. Pokorski and J. Wang, Phys. Rev. **D64** (2001) 105005.

H. C. Cheng, C. T. Hill and J. Wang, Phys. Rev. **D64** (2001) 095003.

H. C. Cheng, C. T. Hill, S. Pokorski and J. Wang, Phys. Rev. **D64** (2001) 065007.

[5] R. Rajaraman, "*Solitons And Instantons* ", Elsevier (1982).

Valery Rubakov and Translated by Stephen S. Wilson, "*Classical Theory of Gauge Fields* " , Princeton University Press (2002).

Nicholas Manton and Paul Sutcliffe, "*Topological Solitons* " , Cambridge University Press (2004).

Edward W. Kolb, Michael S. Turner "*The Early Universe* ", Addison-Wesley Publishing Company. (1990).

Ta-Pei Cheng and Ling-Fong Li, "*Gauge theory of elementary particle physics*", Oxford Science Publications (1984).

Edited by Neil Craigie, "*Theory and Detection of Magnetic Monopoles in Gauge Theories*", World Scientific Publishing Co. Pte. Ltd. (1986).

Graham G. Ross, "*Grand unified theories*", The Benjamin/Cummomgs Publishing Company, Inc. (1985).

[6] Gerardus 't Hooft, "*Magnetic Monopoles in Unified Gauge Theories*", Nucl. Phys. **B79** (1974) 276-284.

[7] Alexander M. Polyakov, "*Particle Spectrum in Quantum Field Theory* ", JETP Lett. **20** (1974) 194-195.

[8] H. J. de Vega and F. A. Schaposnik, "*Classical vortex solution of the Abelian-Higgs model*", Phys. Rev. **D14** (1976) 1100.

F. A. Schaposnik, "*Vortices*", [arXiv:hep-th/0611028].

[9] A. Vilenkin and E. P. S. Shellard, "*Cosmic Strings and Other Topological Defects*", Cambridge University Press (1994).

[10] N. Kan and K. Shiraishi, J. Math. Phys. **46** (2005) 112301.

[11] Teruki Hanada, Koichiro Kobayashi, Kazuhiko Shinoda and Kiyoshi Shiraishi, "*Classical and quantum cosmology of multigravity*", Class. Quantum Grav. **27** (2010) 225010 ; [arXiv:gr-qc/1004.5435].

[12] For a example, R. J. Wilson, "*Introduction to Graph Theory*" (4th Edition), Longman, New York, (1997).

[13] C. Csaki, Christophe Grojean, Luigi Pilo and John Terning, "*Towards a Realistic Model of Higgsless Electroweak Symmetry Breaking*", Phys. Rev. Lett. **92** (2004) 101802 [arXiv:hep-ph/0308038].

C. Csaki, Christophe Grojean, Hitoshi Murayama, Luigi Pilo and John Terning, "*Gauge theories on an interval: Unitarity without a Higgs boson*", Phys. Rev. **D69** (2004) 055006 [arXiv:hep-ph/0305237].

[14] L. Randall and R. Sundrum, "*An Alternative to Compactification*", Phys. Rev. Lett. **83** (2009) 4690 [arXiv:hep-th/9906064v1].

L. Randall and R. Sundrum, "*Large Mass Hierarchy from a Small Extra Dimension*", Phys. Rev. Lett. **83** (2009) 3370 [arXiv:hep-ph/9905221v1].

[15] R. Sekhar Chivukula, B. Coleppa, S. Di Chiara, E. H. Simmons, H. J. He, M. Kurachi and M. Tanabashi, "*A Three Site Higgsless Model*", Phys. Rev. **D74** (2006) 075011 ; [arXiv:hep-ph/0607124].

Niel D. Christensen, "*Some Details of The Minimal Higgsless Model*", (2008).

[16] R.Sekhar Chivukula, Elizabeth H. Simmons, Hong-Jian He, Masafumi Kurachi and Masaharu Tanabashi, "*Ideal fermion delocalization in Higgsless models*", Phys. Rev. D72 (2005) 015008 ; [arXiv:hep-ph/0504114].

Riccardo Barbieri, Alex Pomarol, Riccardo Rattazzi and Alessandro Strumia, "*Electroweak symmetry breaking after LEP-1 and LEP-2*", Nucl.Phys.B703 (2004) 127-146 ; [arXiv:hep-ph/0405040].

R.Sekhar Chivukula, Elizabeth H. Simmons, Hong-Jian He, Masafumi Kurachi and Masaharu Tanabashi, "*Deconstructed Higgsless models with one-site delocalization*", Phys. Rev. D71 (2005) 115001 ; [arXiv:hep-ph/0502162].

R.Casalbuoni, S. De Curtis, D. Dolce and D. Dominici, "*Playing with fermion couplings in Higgsless models*", Phys. Rev. D71 (2005) 075015 ; [arXiv:hep-ph/0502209].

Howard Georgi, "*Chiral fermion delocalization in deconstructed Higgsless theories*", [arXiv:hep-ph/0508014].

R.Sekhar Chivukula, Elizabeth H. Simmons, Hong-Jian He, Masafumi Kurachi and Masaharu Tanabashi, "*Multi-gauge-boson vertices and chiral Lagrangian parameters in Higgsless models with ideal fermion delocalization*", Phys. Rev. D72 (2005) 075012 ; [arXiv:hep-ph/0508147].

R.Sekhar Chivukula, Elizabeth H. Simmons, Hong-Jian He, Masafumi Kurachi and Masaharu Tanabashi, "*Ideal fermion delocalization in five dimensional gauge theories*", Phys. Rev. D72 (2005) 095013 ; [arXiv:hep-ph/0509110].

Stefania De Curtis, "*Fermion delocalization in Higgsless models*", PoS HEP2005:353,2006 ; [arXiv;hep-ph/0512158].

[17] I. L. Buchbinder and S. M. Kuzenko, "*Ideas and Methods of Supersymmetry and Supergravity Or a Walk Through Superspace*", IOP, Bristol, Revised edition (1998).

[18] S. V. Kuzmin and D. G. C. McKeon, Mod. Phys. Lett. **A17** (2002) 2605; [arXiv;hep-th/0211166].

B. Körs and P. Nath, JHEP **0507** (2005) 069 "Aspects of the Stueckelberg Extension", [arXiv;hep-ph/0503208].

T. Kawano, [arXiv;hep-th:/07122351].

[19] J. D. Edelstein, C. Núñez, and F. A. Schaposnik, Phys. Lett. **B329**, 39 (1994) ; [arXiv:hep-th/9311055].

[20] E. B. Bogomolnyi, Sov. J. Nucl. Phys. **24** (1976) 449.

[21] E. J. Weinberg, Phys. Rev. **D19** (1979) 3008.

C. H. Taubes, Commun. Math. Phys. **72** (1980) 277.

[22] A. Achúcarro, A. C. Davis, M. Pickles and J. Urrestilla, Phys. Rev. **D66** (2002) 105013; Phys. Rev. **D68** (2003) 065006.

Y. Cui, S. P. Martin, D. E. Morrissey and J. D. Wells, Phys. Rev. **D77** (2008) 043528.

[23] A. Rebhan, P. van Nieuwenhuizen and R. Wimmer, Nucl. Phys. **B679** (2004) 382; Braz. J. Phys. **34** (2004) 1273.

A. S. Goldhaber, A. Rebhan, P. van Nieuwenhuizen and R. Wimmer, Phys. Rep. **398** (2004), 179.

[24] C. G. Doudoulakis, Physica **D228** (2007) 159 ; Physica **D234** (2007) 1.